Molecular Mechanisms Specifying the Topography of Thalamocortical Projections in the Ventral Telencephalon

Ashton Winfield Powell

A dissertation submitted to the faculty of the University of North Carolina at Chapel Hill in partial fulfillment of the requirements for the degree of Doctor of Philosophy in the Curriculum in Neurobiology.

Chapel Hill
2008

Approved by,
Franck Polleux, Ph.D; Thesis Advisor.
Steve Crews, Ph.D; Committee Chair.
Eva Anton, Ph.D.
Mohanish Deshmukh, Ph.D.
Larysa Pevny, Ph.D.

©2008
Ashton Winfield Powell
ALL RIGHTS RESERVED

ABSTRACT

Ashton Winfield Powell

Molecular Mechanisms Specifying the Topography of Thalamocortical Projections in the Ventral Telencephalon

(Under the direction of Franck Polleux, Ph.D.)

The topographic projection of each thalamic nucleus to a unique set of cortical areas underlies the input specificity characterizing each sensory modality. Although the importance of the patterning of thalamic projections for normal cortical function has long been appreciated, the underlying developmental mechanisms remain largely unknown. The aim of my thesis was to identify some of the cellular and molecular cues patterning thalamocortical projections. First, I developed a novel technique to quantitatively study the topography of thalamocortical axons *in vivo*. Second, I showed that a single gradient of Netrin-1 controls the rostro-caudal topography of thalamocortical axons inside the ventral telencephalon through both attractive and repulsive mechanisms. Third, I confirm that an interaction between corticofugal and thalamic axons inside the VTel acts as a topographic cue for caudal thalamic axons, thus providing the first experimental evidence of the 'handshake hypothesis.'

Solace comes from a comforted heart.
Home is where I find you.
I will love you always,
My Jacqueline

ACKNOWLEDGEMENTS

Mohanish Deshmukh, Eva Anton, Larysa Pevny, Steve Crews, Patricia Maness, Vytas Bankaitis

Lisa Plummer, Dante Bortone, Paul Barnes, Beth Boutte, Takayuki Sassa, Yonqin Wu

Randal Hand, Sabrice Guerrier, Eldon Peters, Rocky Cheung

Amanda Wright, Malika Boukhelifa, Galina Demyanenko

Brent Jones, Gordon Carr, Scott Hutton, Lorelei Taylor, Stacy Foti,

Bruce Herzer, Yukako Yokota, Julie & Brandon Williams

Franny & Bryce, Kathy & Wyman

Brandon, Kari, Decker, Hunter

Mike and Dorothy Blumenthal

Mom, Dad, Diane

Becky

Earl

Franck

Jacqueline de Marchena Powell

TABLE OF CONTENTS

LIST OF FIGURES

Figure

LIST OF ABBREVIATIONS

BDA - Biotinylated-Dextran Amine

CF - Corticofugal

CFA - Corticofugal Axon

CSB - Cortico-Striatal Boundary

DIV - Days *in vitro*

DTel - Dorsal Telencephalon

DTC - Dorsal Thalamus - Caudal Third

DTM - Dorsal Thalamus – Medial Third

DTR - Dorsal Thalamus – Rostral Third

DTh - Dorsal Thalamus

GE - Ganglionic Eminence

LGE - Lateral Ganglionic Eminence

MGE - Medial Ganglionic Eminence

TC - Thalamocortical

TCA - Thalamocortical Axon

VTel - Ventral Telencephalon

VTh - Ventral Thalamus

CHAPTER ONE

Introduction

The functional properties of each structure in the central nervous system are critically dependent on the precision of neuronal connectivity. As each system integrates information from multiple inputs, the segregation of sensory information into functionally distinct processing streams is thought to provide the basis for behavioral responses.

In particular, the cerebral cortex is a highly organized structure defined by both the cytoarchitectural organization in the radial dimension and the efferent and afferent connections in the tangential dimension. The connectivity defines the information send to and from a cortical area while the cytoarchitecture defines how the information is processed. Cortical areas process motor and sensory information as well as higher cognitive functions such as speech.

The thalamus is a symmetric cluster of nuclei located at the midline of the brain along the 3rd ventricle in mammals. All sensory inputs other than olfaction are relayed through the thalamus and project topographically to the cortex. Thalamic nuclei relay specific sensory information (visual, auditory, somatosensory) from the periphery to specific cortical areas (Pallas 2001; Sur and Leamey 2001; O'Leary and Nakagawa 2002; Grove and Fukuchi-Shimogori 2003; Lopez-Bendito and Molnar 2003). Thalamic axons project through one of the most dense axon tracts of the brain, the *internal capsule*, a collection of axons comprising reciprocal projections between the thalamus and cortex as well as all other corticofugal and corticopetal projections.

The separation of projections from each sensory nucleus to distinct cortical areas establishes an initial level of topography in thalamocortical connectivity, also referred to as *inter-areal* specificity. This separation allows the brain to organize and specialize by function according to the

information processed. A second level of organization, referred to as *intra-areal* topography, defines the topographic projection of a single thalamic nucleus within a given cortical area. This separation of input among a single modality creates a central topographic representation of the sensory periphery. The topographic organization of TCA establishes a spatial representation of the peripheral sensory apparatus in the cortex for each sensory modality. The combination of these two levels of topographic projections defines the organizational strategy of the central nervous system.

While the importance of the topography of thalamic projections for normal cortical function has long been appreciated, the developmental mechanisms underlying its establishment remain largely unknown. The focus of this thesis is to identify some of the molecular mechanisms regulating the establishment of *inter-areal* TCA topography.

This thesis will first review some of the molecular mechanisms known to underlie the establishment of the topography of axonal projections in the main model system use to study this question: the retino-tectal projections. This will be followed by an introduction of the current knowledge about the spatial and temporal aspects of thalamocortical development and a review of the developmental mechanisms proposed to control the establishment of TC projections. Finally, this thesis will introduce the specific hypotheses that underlie my doctoral studies on the cellular and molecular mechanisms patterning thalamocortical projections in the ventral telencephalon.

Anatomical development of thalamocortical projections in the mouse

Mouse dorsal thalamic neurons are generated along the ventricular zone of the 3rd ventricle between E10.5 and E13.5 (Angevine 1970). Beginning around E13.5, pioneering axons are directed towards the junction between the diencephalon (thalamus) and ventral telencephalon (VTel), forming the thalamic eminence (**Figure 1A**). The VTel matures into the basal ganglia and striatum and is also the source of most cortical interneurons (Anderson et al. 1997b; Zhu et al. 1999). Upon entering the ventral telencephalon, the growth cones of thalamic axons encounter a diverse and dynamic structure of extracellular matrix, migrating cells and axons.

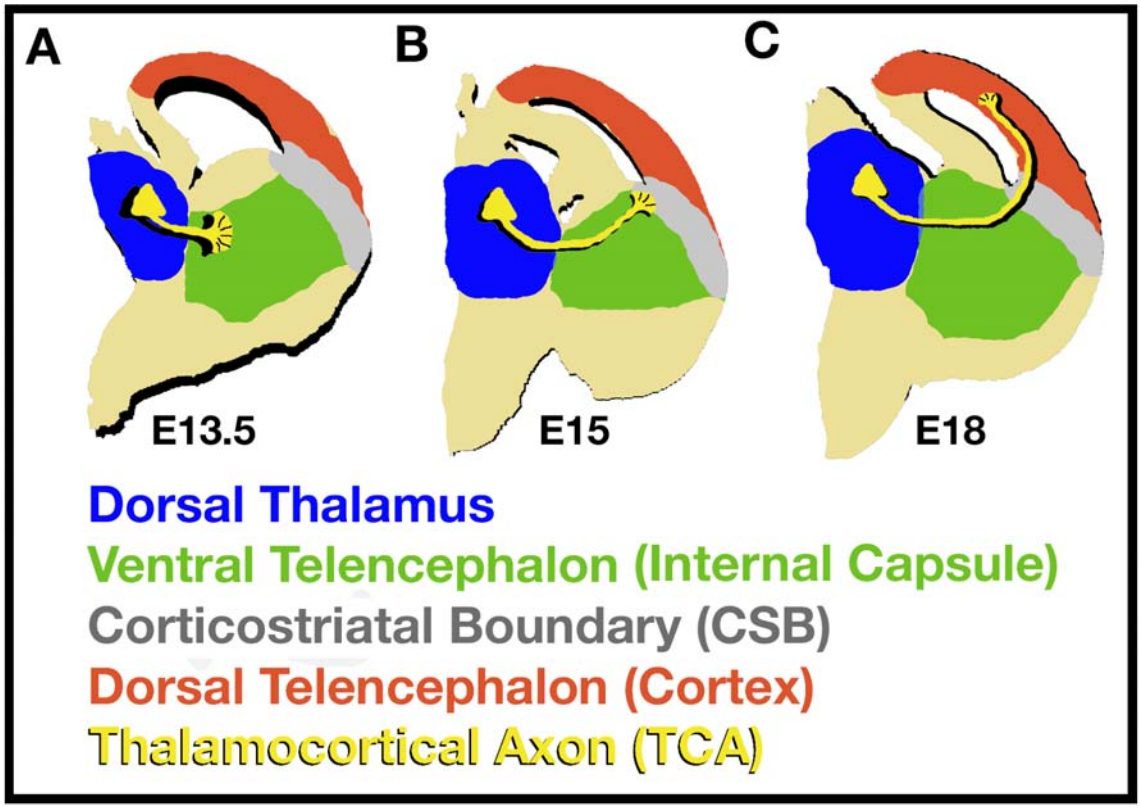

Figure 1. The developmental progression of Thalamocortical axons.

Thalamic neurons projecting axons to the cortex pioneer great distances and complex environments over the course of development.
(**A**) The axons of thalamic neurons (Yellow, TCA) begin leaving the dorsal thalamus (Blue, DTh) at E13.5, entering the ventral telencephalon (Green, VTel).

(**B**) For the next few days, TCA extend through the VTel, encountering a complex environment containing extracellular matrices, axon guidance molecules, migrating cells, and axons from distant regions. TCA extend through the entire rostro-caudal extent of the VTel, a structure almost 2cm long. By E15, most TCA have begun to reach the junction between their intermediate target, the VTel, and their final target the cortex or dorsal telencephalon (Red, DTel). This junction, the cortico-striatal boundary or pallial-subpallial boundary (Grey, CSB or PSPB), separates the VTel and the DTel, genetically distinct regions that form the basal ganglia and cortex respectively in the adult. The specific targeting established by TCA at this point is *inter-areal* topography.

(**C**) By E18, TCA have crossed the CSB and grow dorsally into the intermediate zone of the cortical they will eventually innervate. From this point until postnatal day 7 (P7) TCA will interact with the immature cortex, refining their trajectory inside the DTel. The targeting established by TCA upon crossing the CSB is *intra-areal* topography.

The thalamic growth cones then extend through the VTel, forming the internal capsule, eventually reaching the junction between the ventral and dorsal telencephalon beginning at E13.5 in the mouse (**Figure 1B**) (Bicknese et al. 1994; Molnar and Blakemore 1995a; Molnar et al. 1998a).

Once TC axons cross from the VTel into the dorsal telencephalon (a boundary referred to as cortico-striatal boundary or CSB in the rest of the text), they diverge from their previous trajectory and make a 90° turn dorsally into the intermediate zone of the immature cortex (**Figure 1C**). From E14.5 to E15.5, TCA extend to their general target cortical areas were they interact with subplate neurons and innervate deep layers VIa and V over the course of several days (Agmon et al. 1993; Kageyama and Robertson 1993), which are not their final target. At this point, inter-areal specificity has been established, and during the first postnatal days, thalamic afferents selectively branch and hone their connections with the newly differentiated layer IV neurons (Angevine 1970; Bolz et al. 1992). This period is referred to as the 'waiting period' and varies in duration for different species according to differences in the arrival time of thalamocortical axons to the subplate and the relative birth date of the thalamic neuron (Kostovic and Rakic 1990; Ghosh and Shatz 1992, 1993; Molnar et al. 1998a).

In rodents, inter-areal segregation occurs prenatally, while intra-areal topography is thought to occur postnatally (Lopez-Bendito and Molnar 2003). Until recently, the only molecular cue shown to influence the inter-areal topography of TCA has been ephrin-A5, which is expressed in a high-caudal to low-rostral gradient in the VTel (Gao et al. 1998; Dufour et al. 2003). Initial studies showed that rat TCA grown over ephrinA5 expressing NIH 3T3 cells have a shorter neurite length than control cells, a result that can be proportionally attenuated through increasing concentration of EphA3-Fc in the media (Gao et al. 1998). More recent studies, which will be described in more detail later, showed that EphA4 receptors expressed in a high-rostral to low-caudal gradient in the DTh, contribute to TCA topography by regulating repulsion of rostral TCA to the caudal VTel which expresses high levels of ephrin-A5 (Dufour et al. 2003). Interestingly, the topography of TCA projections is not completely abolished in the ephrinA5-EphA4 double knockout mice, suggesting

that other axon guidance cues work in concert with ephrinA5-EphA4 to establish topography. This cooperativity of different types axon guidance ligand/receptor compliments as mediators of topography has been described in the retino-tectal system from work showing that the medio-lateral projections of retinal ganglion cells (RGC) to the optic tectum is controlled by a coordinated response to ephrinBs (acting on EphBs tyrosine kinase receptors) and Wnt (acting on Ryk tyrosine kinase receptor) (Schmitt et al. 2006).

Basic topography of thalamocortical connectivity

Anatomical studies have shown that the basic topography of thalamic afferents to the mammalian cortex crudely corresponds to cell body position in the thalamus along both the rostral to caudal (R-C) and medial to lateral (M-L) axes (Caviness and Frost 1980; Crandall and Caviness 1984; Hohl-Abrahao and Creutzfeldt 1991). When each axis is addressed individually, the relative rostral to caudal position of neurons within the dorsal thalamus is a good predictor of the rostro-caudal position of the cortical area innervated (**Figure 2**). For example, the R-C axis can be demonstrated by comparing axons originating from the Ventrolateral nucleus (VL), Ventrobasal nucleus (VB), and dorsolateral geniculate (dLGN). All nuclei are spread along the R-C axis of the thalamus and innervate cortical sensory regions (M1, S1, and V1) along the R-C axis of the cortex respectively. Along the M-L axis, comparing the MD, VB, and dLGN gives a similar R-C segregation in the cortex. Together the axis of projection of thalamic neurons onto the cortex can be defined as rostral-medial to caudal-lateral (**Figure 2A & B**) (Caviness and Frost 1980; Crandall and Caviness 1984). This general axis of topography does not hold for all thalamic neurons, as associative thalamic nuclei project to the cortex in a diffuse manner (Jones 2001). This topography is well conserved in mammals, and is specifically maintained in rodents, carnivores and non-human primates (Hohl-Abrahao and Creutzfeldt 1991).

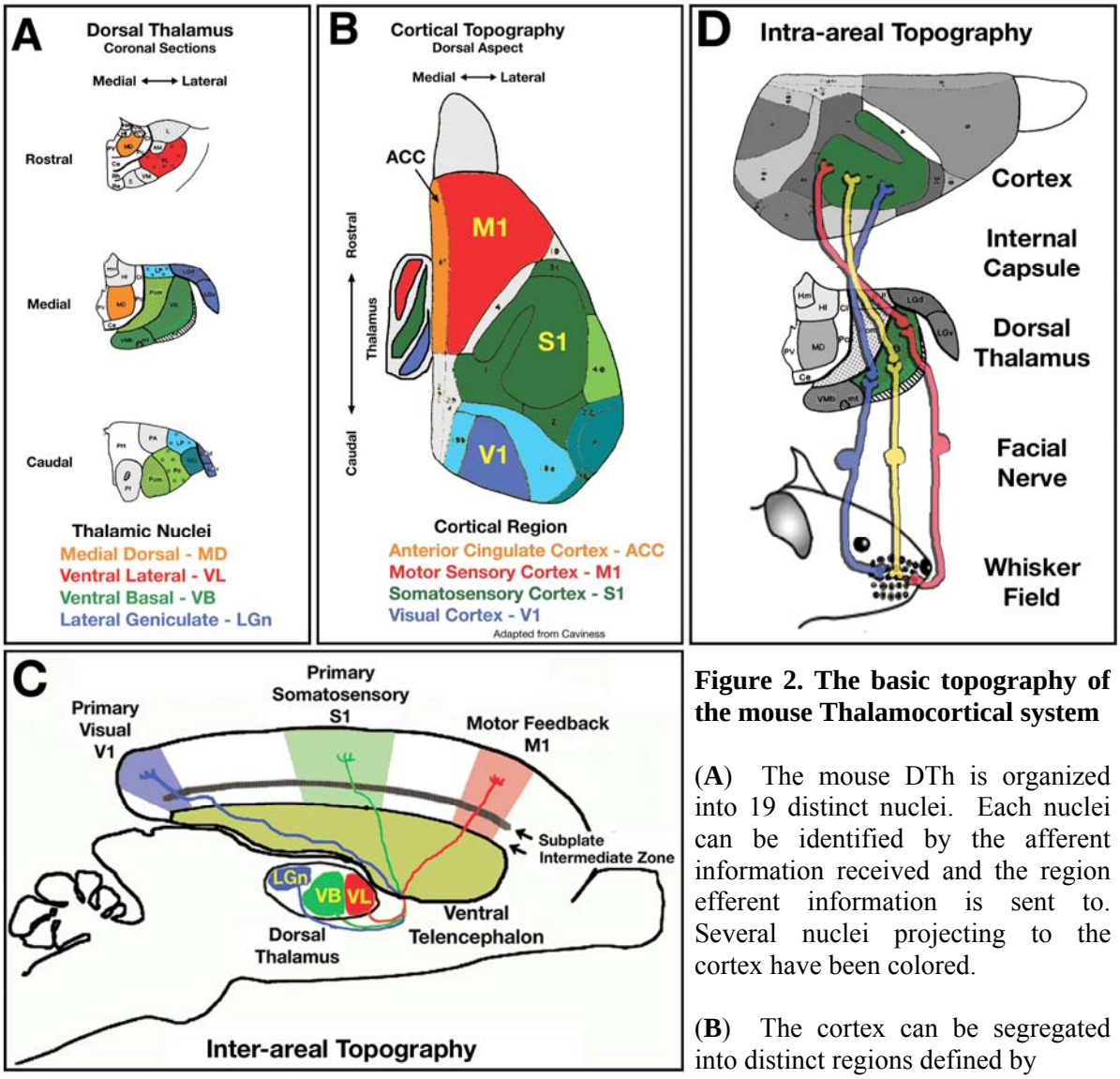

Figure 2. The basic topography of the mouse Thalamocortical system

(**A**) The mouse DTh is organized into 19 distinct nuclei. Each nuclei can be identified by the afferent information received and the region efferent information is sent to. Several nuclei projecting to the cortex have been colored.

(**B**) The cortex can be segregated into distinct regions defined by cyto- architecture, information processed, and the origin of innervating afferent processes. Several cortical regions have been colored to match the thalamic nucleus innervating them. The basic topography of thalamocortical input along the rostro-caudal axis of the cortex correlates with the rostro-medial to caudo-lateral organization of the DTh.

(**C**) *Inter-areal* topography refers to the segregation of thalamic input of the cortex by different thalamic nuclei to distinct cortical regions. This primarily occurs inside the VTel, and is a major determinant for the segregation of cortical regions by functionality.

(**D**) *Intra-areal* topography refers to the organization of input inside a given cortical region. This can be described by a sensory modality like the mouse barrel field, where the innervation of the cortex by the VB creates a physical representation of the sensory apparatus that maintains the spatial relationship of one whisker to another. This topography is refined inside the cortex after *inter-areal* topography has been established.

Mechanisms establishing the inter-areal topography of thalamocortical projections

The role of cortical cues in TCA topography

The topography of TCA projections is developmentally linked to the arealization of the cerebral cortex since the function of individual cortical areas is largely dependent on their afferent and efferent connectivity. This has been well demonstrated in the ferret using experiments where thalamic axons have been re-routed to disparate cortical regions during development (Sur et al. 1988). Interestingly, cortical regions innervated by multiple sensory modalities respond to both their endogenous and experimental sensory stimuli demonstrating that cortical responsiveness is largely dependent on thalamocortical input.

As mentioned previously, cortical areas innervated by the thalamus contain a second level of TCA organization, intra-areal topography, which establishes a physical map of the sensory periphery underlying specific receptive fields for a given modality. The establishment of inter-areal topography occurs during embryonic development in rodents and is generally thought to be activity-independent (Crandall and Caviness 1984; Molnar et al. 1998a; Lopez-Bendito and Molnar 2003). On the other hand, intra-areal topography occurs during early postnatal periods and involves axon guidance mediated and refinement by activity-dependent mechanisms (Monuki and Walsh 2001; Pallas 2001; Ruiz i Altaba et al. 2001; Sur and Leamey 2001; O'Leary and Nakagawa 2002).

In an attempt to address the ability of cortical area-specific cues to regulate the inter-areal specificity of TCA projections, early studies have shown that axons extending from dissected thalamic nuclei fail to differentiate between explants of target or non-target cortical areas *in vitro* (Molnar and Blakemore 1991). These results suggest that either (i) there are no area-specific cortical cues, or (ii) TCA do not respond to cortically derived cues in this in vitro assay, perhaps because they cannot respond to these cues unless they have traversed the intermediate target; a maturation process

similar to that of commissural axons before and after crossing the midline (Flanagan and Van Vactor 1998; Shirasaki et al. 1998).

Whether initial TCA targeting is dependent on cortical identity can be addressed through the timing of thalamic innervation and cortical arealization. There is *in vivo* evidence that the cortex contains intrinsic molecular cues responsible for arealization of the cortex and that this regionalization occurs earlier than and independently of TCA innervation (Miyashita-Lin et al. 1999; Nakagawa et al. 1999; O'Leary and Nakagawa 2002; Grove and Fukuchi-Shimogori 2003). However, regionalized cortical cues have been shown to be involved in establishing intra-areal TCA targeting (Vanderhaeghen et al. 2000; Dufour et al. 2003) and regulating cortical area identity (Bishop et al. 2000; Mallamaci et al. 2000; Zhou et al. 2001), suggesting that these intrinsic cues may act to control inter-areal TCA topography. Until now, no axon guidance cues have been demonstrated to regulate inter-areal specificity of TCA inside of the cortex, enabling them to differentiate between adjacent cortical areas.

The proper patterning of cortical regions, either through regionalized morphogen or transcription factor expression, is required for establishing proper TCA projections (Bishop et al. 2000; Mallamaci et al. 2000; Fukuchi-Shimogori and Grove 2001). Data supporting the role of intrinsic cortical cues that TCA patterning inside the Vtel come from studies of COUP-TFI and Emx2 mutant mice, each of which have caudalized TCA growth inside the VTel correlating to a caudalization of cortical arealization (Bishop et al. 2000; Mallamaci et al. 2000; Zhou et al. 2001).

One morphogen, Fgf8 has been well established as a determinant in the specification of rostral cortical identity (Fukuchi-Shimogori and Grove 2001, 2003; Garel et al. 2003). Despite a prominent role in establishing the cortical protomap, the FGF8 hypomorph, which has a shift in early cortical markers, does not exhibit a deficit in embryonic TCA topography (**Figure 3A & B**) (Garel et al. 2003) reinforcing the concept that the initial topography of TCA projections is at least initially partially independent of the exact position of target cortical areas.

Studies by Grove et al (Fukuchi-Shimogori and Grove 2001; Shimogori and Grove 2005) utilized in utero electroporation to misexpress Fgf8 into caudal regions of the cortical primordium (**Figure 3C**). The effect is a rearrangement of the cortical area map and the formation of a second barrel field (S1) in the caudal cortex. Interestingly, there are significant differences in cortical patterning based upon the timing of the experiment. Specifically performing the experiment at either E10 or E11.5, Fgf8 misexpression has been shown to affect patterning of layer 6b neurons only (E10) or both layer 6b (subplate) and layer 6a neurons (E11.5). At E10, caudal Fgf8 expression caudalizes the expression of rostral markers in both the subplate and cortical plate. Tracing experiments show that TCA axons recognize this shift, innervating the ectopic S1 from the VB nucleus. At E11.5, Fgf8 misexpression creates an alteration of rostral projections only in the cortical plate; the subplate retains the patterning found in control experiments. Interestingly, this out of register, ectopic barrel cortex is similarly capable of being innervated by VB axons. In both cases, TCA reach the CSB with unaltered trajectories compared to control experiments and but deviate from control trajectories upon entering the cortex. In sum, while thalamic projections are sensitive to changes in the cortical area map, alterations of cortical identity have more effect on establishing intra-areal topography in the cortex than inter-areal topography in the VTel. Interestingly, when tracing are done at birth (P1), no inter-areal shifts can be detected. However, a week later (P7) some axons from the presumptive VB project to the caudal ectopic S1, reinforcing the model whereby the initial topography of TCA projections are influenced by extra-cortical cues in ventral telencephalon and the existence of cortical-area specific cues that act postnatally (**Figure 3D**).

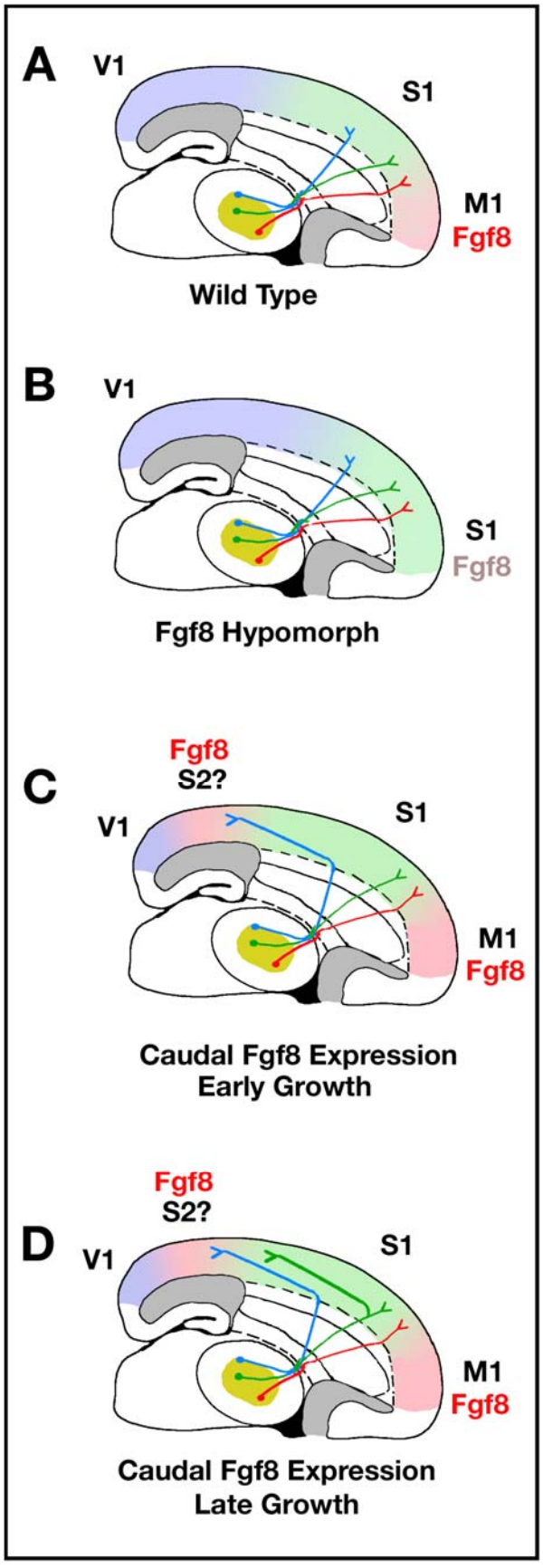

Figure 3. The role of cortical identity in determining TCA topography

(**A**) The morphogen Fgf8 is critical in determining rostral cortical identity. Rostral expression of Fgf8 is necessary for establishing early cortical markers and the boundary between the primary motor and sensory cortices (M1 and S1). Innervation of the cortex by the primary somatosensory nucleus, VB is limited to S1.

(**B**) The early cortical organization of the Fgf8 hypomorph lacks a true M1, with markers for S1 extending more rostrally than in wild-type mice. The innervation of VB however does not extend into the new rostral S1.

(**C**) Misexpression of Fgf8 into the caudal cortex via electroporation creates an ectopic M1 in the caudal cortex. Early tracing studies (P1) show little innervation of this ectopic M1 by the VB.

(**D**) Late tracing studies (P7) of these mice show a significant innervation by the VB, however the projection of these axons inside the VTel appears unaltered.

The role of transcription factors patterning the ventral telencephalon in the topography of TC projections.

For some time, it was thought that the VTel simply provided a permissive, growth promoting intermediate target for TCA to grow through (Metin and Godement 1996). However, results from axon tracing studies suggested that TC axons were first sorted to different cortical domains in the ventral telencephalon (Molnar et al. 1998a; Seibt et al. 2003), strongly suggesting that the VTel contains some axon guidance cues that guide different sub-populations of TC axons mainly along the rostro-caudal axis. However, the identity of these cues remained elusive for many years. If indeed TCA axons have already established topography before reaching the dorsal telencephalon, then the VTel is likely to contain axon guidance cues important for this sorting.

The VTel provides thalamocortical growth cones with a variety of contact-mediated and secreted axon guidance cues that regulate their trajectory to the cortex. During early stages, TCA are deflected from the ventral thalamus and out of the thalamus into the VTel by attractive or outgrowth–promoting cues originating from the mantle region of the VTel combined with a repulsive cue originating from the prethalamus (also called ventral thalamus) (Metin and Godement 1996; Molnar et al. 1998a; Braisted et al. 1999; Tuttle et al. 1999; Braisted et al. 2000). At this point TCA make first contact with the VTel (Metin and Godement 1996; Richards et al. 1997; Molnar and Cordery 1999; Braisted et al. 2000).

Several mutant mice for transcription factors expressed in the VTel such as Ebf1 or Dlx1/2 show pronounced TC axon guidance defects at this level (**Figure 4A**) (Porteus et al. 1994; Anderson et al. 1997a; Casarosa et al. 1999; Garel et al. 1999; Pleasure et al. 2000). The role of the VTel as an intermediate target for TCA patterning was first suggested in Ebf1 mutant mice characterized by abnormal VTel development, which has an effect on the topography of TCA (Garel et al. 2002). Ebf1, an atypical bHLH transcription factor, is expressed in the caudal and lateral GE and controls the

development of striatal neurons. Tracing experiments in Ebf1 mutants show globally caudalized TCA inside the VTel that are not accompanied by changes in either the early outgrowth of CFA or the patterning of gene expression in the cortex and thalamus (**Figure 4B**) (Garel et al. 2002). Unfortunately, the downstream targets genes regulated by this transcription factor and how they interact with TCA has yet to be established. Importantly, Ebf1 is also expressed in both the marginal zone of the cortex and the dorsal thalamus at E14.5, leaving interpretation of TCA phenotypes difficult (Garel et al. 1999).

Dlx1 and Dlx2 are homeobox domain transcription factors that control GABAergic interneuron differentiation in the VTel, although it is also expressed in the ventral thalamus (Anderson et al. 1997c). Dlx1/2 double mutant mice contains two populations of TC axons, one with stalled growth inside the VTel and one that that reaches the cortex in a caudalized trajectory (**Figure 4C**). Considering the cortex and dorsal thalamus do not express either Dlx1 or Dlx2, these results provide more conclusive evidence that the VTel has a cell-non autonomous effect on topographic TCA growth (Garel et al. 2002). It should be noted that expression in the ventral thalamus might inhibit TCA entry *into* the VTel as well. Like the Ebf1 mutant mouse, the downstream target genes of Dlx1/2 and their interactions with TCA are not yet known.

It is likely that the thalamocortical phenotypes described in these mutants are cell non-autonomous, due to a disruption in the patterning of the VTel itself and subsequent expression of axon guidance cues (Casarosa et al. 1999; Garel et al. 1999; Tuttle et al. 1999; Garel et al. 2002; Marin et al. 2002). However, these genes are also expressed in the ventral and dorsal thalamus, which may perturb TCA outgrowth before they reach the VTel.

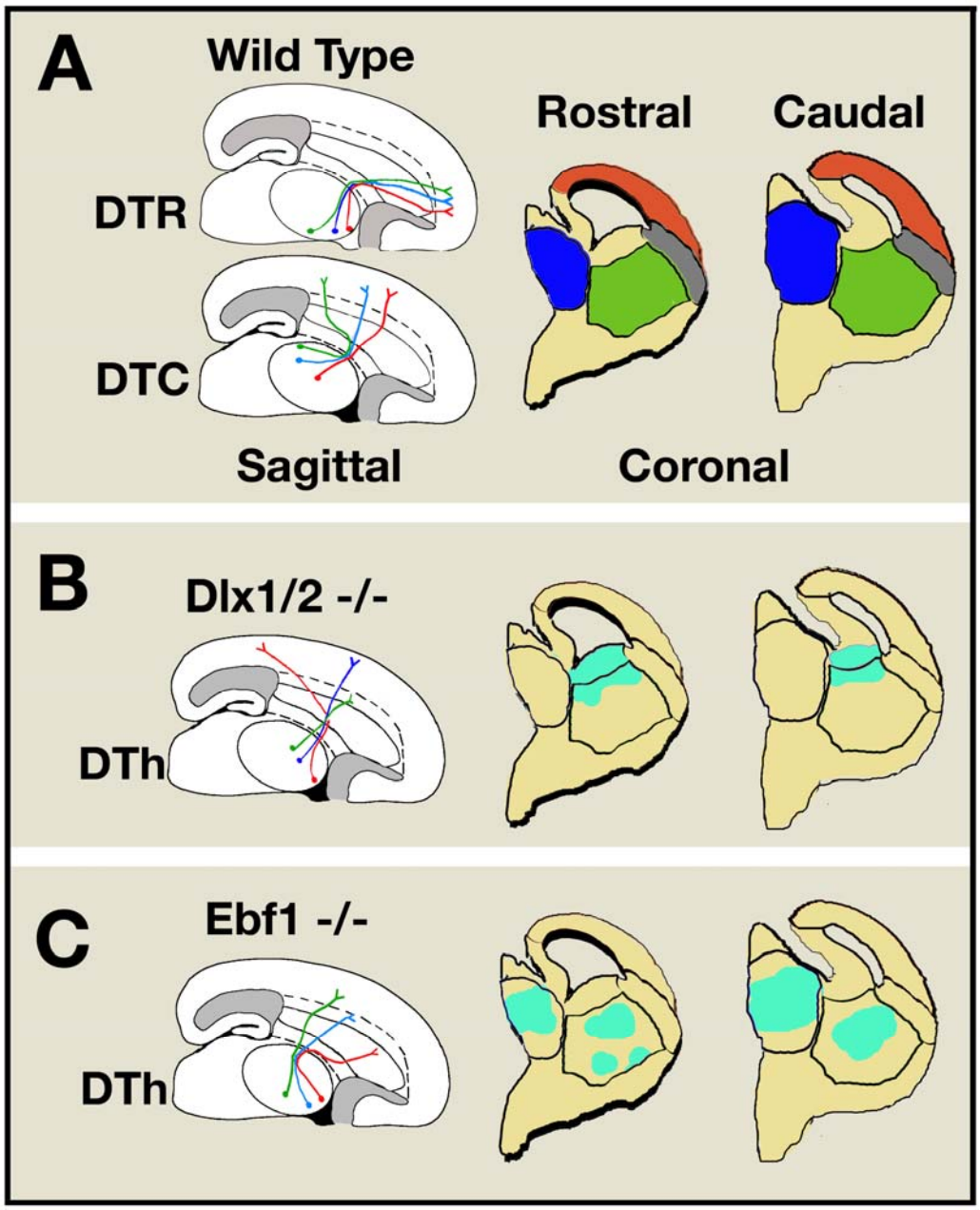

Figure 4. Ventral telencephalic transcription factors involved in establishing TCA topography

(**A**) Wild-type projections schematized on a sagittal section. DTR axons project to the rostral cortex and DTC axons project to the caudal cortex. Coronal schemas are used to depict the expression patterns of transcription factors in rostral and caudal regions.

(**B**) Dlx1/2 are expressed in the mantle region of the VTel. Tracing experiments in Dlx1/2 -/- mice show a pronounced caudalization of DTR axons.

(**C**) Ebf1 is expressed in caudal and lateral regions of the VTel, but is also expressed in the DTh, making interpretation of TCA guidance deficits in mutant mice difficult. Tracing experiments in Ebf1 -/- mice show severe caudalization of TCA inside the VTel.

Molecular mechanism establishing the topography of retino-tectal projections: a model system

Retinal ganglion cells (RGCs) project topographically to three main targets in the mammalian visual system: the dorsal part of the lateral geniculate nucleus (dLGN), the pretectum and the optic tectum (superior colliculus). Two features of RGC axon projections have been intensively studied. First, RGC axons leaving the retina have the choice of whether to cross the midline at the level of the optic chiasm. Second, axons originating along the dorso-ventral and naso-temporal axes of the retina project topographically along the antero-posterior and medio-lateral axes, respectively, of their final targets. These two features of RGC axon projection underlie binocular vision and the retinotopic representation of visual space, respectively.

Control of Retinal Ganglion Cell midline crossing.

Recent studies indicate that the axon guidance choice made by RGC axons at the optic chiasm is determined by the expression of transcription factors (Herrera et al. 2003; Pak et al. 2004). The zinc-finger transcription facto Zic2 is specifically expressed in the ventro-temporal part of the retina that contains RGCs that project axons ipsilaterally, rather than crossing the midline (Nagai et al. 1997; Herrera et al. 2003). Interestingly, Zic2 is expressed by these RGCs before their axons reach the midline but is down-regulated soon after their axons cross the optic chiasm (Herrera et al. 2003). Mice with reduced expression of Zic2 (Zic2 knockdown or $Zic2^{KD/KD}$) have abnormal eye development (Nagai et al. 2000) as well as malformations of the ventral diencephalon, including altered expression of axon guidance molecules that are known to control axon crossing at the optic chiasm, such as ephrin-B2. Heterozygous $Zic2^{KD/+}$ mice were compared with with $Zic2^{KD/KD}$ homozygous and wild-type littermates, revealing a direct correlation between the level of Zic2 expression in RGCs and the proportion of axons that projected ipsilaterally. This suggests that the

expression of Zic2 might drive the decision to project ipsilaterally. Furthermore, over-expression of Zic2 in dorsal RGCs was sufficient to make their axons sensitive to midline repulsive cues, an effect that required the presence of an intact DNA-binding domain in Zic2 (Herrera et al. 2003). These results show that Zic2 has an instructive role in the responsiveness of RGC axons to midline repulsive cues at the optic chiasm

One of the most likely candidate molecules to mediate the effects of Zic2 at the optic chiasm is the ephrin-B receptor EphB1, which is specifically expressed in the ventrotemporal retina, where Zic2 is expressed, and has been shown to help to prevent axon crossing at the optic chiasm (Williams et al. 2003). However, whether Zic2 controls EphB1 expression directly or instead specifies ipsilateral RGC projections in an EphB1-independent manner remains to be determined. The percentage of RGCs that project ipsilaterally at the optic chiasm correlates with the degree of binocularity in different species, ranging from 40% in humans to 15% in ferrets and only 3-5% in rodents. There is also a strong correlation between the number of Zic2-expressing RGCs in the ventrotemporal retina and the increasing degree of binocularity in ferrets, mice, *Xenopus* and chicks (Herrera et al. 2003). What regulates the number of neurons that express Zic2 in the ventrotemporal retina? A recent study shows that the LIM-homeodomain transcription factor Islet2 (Isl-2) is expressed in almost all RGCs except those in the ventrotemporal retina and might inhibit Zic2 expression (Pak et al. 2004). Interestingly, some Isl2+ RGCs are found in the ventrotemporal retina, but these are clearly distinct from RGCs that express Zic2 and EphB1. *Isl2* knockout mice have increased numbers of axons projecting ipsilaterally from RGCs located in or close to the ventrotemporal retina. The ventrotemporal retina of these mice contains more RGCs that co-express Zic2 and EphB1. These results suggest that, in ventro-temporal RGCs, Isl2 represses the expression of Zic2 and EphB1 and therefore represses the genetic program that underlies binocularity (Pak et al. 2004).

Specification of retinal ganglion cell topography on the tectum.

Analysis of the projection of RGC axons to the optic tectum (retinotectal projections) has led to important insights into the establishment of topographic maps (Flanagan and Vanderhaeghen 1998). Importantly, the graded expression of EphA receptors in RGCs along the naso-temporal axis of the retina is crucial for the establishment of the topography of axon projection along the antero-posterior axis of the tectum, whereas graded EphB receptor expression along the dorso-ventral axis of the retina confers on RGC axons the ability to project topographically along the latero-medial axis of the developing tectum (McLaughlin et al. 2003) (**Figure 5**).

The graded expression of EphA and EphB receptors appears to be regulated by homeobox transcription factors. The homeobox gene Vax2 is expressed in a ventral-high to dorsal-low gradient in the retina, and both misexpression experiments in mice and chicks (Schulte et al. 1999) and genetic loss-of-function studies in mice (Mui et al. 2002) point to a role for Vax2 in patterning the expression of EphA5, EphB2-B3 and ephrin-B1-B2 along the dorso-ventral axis of the retina (**Figure 5B**). Retinotectal axons are misrouted in Vax2-knockout mice along the medio-lateral axis of the tectum, supporting the idea that Vax2 helps to specify the projection patterns of RGCs (Barbieri et al. 2002).

Tbx5 is a T-box transcription factor that is expressed in a dorsal-high to caudal-low gradient in the retina, and has been shown to repress expression of Pax2 and Vax2 in the dorsal half of the retina (Koshiba-Takeuchi et al. 2000). Misexpression of Tbx5 is sufficient to induce the expression of ephrinB1 and B2 in the ventral half of the retina, leading to misprojection of RGC axons in the tectum. This supports a model in which patterning of Tbx5, Pax2 and Vax2 along the dorso-ventral axis of the retina, which is possibly regulated by a combination of bone morphogenetic protein (BMP) and retinoic acid signaling (Wagner et al. 2000; Sakuta et al. 2001; Zhao et al. 2002; Lupo et al. 2005; Sen et al. 2005), leads to the patterning of ephrinB-EphB expression that specifies RGC axon projections along the latero-medial axis of the tectum (Mann et al. 2002).

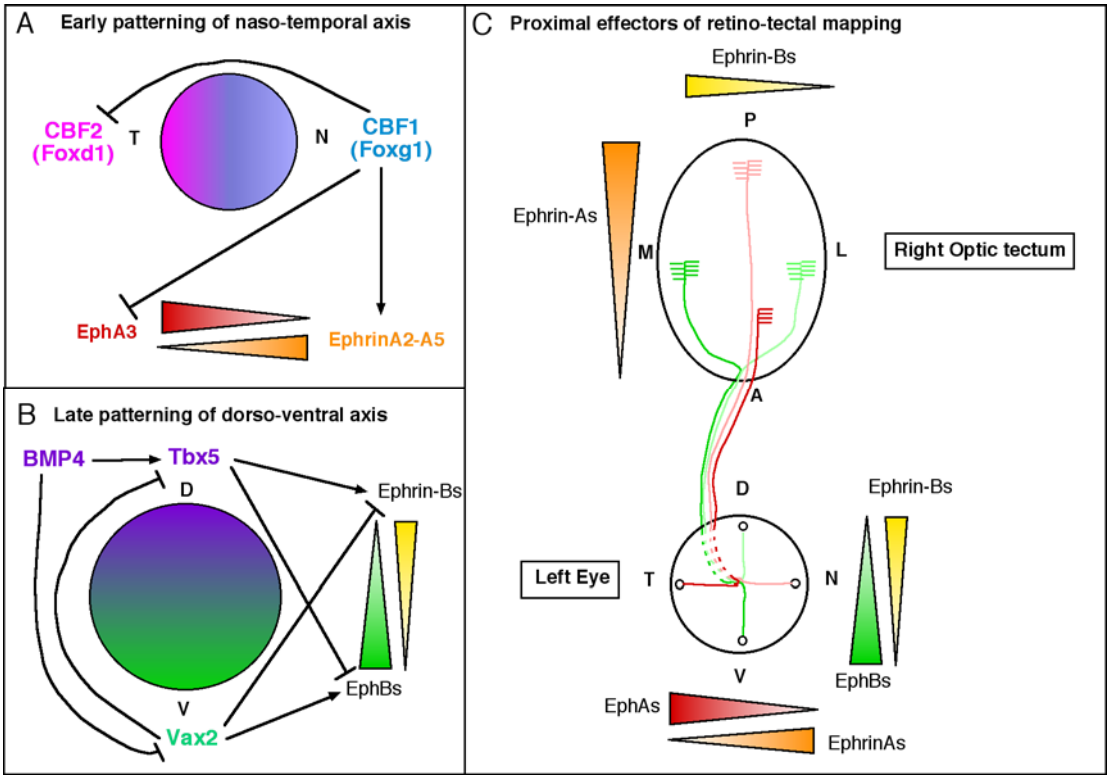

Figure 5. Transcriptional regulation of the topography of retino-tectal projections.

(**A**) Early patterning of the naso-temporal axis of the retina. Two Forkhead-transcription factors called Foxg1 (CBF1 in chick) and Foxd1 (CBF2 in chick) are expressed in complementary patterns in the nasal and temporal retina respectively. Using misexpression studies, CBF1 has been suggested to repress CBF1 and EphA3 receptor expression but induce ephrinA2-A5 ligands expression in the nasal retina

(**B**) Late patterning of the dorso-ventral axis of the retina. Two transcription factors (Tbx5 and Vax2) are expressed in complementary patterns in the dorsal and ventral part of the retina. BMP4 has been proposed to induce Tbx5 expression in the dorsal retina. Tbx5 and Vax2 repress each other's expression. Tbx5 represses the expression of EphB receptors but induces expression of EphrinB ligands in the dorsal retina. Conversely, Vax2 induces EphB receptor expression but represses EphrinBs expression in the ventral retina.

(**C**) Ephrin/Eph signaling in the patterning of retino-tectal projections. The topography of retino-tectal projections is largely determined by EphA receptor expression which determines the projections along the low-anterior and high-posterior gradient of ephrinA2-A5 of the tectum and by EphB receptors which determine the projection along the high-medial to low-lateral gradient of Eph of the body wall.

Adapted from Polleux, et al Nature Reviews Neuroscience (2007).

In chicks, the winged-helix transcription factors CBF1 and CBF2 (orthologs of Foxg1 and Foxd1, respectively, in the mouse and human) are enriched in the nasal and temporal retina respectively, and misexpression of CBF1 in the temporal retina results in misprojection of axons along the anterior-posterior axis of the tectum (Yuasa et al. 1996) (**Figure 5A**). Recent misexpression studies have shown that CBF1 represses CBF2 and EphA3 expression and induces the expression of ephrinA2-A5 (Takahashi et al. 2003).

Interestingly, mice lacking Foxd1 and Foxg1 show deficits earlier in the visual projection pathway, at the level of the optic chiasm (Herrera et al. 2004; Pratt et al. 2004). In Foxd1-knockout mice, RGCs in the ventrotemporal retina, which normally project axons ipsilaterally, end up projecting axons contralaterally, probably because they do not respond to chemorepulsive cues at the chiasm (Herrera et al. 2004). Foxg1 is expressed predominantly in the nasal part of the retina as well as in the optic chiasm. Foxg1-knockout mice have an eight-fold increase in the numbers of RGC axons projecting ipsilaterally, a defect that might be due to a mis-patterning of axon guidance cues at the level of the midline in the optic chiasm (Pratt et al. 2004).

Overall, these results indicate that the combinatorial expression of transcription factors along the dorso-ventral and naso-temporal axes of the retina specifies the pattern of expression of ephrins and Eph receptors that underlies the topographic projections of RGC axons to the visual centers. However, many questions remain to be addressed. For example, what are the patterning mechanisms that specify the graded expression of transcription factors along the axes of the developing retina? How are the transcriptional mechanisms that specify binocularity and topography coordinated in RGCs? And are any of these transcriptional mechanisms influenced by activity-dependent mechanisms in the retina, such as the 'retinal waves' that have been shown to influence RGC connectivity? Further investigations will be required to answer these important questions.

If the VTel contains topographic cues for TCAs, then the thalamus is likely to be composed of heterogeneous neuron populations. The rationale for this is that for an axon guidance molecule to segregate axons originating from distinct parts of the thalamus, there must be a differential expression

of axon guidance receptors to distinguish between regions of the VTel. A homogenous thalamus would react uniformly to VTel cues. This logic has been studied in the spinal cord, where cell-autonomous mechanisms controlling axon guidance are determined by the transcription factors expressed at the cell's birth

The role of axon guidance cues and cell-autonomous factors in establishing topography

Knockout mice of members of several axon guidance receptors and ligands families revealed pronounced defects in TCA outgrowth inside the VTel (**Figure 6**). Repulsive axon guidance molecules slit1 and slit2 have been implicated in TCA patterning due to their expression at the midline of the thalamus, hypothalamus, and the proliferative regions of the VTel at E14.5 (Bagri et al. 2002). Two slit receptors, Robo1 and Robo2 are also expressed at the medial aspect and throughout the thalamus respectively during this period as well (**Figure 6A**). Double knockout mice for slit1 and slit2 have drastic axon guidance deficits in TCA, CFA and forebrain midline crossing axons (Bagri et al. 2002).

Another axon guidance receptor that may regulate TCA growth through the VTel is Sema6A, which has been shown to regulate a repulsive response of thalamic axon *in vitro* (Bagnard et al. 1998), and is necessary for proper TCA guidance inside the internal capsule *in vivo* (Leighton et al. 2001). The role of Sema6 has not yet been determined in the development of TCA topography, as TCA deficits in Sema6A-/- have only been described globally with lipophilic tracing (**Figure 6B**).

Neuregulin-1 has also been proposed to interact with TCA through the receptor ErbB4, which is expressed in the dorsal thalamus (Lopez-Bendito et al. 2006). It is hypothesized that LGE neurons migrating medially create a permissive corridor through the mantle region of the VTel required for TCA axons growth (**Figure 6C**). As with the previous axon guidance molecules, the contribution of this interaction to initiating inter-areal topography has not yet been tested.

Additional cues residing in the VTel have shown to induce outgrowth in TCA, specifically netrin-G1 in the lateral GE and hepatocyte growth factor in the medial GE, however the role of these cues in directing TCA growth *in vitro*, or in establishing topography *in vivo* has been established (Lin et al. 2003; Powell et al. 2003).

The only axon guidance molecules conclusively known to be involved in controlling the topographic outgrowth of TCA inside the VTel are from the Eph/ephrin family. The Eph/ephrin family represents contact-mediated axon guidance molecules also shown to be involved in establishing topographic axon patterning in structures like the tectum. In order for these receptor-ligand pairs to be involved in topographic patterning, they must be differentially expressed along the rostro-caudal axis of the VTel and in the dorsal thalamus (**Figure 6D**). From E13-E15 there is a high rostromedial to low caudolateral expression gradient of EphA3, EphA4, and EphA7 inside the dorsal thalamus (Dufour et al. 2003). Interestingly, this pattern does not match the expression described in the early postnatal thalamus, implying a developmental change in ephrin responsiveness upon entering the cortex (Gao et al. 1998; Mackarehtschian et al. 1999; Vanderhaeghen et al. 2000). The patterning of these receptors is complemented by a graded expression of one of their ligand inside the VTel. Ephrin-A5 was a prime candidate as a topographic guidance molecule considering the high caudal to low rostral gradient of expression in the VTel paired with a complimentary graded expression of its receptor, EphA4, along the rostro-medial to caudal-lateral axis of the thalamus (Gao et al. 1998; Prakash et al. 2000). Considering the nature of Ephrin-A5/EphA4 binding is repulsive (Tessier-Lavigne 1995; Orioli and Klein 1997; Xu et al. 1999) it is likely for ephrin-A5 to act as a caudal repulsive cue to rostral thalamic axons. Carbocyanine dye tracing of the Ephrin-A5 mutant thalamocortical system revealed caudalized projections from the rostral thalamus indicating a possible loss of repulsion elicited by Ephrin-A5/EphA4 interactions.

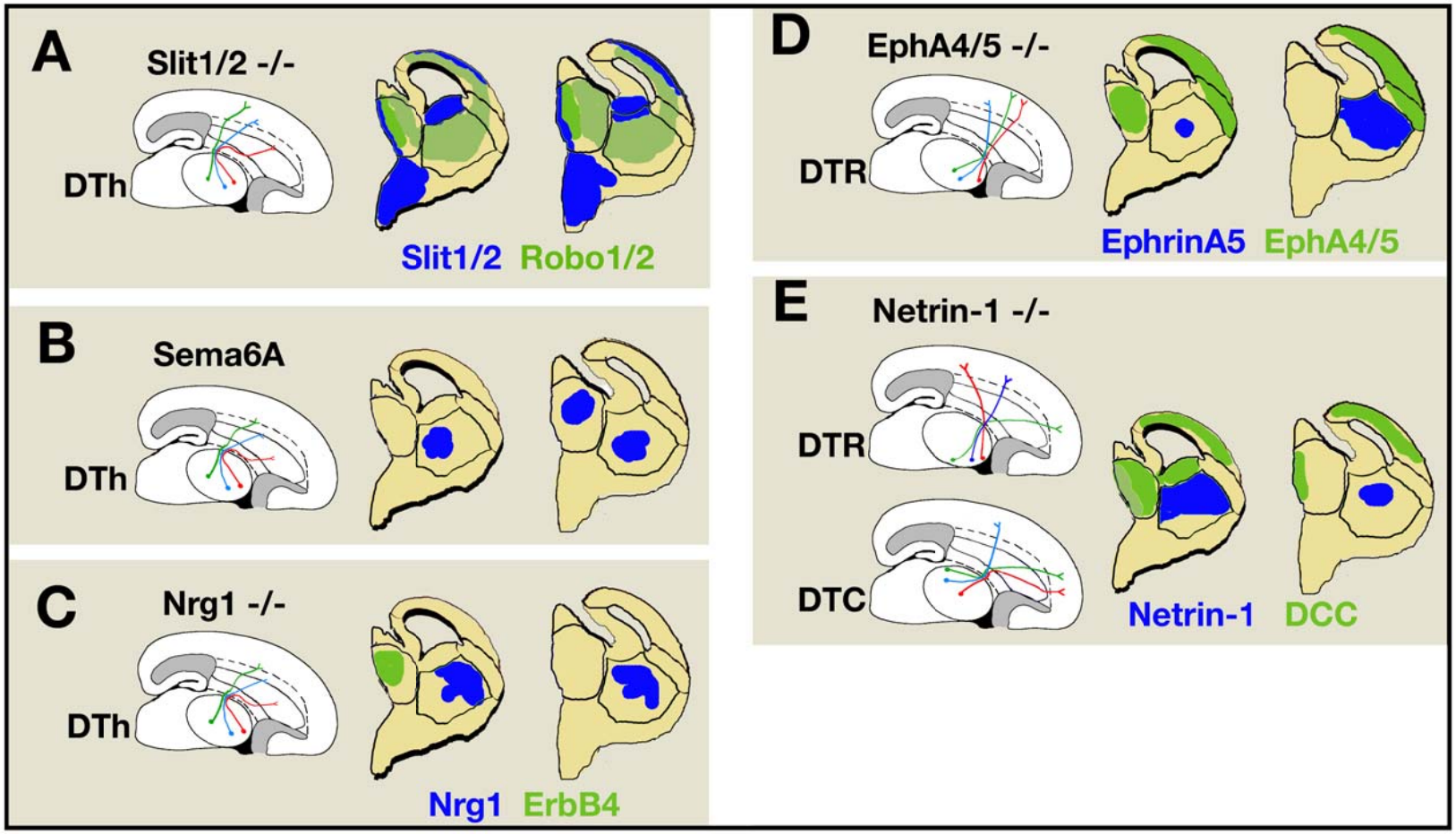

Figure 6. Axon guidance molecules involved in establishing TCA topography inside the VTel. Schematics diagramming the expression patterns of axon guidance ligands (Blue), receptors (Green), and the associated deficits observed in mutant mice. (**A**) Slit1/2 mutants have severe guidance deficits in TCA and midline crossing axons. (**B**) Sema6A mutants have a severe disruption of TCA growth, although Sema6A is also expressed in the caudal DTh. (**C**) Nrg1 is hypothesized to establish a corridor through which TCA can grow inside the VTel. (**D**) EphrinA5 acts as a caudal repulsive cue to rostral TC axons expressing EphA4/5. (**E**) Netrin-1 is expressed in a high-rostral to low-caudal gradient inside the VTel. Netrin-1 mutants have been shown to have severe TCA deficits, which will be further studied in this thesis.

This was tested with the wholemount telencephalic co-culture assay developed by Seibt et al. (2005, **Figure 7**), using WT thalami cultured with telencephalons from Ephrin-A5 mutants, or by depleting Ephrin binding activity in WT cultures with EphA3-Fc. In both conditions, WT axons are caudalized inside the VTel showing the role of graded ephrin-A5 expression in the intermediate target in segregating axon populations by means of responsiveness to a patterned axon guidance molecule.

A final axon guidance molecule shown to be involved in thalamocortical axon guidance is Netrin-1. Netrin-1 has been well characterized as an axonal growth factor and biphasic axon guidance molecule, attractive to growth cones expressing DCC and repulsive to axons co-expressing DCC and an Unc5 homologues (Unc5H) (Keino-Masu et al. 1996; de la Torre et al. 1997; Hong et al. 1999). Additionally, *in vitro* experiments have shown a Netrin-1 mediated chemotrophic effect on both CFA and TCAs in vitro (Metin and Godement 1996; Metin et al. 1997; Richards et al. 1997; Braisted et al. 1999). Netrin-1 mutants have severe axon guidance deficits in multiple axon tracts including midline crossing of commissural and callosal axons (Fazeli et al. 1997; Livesey and Hunt 1997; Shu et al. 2000). Earlier studies have shown that Netrin-1 is expressed in the mantle region of the VTel from E13 to E15 while the receptor DCC is expressed in the thalamus (**Figure 6E**) (Serafini et al. 1996; Metin et al. 1997; Tuttle et al. 1999; Braisted et al. 2000).

Considering the high-rostral to low-caudal gradient of expression of Netrin-1 inside the VTel and the patterned expression of DCC in the rostral thalamus, we propose that Netrin-1 acts as a topographic guidance molecule for TCAs. This thesis will further explore the role of Netrin-1 in establishing the topography of thalamocortical connections inside the VTel (Chapter 2).

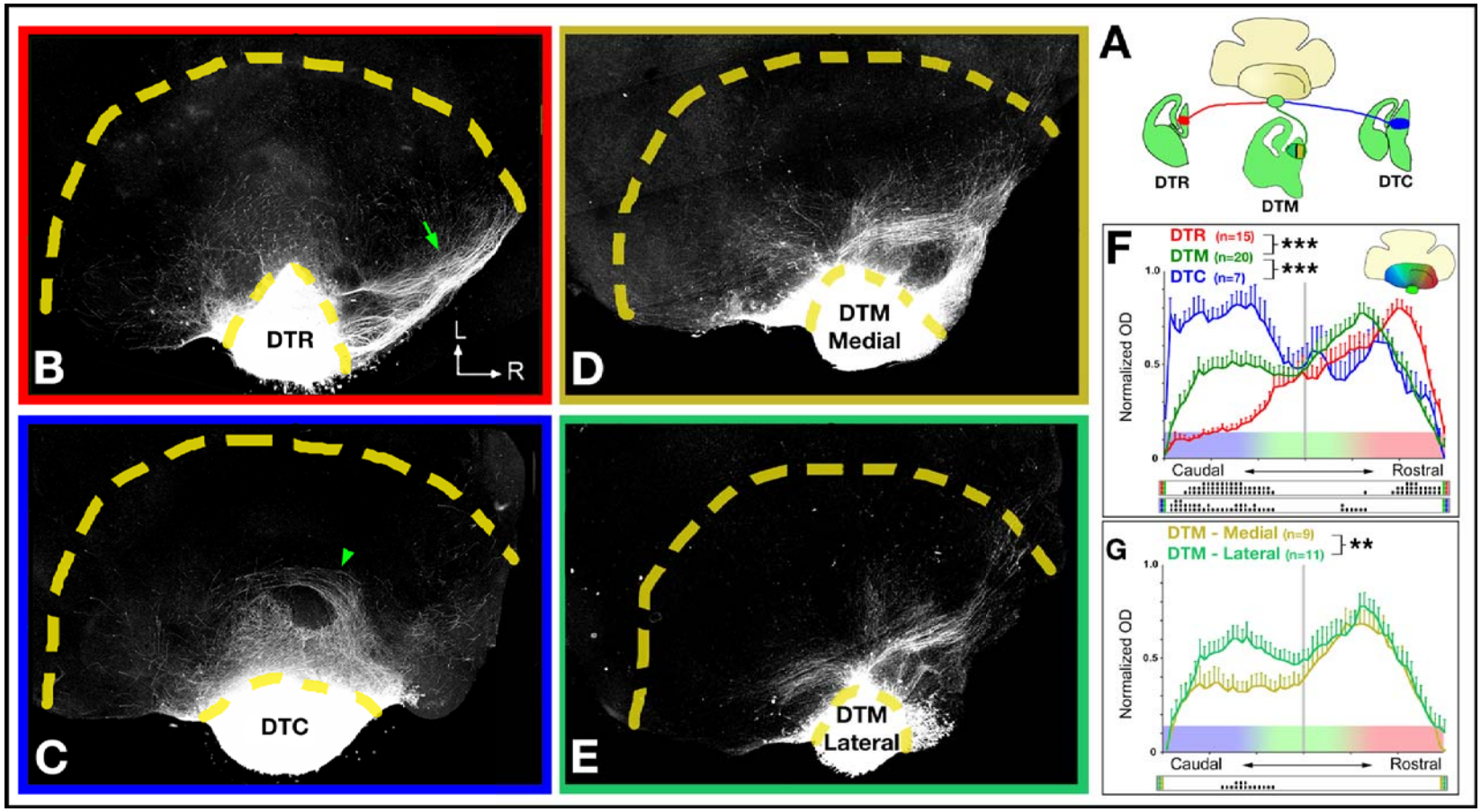

Figure 7. The wholemount telencephalic assay recapitulates in vivo TCA topography

(**A**) Explants isolated from 250 microns thick coronal slices of E14.5 GFP expressing mice are cocultured with a telencephalon from an isochronic wild-type mouse. Explants are from the rostral (DTR), middle (DTM), and caudal (DTC) DTh. DTM explants can be subdivided into medial (DTM-M) and lateral (DTM-L) halves. (**B-C**) DTR and DTC explants grow to the rostral and caudal VTel respectively. (**D-E**) DTM explants grow into more central VTel regions than DTR, with DTM-M having more selective growth into the rostral VTel. (**F-G**) Quantification of B-E shows the progressive topographic growth of thalamic explants in vitro.

The potential role of corticofugal axons in inter-areal topography of TC projections: The 'Handshake hypothesis'

Corticofugal axons (CFA) have been proposed to play a role in the establishment of the topography of TC projections. Tracing studies have shown the close proximity of CFA and TCA inside the internal capsule, leading to the initial proposal of the "handshake" model of reciprocal connectivity (McConnell et al. 1989; Blakemore and Molnar 1990; Molnar and Blakemore 1995b; Molnar et al. 1998a). The primary supposition of this model is that populations of CFA, specifically pioneering subplate axons, interact and fasciculate with ascending TCA (**Figure 8**), allowing for both entry into the cortex and through fasciculation, providing region specific cues to thalamic afferents (McConnell et al. 1989; Ghosh et al. 1990; Ghosh and Shatz 1993; Ghosh 1995; Molnar et al. 1998b).

The postulated interaction of one population of growing axons with another is not isolated to CFA and TCA. Many anatomical studies have hypothesized the existence of extra-cortical cues consisting of guidepost cells in establishing thalamocortical connectivity in the mouse, rat, and ferret (Mitrofanis and Guillery 1993; Metin and Godement 1996; Richards et al. 1997; Molnar and Cordery 1999; Braisted et al. 2000). It has also been proposed that transient striatal projections fasciculate with TCA, establishing a guidance route for thalamic axons (Mitrofanis and Baker 1993; Metin and Godement 1996). These transient projections are abolished in Emx2, Pax6, and Mash1 mutant mice and are believed to contribute to the aberrant TCA projections observed inside the VTel (Tuttle et al. 1999; Jones et al. 2002; Lopez-Bendito et al. 2002).

However, there are confounding results in the literature that bring doubt to the validity of the 'handshake' model. Specifically, changing in the identity of the rostral cortex into more caudal regions as seen in Fgf8 hypomorphs does not alter the trajectory of TCA inside the VTel (Garel et al. 2003). Whether subplate axons play a permissive role for thalamic axons entering the cortex or if they are also involved in establishing inter-areal topography is a contentious debate.

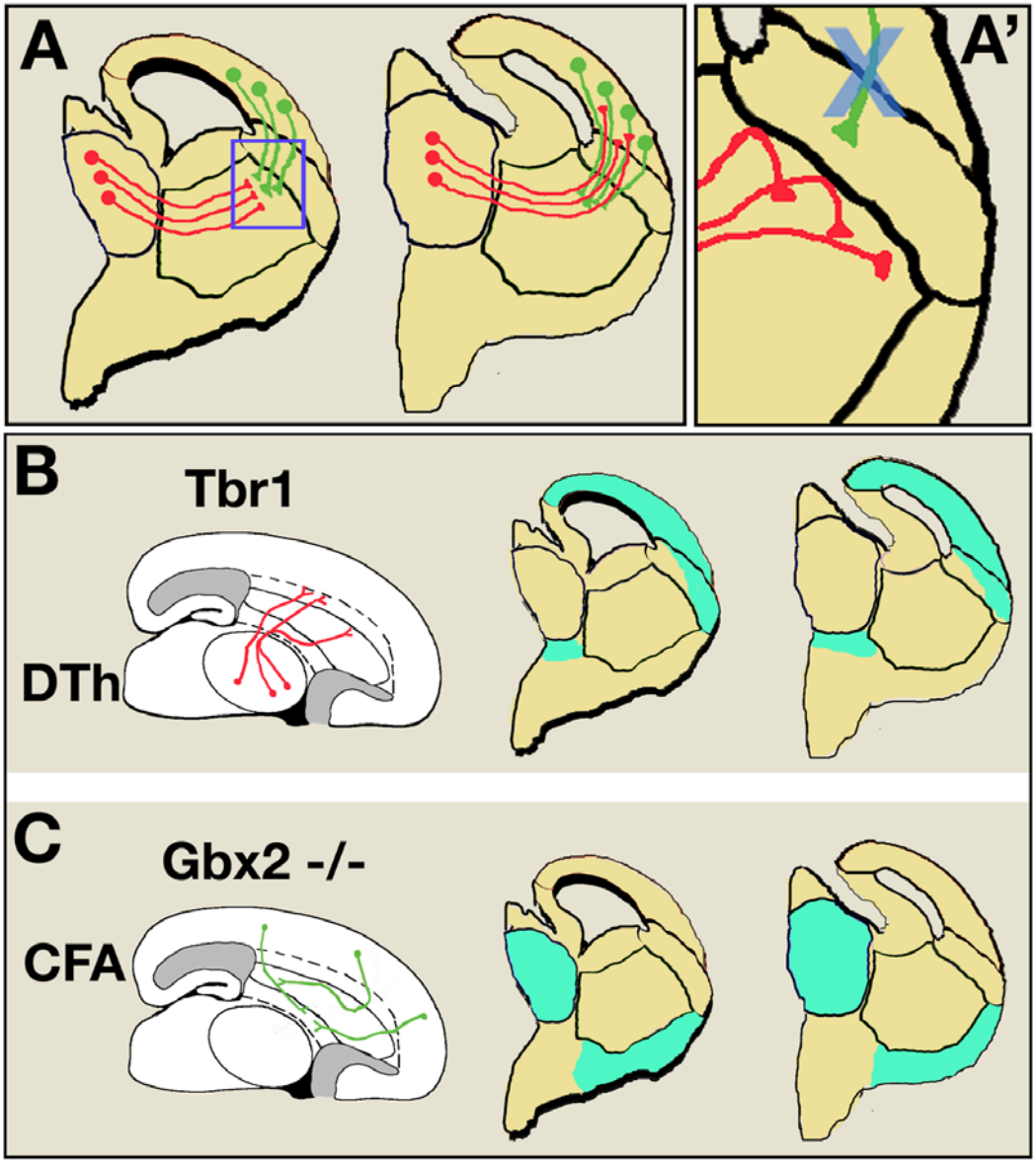

Figure 8. The 'Handshake Hypothesis' of reciprocal connectivity between the thalamus and cortex

(**A**) The 'Handshake Hypothesis' states that TCA (Red) interact with CFA (Green) inside the VTel, providing a contact-mediated topographic cue that guides each population to the proper target. This interaction would constitute a cortical contribution to the establishment of *intra-areal* TCA topography. (**A'**) Studies of mutant mice lacking subplate neurons have shown deficits in TCA growth, primarily an inability for TCA to cross the CSB, although topographic deficits have not been thoroughly evaluated.

(**B**) Tbr1 is a transcription factor expressed in the cortex and ventral thalamus at E14.5. Tbr1 -/- mice show deficits in TCA growth, which was explained to be the consequence of cortically derived cues. However, expression in the ventral thalamus makes this interpretation difficult.

(**C**) Gbx2 is a transcription factor expressed in the DTh, but also at low levels in the VTel. Gbx2 -/- mice have aberrant CFA projections, which was interpreted as being due to a TCA deficit. However the expression of Gbx2 inside the VTel makes this analysis difficult.

Evidence for a relationship between subplate neurons and TCAs come from mice with known subplate abnormalities, specifically COUP-TFI, Emx2, p75, and Tbr1 mutant mice in which TCA axons are misdirected inside the VTel (Zhou et al. 1999; Hevner et al. 2001; Hevner et al. 2002; McQuillen et al. 2002). Tbr1 and p75 mutant TCAs indeed have difficulty crossing the CSB, providing evidence for the role of subplate neurons in allowing cortical entry (Hevner et al. 2001; Hevner et al. 2002; McQuillen et al. 2002). Additionally, TCA have aberrant growth in all these mutants, supporting a role for CFA in stimulating their outgrowth in the internal capsule. However, the role of subplate axons in the establishment of TCA topography is difficult to determine considering the pathfinding deficits observed in COUP-TFI and Emx2 mutants occur immediately upon entering the VTel and expression of these transcription factors can be observed in the dorsal thalamus and VTel respectively (Bishop et al. 2000; Mallamaci et al. 2000; Zhou et al. 2001; Lopez-Bendito et al. 2002) rendering difficult the interpretation of the requirement of COUP-TF1 and Emx2 in specifying the expression of axon guidance cues in CFA growth only.

There are additional mouse knockouts that show interesting deficits in both populations of axons in the internal capsule, however caveats accompany them as well. Important to note, similarly to TCA, the VTel has been proposed to contain regionally expressed cues that regulate the projection of CFA to subcortical targets such as the thalamus, brainstem, and spinal cord (Metin et al. 1997; Richards et al. 1997; Bagnard et al. 1998; Bagri et al. 2002). The impact of this is that in order to test the influence of one axon population on another, it would be essential to be able to manipulate the genotype of the dorsal thalamus and the cortex separately in vitro or in vivo. In several of the knockout mice described earlier (Ebf1, Dlx1/2, and Slit1/2) CFA projections are disrupted in addition to TCAs, again showing the complexity associated with studying the Handshake (Bagri et al. 2002; Garel et al. 2002).

There are two mutant mice with internal capsule deficits that attempt to address the issues of tissue specificity, claiming limited expression to either the cortex or thalamus. The capsular connections of Tbr1 and Gbx2 mutants, transcription factors expressed in the cortex and thalamus

respectfully, show topographic deficits to CFA and TCA (**Figure 8B & C**) (Hevner et al. 2002). In each mouse, a reciprocal deficit can be observed with lipophilic tracing, however the mechanism responsible was not determined. However, it should be noted that Gbx2 expression can be found at low levels inside the VTel at E14.5 and Tbr1 is highly expressed in the ventral thalamus at E15. Again reinforcing the problem in interpreting if the defects characterizing CFA and TCA in Gbx2 and Tbr1 mutant mice are due either to cell non-autonomous effects due to reciprocal interactions of these two populations of axons as the authors propose (Hevner et al. 2002) or to the expression of Gbx2 in the ventral telencephalon itself and Tbr1 expression in the thalamus.

The second goal of this thesis was to test the Handshake hypothesis using a recently identified genetic model where CFA projection do not form and attempt to identify some of the molecular mechanisms underlying the interaction between CFA and TCA (Chapter 3).

Heterogeneity of Thalamic axons: another combinatorial code?

Spinal motor neurons are perhaps the best-studied model of the transcriptional regulation of cell identity. Motor neurons that project to specific muscle groups are clustered in specific pools (Pfaff et al. 1996). Motor neurons that innervate axial muscles are located in the median motor column (MMC) and are present at all segmental levels of the spinal cord. By contrast, motor neurons that innervate limb muscles are located in the lateral motor column (LMC) and are generated only at levels of the neural tube in register with the limb fields (Landmesser 1978; Hollyday 1980; Lance-Jones and Landmesser 1981). Classical experiments on the developing chick spinal cord showed that innervation of a specific muscle by motor neurons is initiated before target innervation by sorting of axons into specific fascicles. These early studies demonstrated indirectly that the projection of distinct pools of motorneurons to a specific muscle is probably determined intrinsically (Lance-Jones and Landmesser 1981; Landmesser 1992).

The discovery that specific pools of motor neurons are organized by the expression of combinations of LIM-homeobox transcription factors such as Lim1 and Islet1 represented a key step in our understanding of the molecular mechanisms that determine motor neuron projections (Tsuchida et al. 1994; Briscoe et al. 2000; Sharma et al. 2000). More recently, a combinatorial code of Hox transcription factors expressed along the rostro-caudal axis of the spinal cord has been shown to have a key function in defining the identity of motor neuron pools, including the specification of a particular target muscle (Dasen et al. 2005).

How does the expression of combinations of transcription factors specify the projection of motor neuron axons to specific muscles? At the brachial level of the developing mammalian spinal cord, two LIM-homeodomain transcription factors (Lim1 and Lmx1b) control the initial trajectory of motor axons in the developing limb (Kania et al. 2000). The expression of Lim1 by a lateral set of LMC neurons ensures that their axons select a dorsal trajectory in the limb. Furthermore, Lmx1b functions within limb mesenchymal cells to control the dorsoventral axonal trajectory of both medial and lateral LMC neurons (Kania et al. 2000). Studies in *Drosophila* and *C. elegans* have indicated that LIM-homeodomain proteins have an evolutionarily conserved role in the control of motor axon trajectories (Hobert et al. 1998; Thor et al. 1999). There is also evidence that EphA-ephrin-A interactions control motor axon projections at the level of the ventral base of the limb (Iwamasa et al. 1999; Eberhart et al. 2000; Helmbacher et al. 2000; Eberhart et al. 2004). Kania et al. (Kania and Jessell 2003) have shown that Lim1 and Isl1 control the dorso-ventral specificity of motor axon projections at least in part by controlling the expression of EphA4 in lateral LMC neurons, and thereby conferring responsiveness to ephrin-A ligands that are induced by Lmx1b in the ventral portion of the limb (Kania and Jessell 2003). These results indicate that Lim1 specifies the dorso-ventral specificity of axon projection by controlling EphA4 expression, whereas the expression of Lmx1b by mesenchymal cells in the ventral half of the developing limb controls the expression of ephrinA5 and thereby defines a territory that is avoided by lateral LMC axons (Kania and Jessell 2003).

Another class of receptors (Neuropilins) that mediates repulsion in response to class 3 semaphorins has been implicated in the early dorso-ventral segregation of LMC axons in the limb (Huber et al. 2005). Sema3A-Npn1 signaling controls the timing of the ingrowth of motor axons into the limb, whereas Sema3F-Npn2 signaling guides the axons of a medial subset of LMC neurons to the ventral limb (Huber et al. 2005).

Members of the fibroblast growth factor family, such as FGF8, that are expressed in the dermomyotome also attract the axons of brachial motor neurons (Shirasaki et al. 2006). Interestingly, reprogramming limb-innervating motorneurons to become dermomyotome-innervating the medial subset of the MMC (MMCm) neurons using the LIM-homeodomain transcriptional factor Lhx3 is sufficient to induce FGF receptor 1 expression and as a consequence induce FGF-responsiveness in the motor neuron axons (Shirasaki et al. 2006). These results indicate that in addition to its well-characterized function as a patterning cue early in development, FGF signaling might also be a novel effector pathway of the LIM-homeodomain transcriptional code in the guidance of motor neuron axons to their targets.

The findings in spinal cord development further support the notion that transcription factors influence axonal projections by regulating the expression of guidance receptors. It remains to be determined how specific combinations of transcription factors specify the expression of axon guidance receptors. It is also not known how interactions between different types of axon guidance receptors contribute to the guidance of motor axons in a local environment that contains multiple axon guidance cues.

Combinatorial codes regulating axon targeting have also been proposed for thalamic axons, due to the expression of transcription factors during embryogenesis prior to and during axon pathfinding. An important study by Nakagawa and O'Leary (Nakagawa and O'Leary 2001) showed the progressive parsing of the mouse DTh into distinct populations based upon transcription factor expression (**Figure 9A**). This study begins at E10.5 and continues through P2, covering the time course of thalamic neuron generation, inter-areal axon guidance, and the beginning of activity

dependant intra-areal refinement. Using in situ hybridization on coronal slices along the rostro-caudal extent of the thalamus, Nakagawa and O'Leary probed for *Gbx2*, *Ngn2*, and LIM-homeodomain transcription factors, *Lhx2*, and *Lhx9*. At P2, the Dth contains 19 cytoarchitecturally distinct nuclei resembling what is found in the adult. At P2, these nuclei express a complex pattern of Lhx2, Lhx9, and Gbx2 indicating these transcription factors may regulate the phenotype of a given thalamic nucleus. The authors then asked at which point the thalamus segregates into transcriptionally identifiable regions.

At E12.5, the DTh contains subtle differences in *Lhx2*, *Lhx9*, *Gbx2*, and *Ngn2*, expression along the rostral-caudal and medial-lateral axes. Specifically, for all the above factors, there is greater medial expression than lateral and for Ngn2 there is an additional higher rostral than caudal expression. At E14.5, these patterns become more refined, with distinct patterns of expression occurring throughout the DTh (**Figure 9A**). Specifically, Lhx2 is expressed selectively in the medial portion of the thalamus while Lhx9 and Gbx2 have a sometimes overlapping graded expressed along the medial-lateral axis. Ngn2 has a distinct graded expression in the Dth, described as high-rostral to low-caudal. By E16.5, this regionalization is much more defined, with the patterning of the DTh looking quite similar to that of P2. The exception to this is *Ngn2*, which still has a graded high-rostral to low-caudal expression at E16.5, but no expression at P2. These data show that at a transcriptional level, the early embryonic DTh contains heterogeneous populations of neurons that are organized similarly to the neonatal DTh. Importantly, these populations are transcriptionally patterned before TCA leave the thalamus, before reaching the cortex, and before thalamic nuclei are cytoarchitecturally identifiable. This is a crucial point as the topography of TC axon projections in the ventral telencephalon (E14-15) are established before individual thalamic nuclei are formed, meaning that thalamic neurons segregate into specific nuclei after their axons have reached the cortex. This also means that experiments testing how topography is established in the ventral telencephalon need to be performed at E14.5 at the latest.

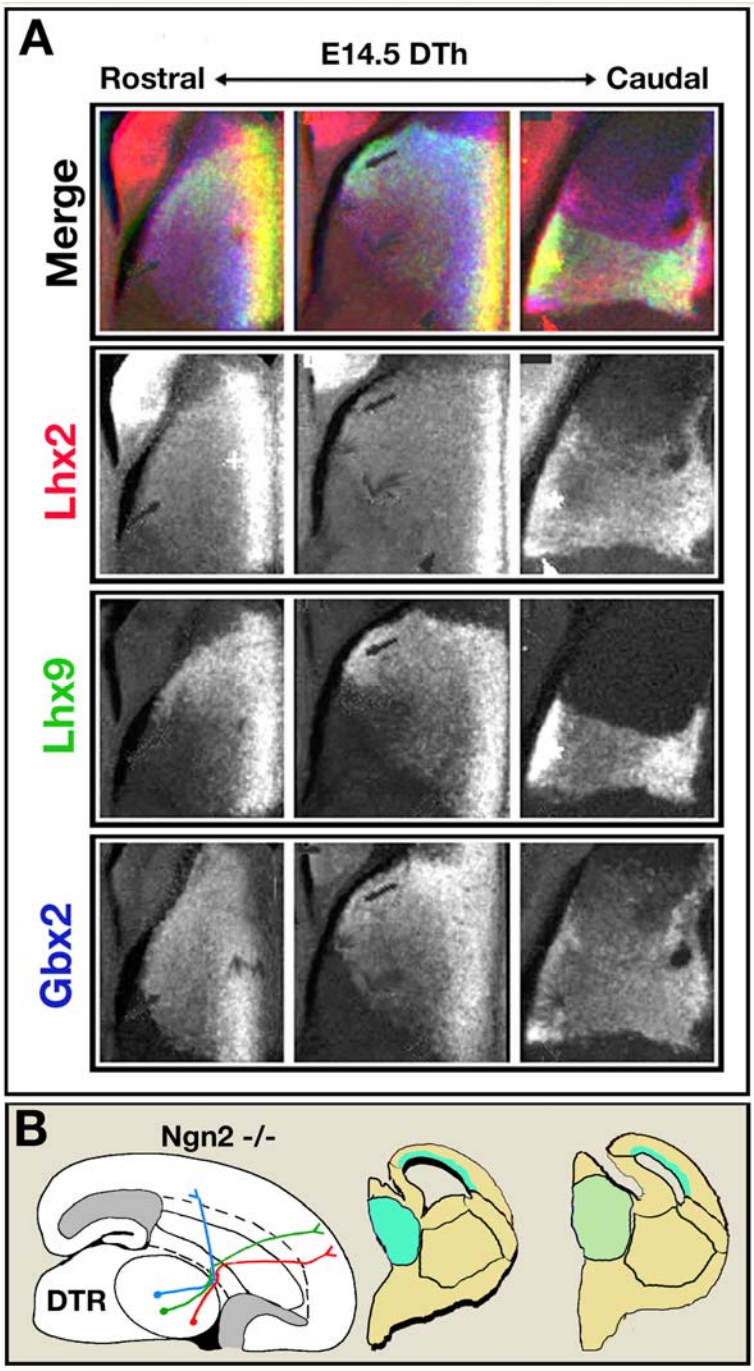

Figure 9. Possibility of combinatorial codes in the DTh

(**A**) At E14.5, transcription factors are differentially expressed in the DTh before thalamic nuclei can be identified using *in situ* hybridization. Lhx2 (Red) is highly expressed in the medial and caudal regions of the DTh. Lhx9 (Green) is expressed in medial, dorsal, and central regions of the DTh. Gbx2 (Blue) is evenly expressed along the rostro-caudal extent of the DTh, but more highly along the medial regions. Overlays show the combinatorial patterning of these transcription factors.

(**B**) At E14.5, Ngn2, a bHLH transcription factor, is expressed in a high-rostral to low-caudal gradient in the DTh. Studies of Ngn2 -/- mice show a deficit in rostral growth inside the VTel by rostral TCA.

The hypothesis that the inter-areal topography of TCA projection is determined in part by transcriptionally regulated axon guidance receptor expression is compelling, however little research has been conducted to test this. In searching for cell-autonomous mechanisms establishing TCA topography, the bHLH transcription factor Ngn2 was a candidate due to known proneural activity and a graded rostral-caudal expression in the thalamus at E14 (Nakagawa and O'Leary 2001). Carbocyanine dye tracing experiments of mice lacking Ngn2 showed a dramatic shift in the trajectory of axons originating from the rostral thalamus to cortical areas normally innervated by central thalamic regions (**Figure 9B**) (Seibt et al. 2003). While these results suggest that Ngn2 may regulate the expression of proteins associated with axon guidance machinery, it is difficult to decipher whether this phenotype is due to cell-autonomous mechanisms as Ngn2 is highly expressed in the cortex. To describe the role of Ngn2 solely in TCA guidance, thalamic explants taken from GFP expressing/Ngn2 mutant mice were co-cultured with WT telencephalon using a novel wholemount telencephalic coculture assay (Seibt et al. 2003). In these experiments, the authors found that axons emerging from the rostro-medial dorsal thalamus are preferentially targeted to the anterior ventral telencephalon, ultimately invading anterior cortical territories. Conversely, axons that emerge from progressively more caudo-lateral parts of the thalamus grow preferentially towards more caudal parts of the ventral telencephalon (**Figure 7**). Rostral thalamic explants from Ngn2 mutants lost anterior selectivity, mirroring the tracing experiments by growing to caudal regions of the VTel (**Figure 9B**). These results show that Ngn2 controls the topography of thalamocortical projections by controlling the responsiveness of thalamocortical axons to intermediate target cues in the ventral telencephalon (Seibt et al. 2003).

It is unclear whether the relative responsiveness of TCA to axon guidance cues, corresponding to their cell body location inside the thalamus, is the mechanism by which the VTel establishes crude topography. Thalamic expression of Ngn2 is in a high rostral to low caudal gradient, suggesting that this may be the case as a subtractive hybridization screen performed in the cortex showed that Netrin-1 receptor DCC is regulated by Ngn2 (Mattar et al. 2004). Considering the

patterned Netrin-1 expression in the VTel, it is possible that a lack of recognition to this attractive rostral cue could be partially responsible for the caudalization found in Ngn2 mutants. In a pathway as complex and specific as the thalamocortical system, it is likely that topography is created by an equally complex combination of axon guidance cues and receptors.

References

Agmon A, Yang LT, O'Dowd DK, Jones EG (1993) Organized growth of thalamocortical axons from the deep tier of terminations into layer IV of developing mouse barrel cortex. J Neurosci 13(12): 5365-5382.

Anderson SA, Eisenstat DD, Shi L, Rubenstein JL (1997a) Interneuron migration from basal forebrain to neocortex: dependence on Dlx genes [see comments]. Science 278(5337): 474-476.

Anderson SA, Eisenstat DD, Shi L, Rubenstein JL (1997b) Interneuron migration from basal forebrain to neocortex: dependence on Dlx genes. Science 278(5337): 474-476.

Anderson SA, Qiu M, Bulfone A, Eisenstat DD, Meneses J et al. (1997c) Mutations of the homeobox genes Dlx-1 and Dlx-2 disrupt the striatal subventricular zone and differentiation of late born striatal neurons. Neuron 19(1): 27-37.

Angevine JBJ (1970) Time of neuron origin in the diencephalon of the mouse. An autoradiographic study. J Comp Neurol 139: 129-188.

Bagnard D, Lohrum M, Uziel D, Puschel AW, Bolz J (1998) Semaphorins act as attractive and repulsive guidance signals during the development of cortical projections. Development 125(24): 5043-5053.

Bagri A, Marin O, Plump AS, Mak J, Pleasure SJ et al. (2002) Slit proteins prevent midline crossing and determine the dorsoventral position of major axonal pathways in the mammalian forebrain. Neuron 33(2): 233-248.

Barbieri AM, Broccoli V, Bovolenta P, Alfano G, Marchitiello A et al. (2002) Vax2 inactivation in mouse determines alteration of the eye dorsal-ventral axis, misrouting of the optic fibres and eye coloboma. Development 129(3): 805-813.

Bicknese AR, Sheppard AM, O'Leary DD, Pearlman AL (1994) Thalamocortical axons extend along a chondroitin sulfate proteoglycan-enriched pathway coincident with the neocortical subplate and distinct from the efferent path. J Neurosci 14(6): 3500-3510.

Bishop KM, Goudreau G, O'Leary DD (2000) Regulation of area identity in the mammalian neocortex by Emx2 and Pax6. Science 288(5464): 344-349.

Blakemore C, Molnar Z (1990) Factors involved in the establishment of specific interconnections between thalamus and cerebral cortex. Cold Spring Harb Symp 55: 491-504.

Bolz J, Novak N, Staiger V (1992) Formation of specific afferent connections in organotypic slice cultures from rat visual cortex cocultured with lateral geniculate nucleus. J Neurosci 12(8): 3054-3070.

Braisted JE, Tuttle R, O'Leary D D (1999) Thalamocortical axons are influenced by chemorepellent and chemoattractant activities localized to decision points along their path. Dev Biol 208(2): 430-440.

Braisted JE, Catalano SM, Stimac R, Kennedy TE, Tessier-Lavigne M et al. (2000) Netrin-1 promotes thalamic axon growth and is required for proper development of the thalamocortical projection. J Neurosci 20(15): 5792-5801.

Briscoe J, Pierani A, Jessell TM, Ericson J (2000) A homeodomain protein code specifies progenitor cell identity and neuronal fate in the ventral neural tube. Cell 101(4): 435-445.

Casarosa S, Fode C, Guillemot F (1999) Mash1 regulates neurogenesis in the ventral telencephalon. Development 126(3): 525-534.

Caviness VS, Jr., Frost DO (1980) Tangential organization of thalamic projections to the neocortex in the mouse. J Comp Neurol 194(2): 335-367.

Crandall JE, Caviness VS, Jr. (1984) Thalamocortical connections in newborn mice. J Comp Neurol 228(4): 542-556.

Dasen JS, Tice BC, Brenner-Morton S, Jessell TM (2005) A Hox regulatory network establishes motor neuron pool identity and target-muscle connectivity. Cell 123(3): 477-491.

de la Torre JR, Hopker VH, Ming GL, Poo MM, Tessier-Lavigne M et al. (1997) Turning of retinal growth cones in a netrin-1 gradient mediated by the netrin receptor DCC. Neuron 19(6): 1211-1224.

Dufour A, Seibt J, Passante L, Depaepe V, Ciossek T et al. (2003) Area specificity and topography of thalamocortical projections are controlled by ephrin/Eph genes. Neuron 39(3): 453-465.

Eberhart J, Swartz M, Koblar SA, Pasquale EB, Tanaka H et al. (2000) Expression of EphA4, ephrin-A2 and ephrin-A5 during axon outgrowth to the hindlimb indicates potential roles in pathfinding. Dev Neurosci 22(3): 237-250.

Eberhart J, Barr J, O'Connell S, Flagg A, Swartz ME et al. (2004) Ephrin-A5 exerts positive or inhibitory effects on distinct subsets of EphA4-positive motor neurons. J Neurosci 24(5): 1070-1078.

Fazeli A, Dickinson SL, Hermiston ML, Tighe RV, Steen RG et al. (1997) Phenotype of mice lacking functional Deleted in colorectal cancer (Dcc) gene. Nature 386(6627): 796-804.

Flanagan JG, Van Vactor D (1998) Through the looking glass: axon guidance at the midline choice point. Cell 92(4): 429-432.

Flanagan JG, Vanderhaeghen P (1998) The ephrins and Eph receptors in neural development. Annu Rev Neurosci 21: 309-345.

Fukuchi-Shimogori T, Grove EA (2001) Neocortex patterning by the secreted signaling molecule FGF8. Science 294(5544): 1071-1074.

Fukuchi-Shimogori T, Grove EA (2003) Emx2 patterns the neocortex by regulating FGF positional signaling. Nat Neurosci 6(8): 825-831.

Gao PP, Yue Y, Zhang JH, Cerretti DP, Levitt P et al. (1998) Regulation of thalamic neurite outgrowth by the Eph ligand ephrin-A5: implications in the development of thalamocortical projections. Proc Natl Acad Sci U S A 95(9): 5329-5334.

Garel S, Huffman KJ, Rubenstein JL (2003) Molecular regionalization of the neocortex is disrupted in Fgf8 hypomorphic mutants. Development 130(9): 1903-1914.

Garel S, Marin F, Grosschedl R, Charnay P (1999) Ebf1 controls early cell differentiation in the embryonic striatum. Development 126(23): 5285-5294.

Garel S, Yun K, Grosschedl R, Rubenstein JL (2002) The early topography of thalamocortical projections is shifted in Ebf1 and Dlx1/2 mutant mice. Development 129(24): 5621-5634.

Ghosh A (1995) Subplate neurons and the patterning of thalamocortial connections. Ciba Found Symp 193: 150-172; discussion 192-159.

Ghosh A, Shatz CJ (1992) Pathfinding and target selection by developing geniculocortical axons. J Neurosci 12(1): 39-55.

Ghosh A, Shatz CJ (1993) A role for subplate neurons in the patterning of connections from thalamus to neocortex. Development 117(3): 1031-1047.

Ghosh A, Antonini A, McConnell SK, Shatz CJ (1990) Requirement for subplate neurons in the formation of thalamocortical connections. Nature 347(6289): 179-181.

Grove EA, Fukuchi-Shimogori T (2003) Generating the cerebral cortical area map. Annu Rev Neurosci 26: 355-380.

Helmbacher F, Schneider-Maunoury S, Topilko P, Tiret L, Charnay P (2000) Targeting of the EphA4 tyrosine kinase receptor affects dorsal/ventral pathfinding of limb motor axons. Development 127(15): 3313-3324.

Herrera E, Marcus R, Li S, Williams SE, Erskine L et al. (2004) Foxd1 is required for proper formation of the optic chiasm. Development 131(22): 5727-5739.

Herrera E, Brown L, Aruga J, Rachel RA, Dolen G et al. (2003) Zic2 patterns binocular vision by specifying the uncrossed retinal projection. Cell 114(5): 545-557.

Hevner RF, Miyashita-Lin E, Rubenstein JL (2002) Cortical and thalamic axon pathfinding defects in Tbr1, Gbx2, and Pax6 mutant mice: evidence that cortical and thalamic axons interact and guide each other. J Comp Neurol 447(1): 8-17.

Hevner RF, Shi L, Justice N, Hsueh Y, Sheng M et al. (2001) Tbr1 regulates differentiation of the preplate and layer 6. Neuron 29(2): 353-366.

Hobert O, D'Alberti T, Liu Y, Ruvkun G (1998) Control of neural development and function in a thermoregulatory network by the LIM homeobox gene lin-11. J Neurosci 18(6): 2084-2096.

Hohl-Abrahao JC, Creutzfeldt OD (1991) Topographical mapping of the thalamocortical projections in rodents and comparison with that in primates. Exp Brain Res 87(2): 283-294.

Hollyday M (1980) Organization of motor pools in the chick lumbar lateral motor column. J Comp Neurol 194(1): 143-170.

Hong K, Hinck L, Nishiyama M, Poo MM, Tessier-Lavigne M et al. (1999) A ligand-gated association between cytoplasmic domains of UNC5 and DCC family receptors converts netrin-induced growth cone attraction to repulsion. Cell 97(7): 927-941.

Huber AB, Kania A, Tran TS, Gu C, De Marco Garcia N et al. (2005) Distinct roles for secreted semaphorin signaling in spinal motor axon guidance. Neuron 48(6): 949-964.

Iwamasa H, Ohta K, Yamada T, Ushijima K, Terasaki H et al. (1999) Expression of Eph receptor tyrosine kinases and their ligands in chick embryonic motor neurons and hindlimb muscles. Dev Growth Differ 41(6): 685-698.

Jones EG (2001) The thalamic matrix and thalamocortical synchrony. Trends Neurosci 24(10): 595-601.

Jones L, Lopez-Bendito G, Gruss P, Stoykova A, Molnar Z (2002) Pax6 is required for the normal development of the forebrain axonal connections. Development 129(21): 5041-5052.

Kageyama GH, Robertson RT (1993) Development of geniculocortical projections to visual cortex in rat: evidence for early ingrowth and synaptogenesis. J Comp Neurol 335: 123-148.

Kania A, Jessell TM (2003) Topographic motor projections in the limb imposed by LIM homeodomain protein regulation of ephrin-A:EphA interactions. Neuron 38(4): 581-596.

Kania A, Johnson RL, Jessell TM (2000) Coordinate roles for LIM homeobox genes in directing the dorsoventral trajectory of motor axons in the vertebrate limb. Cell 102(2): 161-173.

Keino-Masu K, Masu M, Hinck L, Leonardo ED, Chan SS et al. (1996) Deleted in Colorectal Cancer (DCC) encodes a netrin receptor. Cell 87(2): 175-185.

Koshiba-Takeuchi K, Takeuchi JK, Matsumoto K, Momose T, Uno K et al. (2000) Tbx5 and the retinotectum projection. Science 287(5450): 134-137.

Kostovic I, Rakic P (1990) Developmental history of the transient subplate zone in the visual and somatosensory cortex of the macaque monkey and human brain. J Comp Neurol 297(3): 441-470.

Lance-Jones C, Landmesser L (1981) Pathway selection by embryonic chick motoneurons in an experimentally altered environment. Proc R Soc Lond B Biol Sci 214(1194): 19-52.

Landmesser L (1978) The distribution of motoneurones supplying chick hind limb muscles. J Physiol 284: 371-389.

Landmesser L (1992) The relationship of intramuscular nerve branching and synaptogenesis to motoneuron survival. J Neurobiol 23(9): 1131-1139.

Leighton PA, Mitchell KJ, Goodrich LV, Lu X, Pinson K et al. (2001) Defining brain wiring patterns and mechanisms through gene trapping in mice. Nature 410(6825): 174-179.

Lin JC, Ho WH, Gurney A, Rosenthal A (2003) The netrin-G1 ligand NGL-1 promotes the outgrowth of thalamocortical axons. Nat Neurosci 6(12): 1270-1276.

Livesey FJ, Hunt SP (1997) Netrin and netrin receptor expression in the embryonic mammalian nervous system suggests roles in retinal, striatal, nigral, and cerebellar development. Mol Cell Neurosci 8(6): 417-429.

Lopez-Bendito G, Molnar Z (2003) Thalamocortical development: how are we going to get there? Nat Rev Neurosci 4(4): 276-289.

Lopez-Bendito G, Chan CH, Mallamaci A, Parnavelas J, Molnar Z (2002) Role of Emx2 in the development of the reciprocal connectivity between cortex and thalamus. J Comp Neurol 451(2): 153-169.

Lopez-Bendito G, Cautinat A, Sanchez JA, Bielle F, Flames N et al. (2006) Tangential neuronal migration controls axon guidance: a role for neuregulin-1 in thalamocortical axon navigation. Cell 125(1): 127-142.

Lupo G, Liu Y, Qiu R, Chandraratna RA, Barsacchi G et al. (2005) Dorsoventral patterning of the Xenopus eye: a collaboration of Retinoid, Hedgehog and FGF receptor signaling. Development 132(7): 1737-1748.

Mackarehtschian K, Lau CK, Caras I, McConnell SK (1999) Regional differences in the developing cerebral cortex revealed by ephrin-A5 expression. Cereb Cortex 9(6): 601-610.

Mallamaci A, Muzio L, Chan CH, Parnavelas J, Boncinelli E (2000) Area identity shifts in the early cerebral cortex of Emx2-/- mutant mice. Nat Neurosci 3(7): 679-686.

Mann F, Ray S, Harris W, Holt C (2002) Topographic mapping in dorsoventral axis of the Xenopus retinotectal system depends on signaling through ephrin-B ligands. Neuron 35(3): 461-473.

Marin O, Baker J, Puelles L, Rubenstein JL (2002) Patterning of the basal telencephalon and hypothalamus is essential for guidance of cortical projections. Development 129(3): 761-773.

Mattar P, Britz O, Johannes C, Nieto M, Ma L et al. (2004) A screen for downstream effectors of Neurogenin2 in the embryonic neocortex. Dev Biol 273(2): 373-389.

McConnell SK, Ghosh A, Shatz CJ (1989) Subplate neurons pioneer the first axon pathway from the cerebral cortex. Science 245(4921): 978-982.

McLaughlin T, Hindges R, O'Leary DD (2003) Regulation of axial patterning of the retina and its topographic mapping in the brain. Curr Opin Neurobiol 13(1): 57-69.

McQuillen PS, DeFreitas MF, Zada G, Shatz CJ (2002) A novel role for p75NTR in subplate growth cone complexity and visual thalamocortical innervation. J Neurosci 22(9): 3580-3593.

Metin C, Godement P (1996) The ganglionic eminence may be an intermediate target for corticofugal and thalamocortical axons. J Neurosci 16(10): 3219-3235.

Metin C, Deleglise D, Serafini T, Kennedy TE, Tessier-Lavigne M (1997) A role for netrin-1 in the guidance of cortical efferents. Development 124(24): 5063-5074.

Mitrofanis J, Guillery RW (1993) New views of the thalamic reticular nucleus in the adult and the developing brain. Trends Neurosci 16(6): 240-245.

Mitrofanis J, Baker GE (1993) Development of the thalamic reticular and perireticular nuclei in rats and their relationship to the course of growing corticofugal and corticopetal axons. J Comp Neurol 338(4): 575-587.

Miyashita-Lin EM, Hevner R, Wassarman KM, Martinez S, Rubenstein JL (1999) Early neocortical regionalization in the absence of thalamic innervation. Science 285(5429): 906-909.

Molnar Z, Blakemore C (1991) Lack of regional specificity for connections formed between thalamus and cortex in coculture. Nature 351(6326): 475-477.

Molnar Z, Blakemore C (1995a) Guidance of thalamocortical innervation. Ciba Found Symp 193: 127-149.

Molnar Z, Blakemore C (1995b) How do thalamic axons find their way to the cortex? Trends Neurosci 18(9): 389-397.

Molnar Z, Cordery P (1999) Connections between cells of the internal capsule, thalamus, and cerebral cortex in embryonic rat. J Comp Neurol 413(1): 1-25.

Molnar Z, Adams R, Blakemore C (1998a) Mechanisms underlying the early establishment of thalamocortical connections in the rat. Journal of Neuroscience 18(15): 5723-5745.

Molnar Z, Adams R, Goffinet AM, Blakemore C (1998b) The role of the first postmitotic cortical cells in the development of thalamocortical innervation in the reeler mouse. Journal of Neuroscience 18(15): 5746-5765.

Monuki ES, Walsh CA (2001) Mechanisms of cerebral cortical patterning in mice and humans. Nat Neurosci 4 Suppl: 1199-1206.

Mui SH, Hindges R, O'Leary DD, Lemke G, Bertuzzi S (2002) The homeodomain protein Vax2 patterns the dorsoventral and nasotemporal axes of the eye. Development 129(3): 797-804.

Nagai T, Aruga J, Takada S, Gunther T, Sporle R et al. (1997) The expression of the mouse Zic1, Zic2, and Zic3 gene suggests an essential role for Zic genes in body pattern formation. Dev Biol 182(2): 299-313.

Nagai T, Aruga J, Minowa O, Sugimoto T, Ohno Y et al. (2000) Zic2 regulates the kinetics of neurulation. Proc Natl Acad Sci U S A 97(4): 1618-1623.

Nakagawa Y, O'Leary DD (2001) Combinatorial expression patterns of LIM-homeodomain and other regulatory genes parcellate developing thalamus. J Neurosci 21(8): 2711-2725.

Nakagawa Y, Johnson JE, O'Leary DD (1999) Graded and areal expression patterns of regulatory genes and cadherins in embryonic neocortex independent of thalamocortical input. J Neurosci 19(24): 10877-10885.

O'Leary DD, Nakagawa Y (2002) Patterning centers, regulatory genes and extrinsic mechanisms controlling arealization of the neocortex. Curr Opin Neurobiol 12(1): 14-25.

Orioli D, Klein R (1997) The Eph receptor family: axonal guidance by contact repulsion. Trends Genet 13(9): 354-359.

Pak W, Hindges R, Lim YS, Pfaff SL, O'Leary DD (2004) Magnitude of binocular vision controlled by islet-2 repression of a genetic program that specifies laterality of retinal axon pathfinding. Cell 119(4): 567-578.

Pallas SL (2001) Intrinsic and extrinsic factors that shape neocortical specification. Trends Neurosci 24(7): 417-423.

Pfaff SL, Mendelsohn M, Stewart CL, Edlund T, Jessell TM (1996) Requirement for LIM homeobox gene Isl1 in motor neuron generation reveals a motor neuron-dependent step in interneuron differentiation. Cell 84(2): 309-320.

Pleasure SJ, Anderson S, Hevner R, Bagri A, Marin O et al. (2000) Cell migration from the ganglionic eminences is required for the development of hippocampal GABAergic interneurons. Neuron 28(3): 727-740.

Polleux F, Ince-Dunn G, Ghosh A (2007) Transcriptional regulation of vertebrate axon guidance and synapse formation. Nature Reviews Neuroscience 8, 331-340.

Porteus MH, Bulfone A, Liu JK, Puelles L, Lo LC et al. (1994) DLX-2, MASH-1, and MAP-2 expression and bromodeoxyuridine incorporation define molecularly distinct cell populations in the embryonic mouse forebrain. J Neurosci 14(11 Pt 1): 6370-6383.

Powell EM, Muhlfriedel S, Bolz J, Levitt P (2003) Differential regulation of thalamic and cortical axonal growth by hepatocyte growth factor/scatter factor. Dev Neurosci 25(2-4): 197-206.

Prakash N, Vanderhaeghen P, Cohen-Cory S, Frisen J, Flanagan JG et al. (2000) Malformation of the functional organization of somatosensory cortex in adult ephrin-A5 knock-out mice revealed by in vivo functional imaging. J Neurosci 20(15): 5841-5847.

Pratt T, Tian NM, Simpson TI, Mason JO, Price DJ (2004) The winged helix transcription factor Foxg1 facilitates retinal ganglion cell axon crossing of the ventral midline in the mouse. Development 131(15): 3773-3784.

Richards LJ, Koester SE, Tuttle R, O'Leary DDM (1997) Directed Growth of Early Cortical Axons Is Influenced by a Chemoattractant Released from an Intermediate Target. J Neurosci 17: 2445-2458.

Ruiz i Altaba A, Gitton Y, Dahmane N (2001) Embryonic regionalization of the neocortex. Mech Dev 107(1-2): 3-11.

Sakuta H, Suzuki R, Takahashi H, Kato A, Shintani T et al. (2001) Ventroptin: a BMP-4 antagonist expressed in a double-gradient pattern in the retina. Science 293(5527): 111-115.

Schmitt AM, Shi J, Wolf AM, Lu CC, King LA et al. (2006) Wnt-Ryk signalling mediates medial-lateral retinotectal topographic mapping. Nature 439(7072): 31-37.

Schulte D, Furukawa T, Peters MA, Kozak CA, Cepko CL (1999) Misexpression of the Emx-related homeobox genes cVax and mVax2 ventralizes the retina and perturbs the retinotectal map. Neuron 24(3): 541-553.

Seibt J, Schuurmans C, Gradwhol G, Dehay C, Vanderhaeghen P et al. (2003) Neurogenin2 specifies the connectivity of thalamic neurons by controlling axon responsiveness to intermediate target cues. Neuron 39(3): 439-452.

Sen J, Harpavat S, Peters MA, Cepko CL (2005) Retinoic acid regulates the expression of dorsoventral topographic guidance molecules in the chick retina. Development 132(23): 5147-5159.

Serafini T, Colamarino SA, Leonardo ED, Wang H, Beddington R et al. (1996) Netrin-1 is required for commissural axon guidance in the developing vertebrate nervous system. Cell 87(6): 1001-1014.

Sharma K, Leonard AE, Lettieri K, Pfaff SL (2000) Genetic and epigenetic mechanisms contribute to motor neuron pathfinding. Nature 406(6795): 515-519.

Shimogori T, Grove EA (2005) Fibroblast growth factor 8 regulates neocortical guidance of area-specific thalamic innervation. J Neurosci 25(28): 6550-6560.

Shirasaki R, Katsumata R, Murakami F (1998) Change in chemoattractant responsiveness of developing axons at an intermediate target. Science 279(5347): 105-107.

Shirasaki R, Lewcock JW, Lettieri K, Pfaff SL (2006) FGF as a target-derived chemoattractant for developing motor axons genetically programmed by the LIM code. Neuron 50(6): 841-853.

Shu T, Valentino KM, Seaman C, Cooper HM, Richards LJ (2000) Expression of the netrin-1 receptor, deleted in colorectal cancer (DCC), is largely confined to projecting neurons in the developing forebrain. J Comp Neurol 416(2): 201-212.

Sur M, Leamey CA (2001) Development and plasticity of cortical areas and networks. Nat Rev Neurosci 2(4): 251-262.

Sur M, Garraghty PE, Roe AW (1988) Experimentally induced visual projections into auditory thalamus and cortex. Science 242: 1437-1441.

Takahashi H, Shintani T, Sakuta H, Noda M (2003) CBF1 controls the retinotectal topographical map along the anteroposterior axis through multiple mechanisms. Development 130(21): 5203-5215.

Tessier-Lavigne M (1995) Eph receptor tyrosine kinases, axon repulsion, and the development of topographic maps. Cell 82(3): 345-348.

Thor S, Andersson SG, Tomlinson A, Thomas JB (1999) A LIM-homeodomain combinatorial code for motor-neuron pathway selection. Nature 397(6714): 76-80.

Tsuchida T, Ensini M, Morton SB, Baldassare M, Edlund T et al. (1994) Topographic organization of embryonic motor neurons defined by expression of LIM homeobox genes. Cell 79(6): 957-970.

Tuttle R, Nakagawa Y, Johnson JE, O'Leary DD (1999) Defects in thalamocortical axon pathfinding correlate with altered cell domains in Mash-1-deficient mice. Development 126(9): 1903-1916.

Vanderhaeghen P, Lu Q, Prakash N, Frisen J, Walsh CA et al. (2000) A mapping label required for normal scale of body representation in the cortex. Nat Neurosci 3(4): 358-365.

Wagner E, McCaffery P, Drager UC (2000) Retinoic acid in the formation of the dorsoventral retina and its central projections. Dev Biol 222(2): 460-470.

Williams SE, Mann F, Erskine L, Sakurai T, Wei S et al. (2003) Ephrin-B2 and EphB1 mediate retinal axon divergence at the optic chiasm. Neuron 39(6): 919-935.

Xu Q, Mellitzer G, Robinson V, Wilkinson DG (1999) In vivo cell sorting in complementary segmental domains mediated by Eph receptors and ephrins. Nature 399(6733): 267-271.

Yuasa J, Hirano S, Yamagata M, Noda M (1996) Visual projection map specified by topographic expression of transcription factors in the retina. Nature 382(6592): 632-635.

Zhao S, Chen Q, Hung FC, Overbeek PA (2002) BMP signaling is required for development of the ciliary body. Development 129(19): 4435-4442.

Zhou C, Tsai SY, Tsai MJ (2001) COUP-TFI: an intrinsic factor for early regionalization of the neocortex. Genes Dev 15(16): 2054-2059.

Zhou C, Qiu Y, Pereira FA, Crair MC, Tsai SY et al. (1999) The nuclear orphan receptor COUP-TFI is required for differentiation of subplate neurons and guidance of thalamocortical axons. Neuron 24(4): 847-859.

Zhu Y, Li H, Zhou L, Wu JY, Rao Y (1999) Cellular and molecular guidance of GABAergic neuronal migration from an extracortical origin to the neocortex. Neuron 23(3): 473-485.

CHAPTER TWO

The attractive and repulsive functions of Netrin-1 are required for the topographic projection of thalamocortical axons in the ventral telencephalon

Ashton Powell [1, 2], Takayuki Sassa [1], Yongqin Wu [1], Marc Tessier-Lavigne [3, 4], and Franck Polleux [1#]

[1] University of North Carolina, Neuroscience Center, Department of Pharmacology, Chapel Hill, NC 27599-7250, USA
[2] Curriculum in Neuroscience, UNC Chapel Hill, NC 27599, USA
[3] Department of Biological Sciences, Howard Hughes Medical Institute, Stanford University, Stanford, California 94305, USA
[4] Present address: Genentech, Inc., 1 DNA Way, South San Francisco, California 94080, USA

[#] Address correspondence to: polleux@med.unc.edu

Franck POLLEUX
University of North Carolina
Neuroscience Center - Dept of Pharmacology
115 mason farm road –CB#7250
Chapel Hill, NC 27599 -7250
USA

Tel: 919-966-1449

Fax: 919-966-9605

SUMMARY

Recent studies demonstrated that the topography of thalamocortical (TC) axon projections is initiated before they reach the cortex, in the ventral telencephalon (VTel). However, at this point the molecular mechanisms patterning the topography of TC projections in the ventral telencephalon remains poorly understood. Here we show that a long-range, high-rostral to low-caudal gradient of Netrin-1 in the VTel is required *in vivo* for the topographic sorting of TC axons to distinct cortical domains. We demonstrate that Netrin-1 is a chemoattractant for rostral thalamic axons but functions as a chemorepulsive cue for caudal thalamic axons. In accordance with this model, *DCC* is expressed in a high rostro-medial to low caudo-lateral gradient in the DTh, whereas three *Unc5* receptors (*Unc5A-C*) show graded expression in the reverse orientation. Finally, we show that DCC is required for the attraction of rostro-medial thalamic axons to the Netrin-1-rich, anterior part of the VTel whereas DCC and Unc5A/C receptors are required for the repulsion of caudo-lateral TC axons from the same Netrin-1-rich region of the VTel. Our results demonstrate that a long-range gradient of Netrin-1 plays a critical role in the topography of thalamocortical projections before they enter the cortex.

INTRODUCTION

In the central nervous system, the vast majority of axonal projections are organized topographically. The dorsal thalamus is a pivotal forebrain structure, receiving sensory inputs from the periphery and communicating with the cerebral cortex via thalamocortical (TC) axons. Each thalamic nucleus projects topographically to a unique set of cortical areas (*inter-areal*, first-order level of topography) and subsequently, axons emerging within a given thalamic nucleus establish a topographic map of a given sensory modality within each cortical area (*intra-areal*, second-order level of topography). Numerous anatomical studies have demonstrated that the *inter-areal* topography of TC projections is organized so that rostro-medial thalamic neurons project to more rostral cortical areas than caudo-lateral nuclei which tend to project to more caudal cortical areas (Caviness and Frost 1980; Crandall and Caviness 1984; Hohl-Abrahao and Creutzfeldt 1991). The developmental mechanisms leading to the initial guidance and topographic sorting of TC axons first in the ventral telencephalon (VTel) and ultimately the dorsal telencephalon (or cortex) are still poorly understood at the molecular level (reviewed in (Garel and Rubenstein 2004; Vanderhaeghen and Polleux 2004)).

Previous results suggested that the precise topography characterizing thalamocortical projections arises from the progressive sorting of axons by a series of cues present along their pathway rather than by those exclusively present in their final target, the cortex (Garel and Rubenstein 2004; Vanderhaeghen and Polleux 2004). First, analysis of mouse knockouts for genes patterning the ventral telencephalon, including *Ebf1* and *Dlx1/2* revealed a severe disruption of the topography of TC axon projections (Garel et al. 2002). Second, genetic manipulation of rostral patterning molecules such as FGF8 affects the relative positioning of cortical areas without initially changing the topography of thalamocortical projections to the appropriate 'cortical domain' (Garel et al. 2003; Shimogori and Grove 2005). These findings suggested a model where TC axons are guided to their appropriate cortical domain by extracortical cues, i.e. *before* reaching the cortex.

Interestingly, at later stages, unidentified cortical cues are able to re-direct thalamic axons outgrowth to the appropriate cortical area inside the cortex proper (Shimogori and Grove 2005), a result also found in heterotopic cortical grafting experiments (Frappe et al. 2001).

Using a novel *in vitro* assay (the 'wholemount telencephalic' assay), a recent study demonstrated that axons originating from different rostro-caudal domains of the dorsal thalamus (DTh) respond differentially to topographic cues present in the ventral telencephalon that guide these axons to specific cortical domains (Seibt et al. 2003). Currently, the only axon guidance cue identified to play a role in the topographic sorting of TC axons is *ephrinA5*, which is expressed in a high-caudal to low-rostral gradient in the ventral telencephalon (Dufour et al. 2003). In a complementary fashion, several EphA receptors, including *EphA4*, *EphA3* and *EphA7,* are expressed in high rostro-medial to low caudo-lateral gradients in the dorsal thalamus (Dufour et al. 2003) (see **Figure 11**). Using the 'wholemount telencephalic' assay developed by Seibt et al., a parallel study demonstrated that the graded expression of *ephrinA5* in the VTel and some of its receptors such as *EphA7* and *EphA4* in the DTh play a role in the topographic sorting of TC axons in the ventral telencephalon. Interestingly, ephrinA5-EphA4 double knockout (dKO) mice show a significant and fully penetrant topographic shift of thalamocortical projections at the level of the VTel leading to the misprojection of some thalamic motor axons to aberrantly more caudal areas such as the primary somato-sensory cortex. However, TC axon projections still display a significant level of topography in the ephrinA5-EphA4 dKO mouse (Dufour et al. 2003) suggesting the existence of other axon guidance cues involved in the topographic sorting of TC axons in the ventral telencephalon (Vanderhaeghen et al. 2000).

In the present study, we demonstrate that *Netrin-1* is expressed in a high-rostral to low-caudal long-range gradient within the ventral telencephalon. Using a novel *quantitative* axon tracing technique with high spatial resolution, we show that *Netrin-1*-deficient embryos show a severe disruption of the topography of thalamocortical projections at the level of ventral telencephalon before they enter the cortex. Interestingly, both rostral and caudal thalamic axons are affected in the

Netrin-1 knockout mouse and we further demonstrate that both the attractive and repulsive functions of Netrin-1 are required for proper topographic projections of thalamocortical axons along the antero-posterior axis of the ventral telencephalon. These results (1) provide new insights into the molecular and cellular mechanisms specifying the topography of TC axons and (2) demonstrate that the secreted ligand Netrin-1 can specify the topography of projection of large ensembles of axons, a function almost exclusively attributed to the membrane-bound ephrin/Eph signaling system and more recently to Wnt/Ryk signaling.

RESULTS

A novel quantitative method to trace and reconstruct the topography of thalamocortical projections *in vivo*

The introduction of fluorescent carbocyanine dyes as axonal tracers represented a technical breakthrough in our ability to map the development of neuronal connectivity, especially at early embryonic stages in mice (Godement et al. 1987). However, fluorescent carbocyanine dyes such as DiI present several important limitations: (i) their diffusion time in fixed tissue is proportional to the axon length to be traced but typically ranges in 3-5 weeks for embryonic axon tracts in rodents; (ii) during this time frame their important diffusion at the site of injection limits their spatial resolution; (iii) in fixed tissues fluorescent carbocyanines diffuse both anterogradely and retrogradely along axons. In order to circumvent these problems we adapted a well-established anterograde axon tracing technique using lysine-fixable low molecular weight biotinylated dextran amine (BDA or biocytin) microinjection in the dorsal thalamus of embryonic mouse ((Fritzsch 1993; Chang et al. 2000); see also Supplemental Material and Methods for details). Following microinjections of BDA in the DTh of mouse embryos (**Suppl. Fig. 1A**), the isolated hemispheres were incubated in oxygenated artificial cerebro-spinal fluid (aCSF) warmed at 37ºC for up to 6 hours, allowing for fast anterograde tracing of thalamic axons in a short amount of time. After fixation and vibratome sectioning, adjacent 100 microns thick coronal sections are permeabilized and incubated with fluorescent Alexa546-conjugated Streptavidin. This technique enables high spatial resolution (few hundreds of neurons labeled; see **Fig. 4A-G** as well as **Suppl. Fig. 1B'-D'**) and is fully compatible with immunofluorescence (**Suppl. Fig. 1B-D**). Complete anterograde filling of the axon is achieved over long distances (1-2 mm) within only 4-6 hours following BDA injection as shown by the presence of large growth cones at the tip of the majority of axons (**Suppl. Fig. 1E**).

In order to normalize, register and quantify the topography of thalamocortical axon projections in the VTel from microinjections performed in multiple mouse embryos, we developed an image analysis tool allowing (i) reconstruction of the size and position of the BDA injection site in the DTh (**Suppl. Fig. 1G-I-K-M**) as well as (ii) tracing of thalamic axon projections throughout the telencephalon (**Suppl. Fig. 1F-H-J-L**) and (iii) quantitative analysis of the mapping of TC axons projections resulting from multiple injections in a large number of individuals. In order to best represent the degree of topographic sorting achieved by thalamic axons in the ventral telencephalon (i.e. just before entering the cortex), we chose an anatomical landmark lying at the interface between the ventral and the dorsal telencephalon: the cortico-striatal boundary (CSB, also known as the pallial-subpallial boundary; **Fig. 1E**, **Suppl. Fig. 1P-R** and **Suppl. Fig 2**). The axon density map shown in **Suppl. Fig. 1S** is a flat, two-dimensional representation of the CSB as viewed from a virtual observer looking at the telencephalon from a lateral perspective (see **Fig. 1E**).

Topography of thalamocortical projections established in the ventral telencephalon

Using this approach, we precisely mapped the organization of the axonal projections originating from different regions of the dorsal thalamus at the level of the ventral telencephalon. To do this, we performed a series of random microinjections of BDA in the dorsal thalamus (DTh) of E15.5 (**Suppl. Fig. 3**), when TC axons are still pioneering the ventral telencephalon *en route* to the cortex, and E18.5 mouse embryos, a stage when all thalamic axons have reached the cortex (Molnar et al. 1998b). Only injections representing less than 5% of the total volume of the DTh were analyzed in order to ensure that small groups of thalamic neurons are labeled, thus maintaining high spatial resolution.

Our results show that at E18.5, thalamic axons are highly segregated at the corticostriatal boundary (CSB) according to their origin along two main axes of the DTh: the rostro-caudal axis (**Fig. 1A-A3**) and the medio-lateral axis (**Fig. 1B-B3** and **1C-C3**). Axons originating from the rostral third of the DTh cross the CSB (and therefore enter the cortex) at a more rostral level (**Fig. 1A1**) than axons originating from progressively more caudo-lateral levels of the DTh (**Fig. 1A2-A3**). The same segregation is found for axons originating at different levels of the medio-lateral axis of the DTh: axons originating from the medial third of the DTh reach the CSB at more rostro-dorsal levels (**Fig. 1C-C1** and **Fig. 1B-B3**) than axons originating from progressively more lateral thalamic domains (**Fig. 1C2-C3** and **Fig. 1B-B3**) which cross the CSB at progressively more caudal levels.

A converse way to represent the topography of thalamic axon projections in the ventral telencephalon is to categorize thalamic axon populations based on where they cross the CSB and ask where they originate within the dorsal thalamus (**Fig. 1D-D3**). This 'reverse anatomy' approach reveals that axons crossing the CSB at rostral levels originate from more rostro-medial levels of the DTh (**Fig. 1D1**) than axons crossing the caudal CSB, which originate from progressively more caudo-lateral levels of the DTh (**Fig. 1D2-D3**).

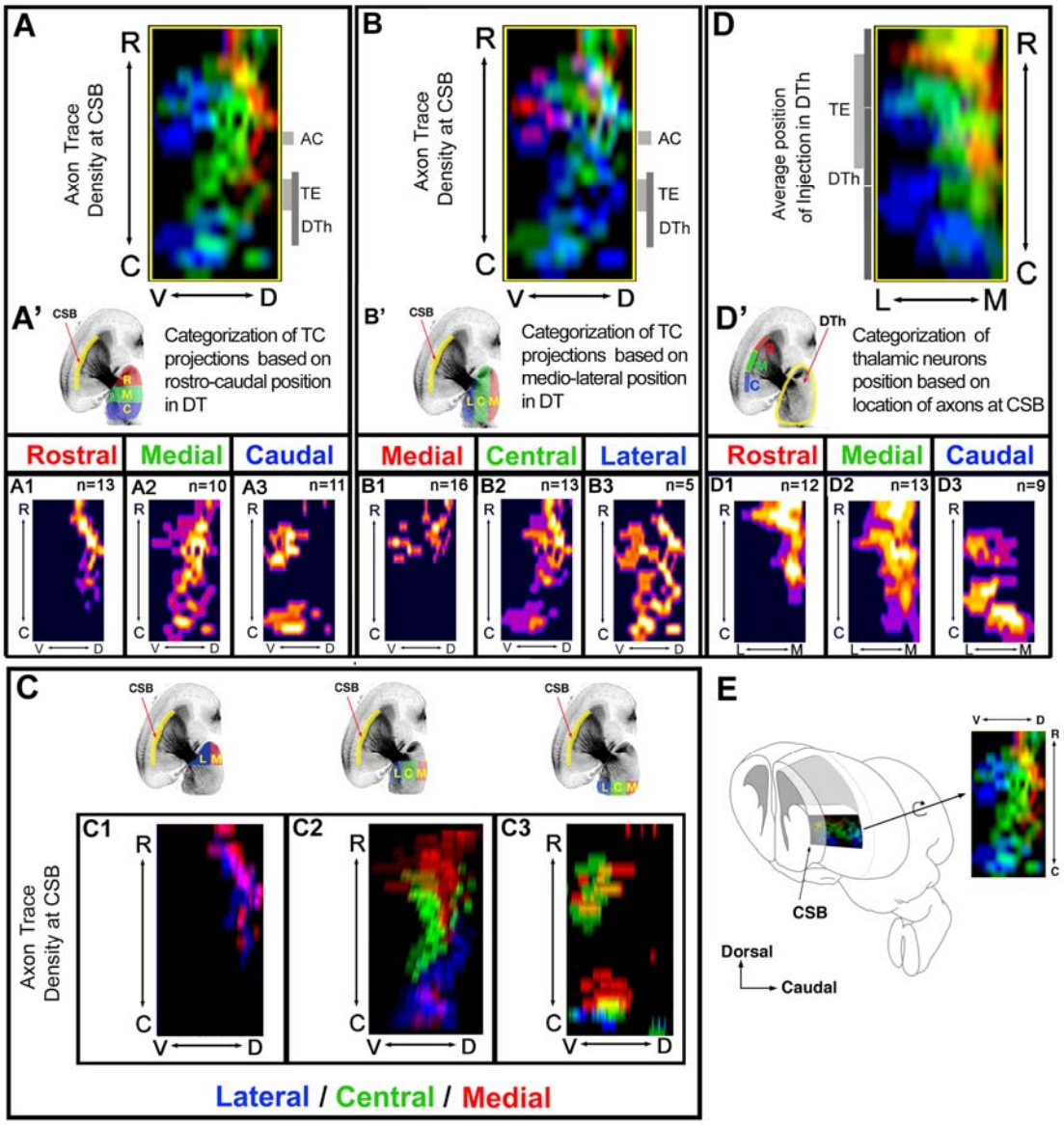

Figure 1. Precise topography of thalamocortical projections achieved at the level of the ventral telencephalon before entering the cortex.

(**A**) Averaged axon density maps quantified from multiple BDA injections (n numbers in A1-A3) clustered in three, arbitrarily-defined thirds along the rostro-caudal axis of the E18.5 mouse DTh (red: rostral, green: medial, blue caudal; as shown in **A'**). (**A1-A3**) Individual average axon density maps for thalamic injections clustered in the rostral (A1), medial (A2) or caudal (A3) most third of the DTh. (**B**) Averaged axon density maps quantified from multiple BDA injections clustered along the medio-lateral axis of the DTh (red: medial, green: central, blue: lateral; as shown in **B'**). (**C**) Averaged axon density maps shown in A1 (rostral third along rostro-caudal extent), A2 (medial third along rostro-caudal extent), and A3 (caudal third along rostro-caudal extent) were further subdivided into three thirds along the medio-lateral axis (C1-C3respectively). (**D-D'**) Averaged position of BDA injection sites in the DTh leading to axons crossing CSB at its most rostral (red), medial (green) or caudal-most (blue) third. (**D1-D3**) Individual averaged density maps of thalamic injection sites leading to axons crossing the CSB at its rostral (D1), medial (D2) or caudal-most (D3) third. (**E**) Schematic representation of the anatomical location of our 2-dimensional, averaged axon density maps shown in this Figure as well as Figure 4.

Interestingly, the general topography of TC projections is already present at E15.5 as demonstrated using the same analysis (see **Suppl. Fig. 3**) confirming that the topographic sorting of TC axons is controlled by axon guidance cues present in the ventral telencephalon when TC axons pioneer this intermediate target while forming the internal capsule (E14-E15; (Seibt et al. 2003)).

These results (i) confirms previous studies that have primarily explored the organization of thalamic projections along the medio-lateral axis of the dorsal thalamus (Molnar and Blakemore 1995; Molnar et al. 1998a; Garel et al. 2002; Garel et al. 2003; Seibt et al. 2003), (ii) reveal that TC projections are also organized along the rostro-caudal axis as proposed previously (Frost and Caviness 1980; Hohl-Abrahao and Creutzfeldt 1991; Dufour et al. 2003; Seibt et al. 2003) and therefore (iii) that the overall axis of topography of TC projections is rostro-medial to caudo-lateral (Vanderhaeghen and Polleux 2004); importantly (iv) this new quantitative tool provides for the first time a framework for the *quantitative* analysis of the function of axon guidance cues in the specification of the topography of thalamocortical projections in the ventral telencephalon *in vivo*.

The rostral part of the ganglionic eminence contains a chemoattractive cue for rostral thalamic axons

These results reveal that thalamocortical axons are organized in a precise 'canvas' at the CSB as a consequence of axon guidance mechanisms specifying the topography of TC projections in the ventral telencephalon i.e. before they enter the dorsal telencephalon (Garel and Rubenstein 2004; Vanderhaeghen and Polleux 2004). In order to identify some of the axon guidance cues patterning the topography of TC axon projections in the VTel, we used a wholemount telencephalic assay recapitulating *in vitro* some of the key aspects of thalamocortical pathfinding observed *in vivo*, including the rostro-caudal axis of TC projections (Seibt et al. 2003). Using this *in vitro* assay, we tested if the mantle region of the rostral part of the ventral telencephalon contains a chemoattractive cue for axons originating from the rostral thalamus by performing grafts of the mantle (post-mitotic) region isolated from the rostral (heterotopic graft) or the caudal VTel (homotopic graft) into the caudal VTel of a wholemount telencephalon (see **Fig. 2A**). In control experiments, homotopic grafts (caudal VTel into the caudal VTel), axons originating from the rostral DTh (DTR; see **Suppl. Fig. 10** for definition) specifically invade the rostral domain of the VTel (arrow in **Fig. 2B**) as observed in control non-grafted wholemount telecenphalic co-cultures (see gray curve in **Fig. 2D** corresponding to the control DTR of Fig. 6B; see also (Dufour et al. 2003; Seibt et al. 2003)). Therefore, grafting itself does not perturb the topography of DTR axon projections in the VTel. However, when a small explant of rostral VTel is grafted heterotopically into the caudal VTel, rostral thalamic axons are significantly attracted towards the caudal VTel (arrows in **Fig. 2C**; see also quantification in **Fig. 2D**), overall randomizing the outgrowth of rostral DTh axons in the VTel. This result strongly suggests the presence of a chemoattractive cue for rostral thalamic axons in the rostral part of the VTel.

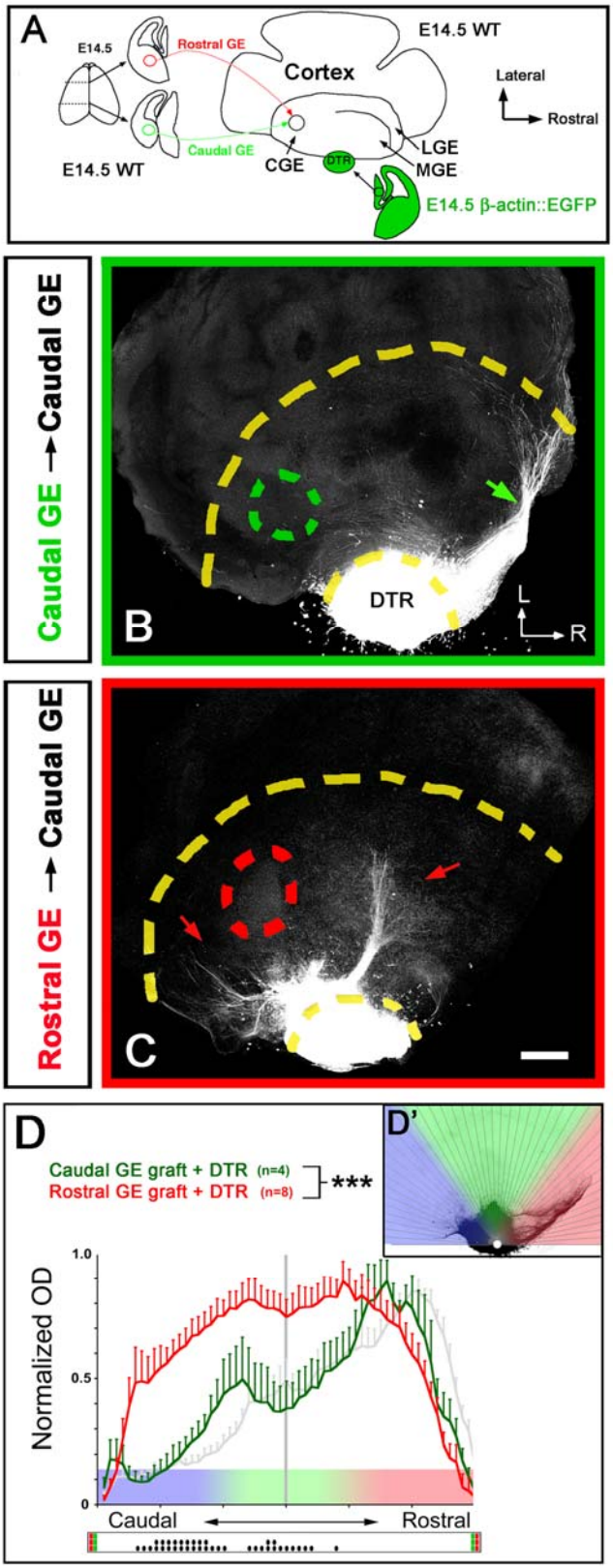

Figure 2. The rostral part of the ganglionic eminence contains a chemoattractant for rostral thalamic axons.

(**A**) Rostral (red) or caudal (green) explants isolated from the mantle region of the ganglionic eminence (VTel) were isolated from 250 microns-thick vibratome sections and grafted into the caudal part of the VTel of a recipient E14.5 wholemount telencephalic vesicle as described previously (Seibt et al. 2003). The rostral part of the DTh (DTR) isolated from coronal slices of an isochronic ß-actin::EGFP-expressing mouse embryos (see **Suppl. Fig. 11** for details on explant isolation) is co-cultured with the wholemount telencephalon for 4 days *in vitro* (div; see Experimental Procedures for detail).

(**B**) Homotopic grafting (caudal VTel into caudal VTel) results in a normal outgrowth of rostral thalamic axons into the rostral domain of the VTel (arrow).

(**C**) In contrast, heterotopic grafting (rostral VTel into the caudal VTel) results in a pronounced change in the topography of DTR axon projections which invade more caudal territories (red arrows) than in control grafts (see B).

(**D**) Quantification of the topography of rostral thalamic axon outgrowth in the VTel presenting homotopic (green) or heterotopic (red) VTel graft into the caudal VTel The gray curve illustrates the topography of DTR axons in control non-grafted experiments shown in Figure 5D. Each histogram represents the average normalized optical density (OD) from the EGFP signal measured in 60 radial bins centered on the thalamic explant as shown in (**D'**).

*** $p<0.001$ ANOVA one-way test (overall effect: bins versus experimental conditions). The raster-like dot plot presented under the histograms represents the significance of individual bin comparisons between the two experimental conditions according to a PLSD-post-hoc test (• $p<0.05$; •• $p<0.01$ and ••• $p<0.001$). Scale bar value: B-C, 250 microns.

Netrin-1 is expressed in a high-rostral to low-medial gradient in the ganglionic eminence

Earlier studies have shown that Netrin-1 is expressed in the mantle (post-mitotic) region of the ventral telencephalon of mouse embryos where the internal capsule forms (Serafini et al. 1996; Metin et al. 1997; Tuttle et al. 1999; Braisted et al. 2000). We carefully examined the spatial pattern of Netrin-1 expression using two independent approaches at E14.5 and E15.5, when the vast majority of TC axons pioneer the ventral telencephalon to form the internal capsule *en route* to the cortex in the mouse embryo (Molnar et al. 1998b; Tuttle et al. 1999). First, using *in situ* hybridization performed on horizontal sections of E14.5 (**Fig. 3A-B**) or E15.5 mouse embryos (**Fig. 3C-E and 3I**), we found that *Netrin-1* mRNA is expressed in a high-rostral to low-caudal gradient in the mantle region of the VTel

We took advantage of a 'gene trap' mouse line where a LacZ reporter cassette was inserted into the first intron of the *Netrin-1* coding sequence (*Ntn1*$^{Gt(pGT1.8TM)629Wcs}$ abbreviated *Ntn1*^{LacZ} allele; (Serafini et al. 1996)). As shown in **Figure 3F-G**, anti-ß-galactosidase immunofluorescence in E15.5 *Ntn1*$^{LacZ/+}$ mouse embryos recapitulates faithfully the graded expression of *Netrin-1* mRNA at the same age (**Fig. 3C-D**). In order to examine the spatial relationship between this gradient of *Netrin-1* expression and thalamocortical axons in the internal capsule, we performed L1 immunofluorescent staining in combination with anti-ß-galactosidase immunofluorescence in *Ntn1*$^{Lacz/+}$ embryos at E15.5 (**Fig. 3H**). A quantitative analysis of both *Netrin-1* mRNA expression and anti-ß-galactosidase immunofluorescence along the rostro-caudal axis of the VTel reveals an almost linear high-rostral to low-caudal gradient (**Fig. 3I**). Therefore, this gradient of Netrin-1 expression represents a good candidate to exert a function in the control of the topography of thalamocortical axons along the rostro-caudal axis of the VTel.

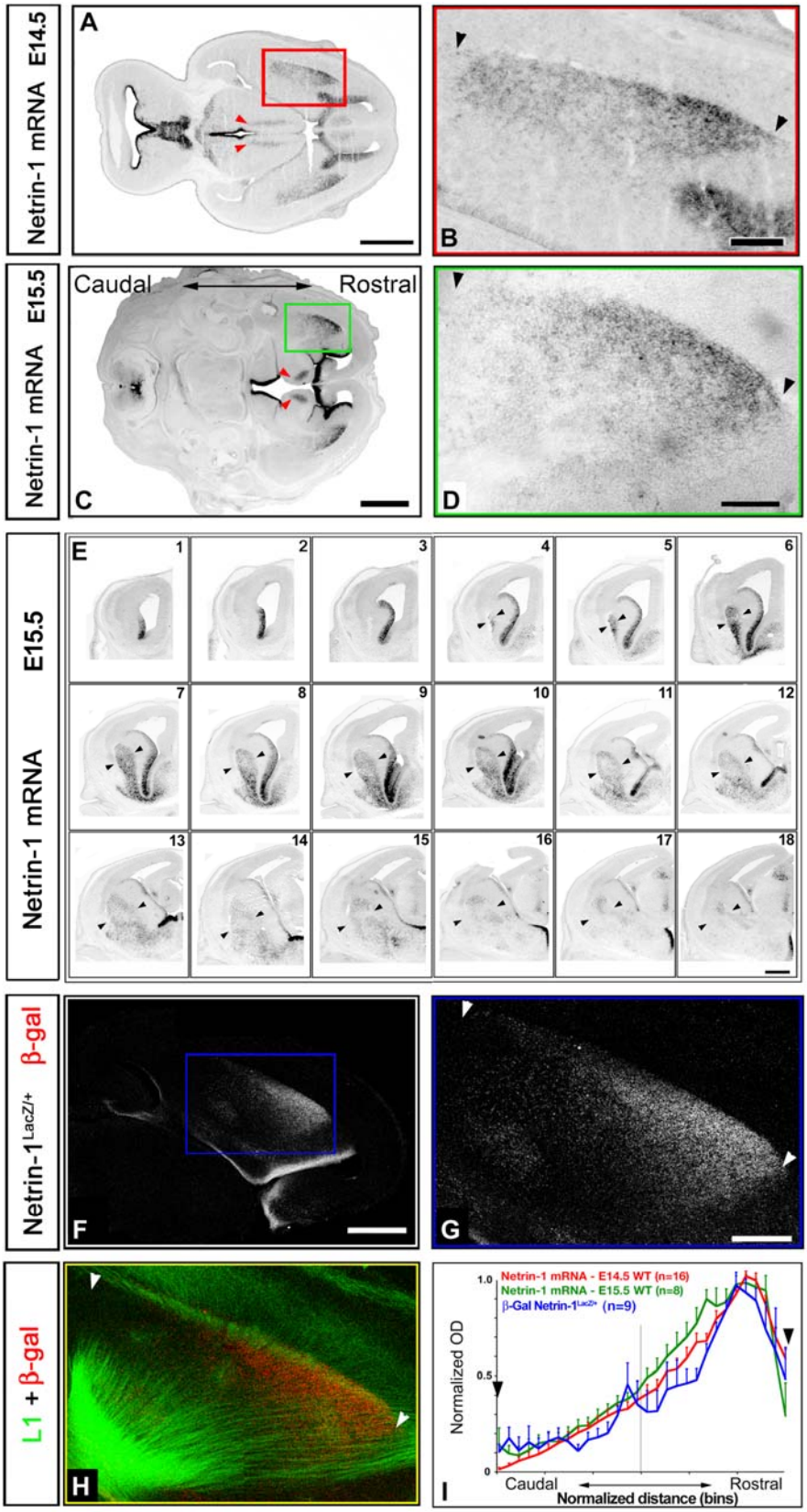

Figure 3. Netrin-1 is expressed in a high-rostral to low-caudal gradient in the ganglionic eminence.

Figure 3. Netrin-1 is expressed in a high-rostral to low-caudal gradient in the ganglionic eminence. Cont.

(**A-D**) mRNA *in situ* hybridization performed on horizontal sections of E14.5 (A-B) and E15.5 (C-D) mouse embryos reveals that Netrin-1 mRNA is expressed in a high-rostral to low-caudal gradient in the ventral telencephalon (VTel). Also note that Netrin-1 is expressed in the dorsal thalamus itself (arrowheads in A and C).

(**E**) Series of eighteen coronal sections from a single E15.5 wild-type mouse brain showing that the high-rostral to low-caudal gradient of Netrin-1 mRNA expression is found in the mantle region of the ganglionic eminence. Sections are numbered from rostral (#1) to caudal (#18). Arrowheads indicate the location of the internal capsule.

(**F-G**) This rostro-caudal gradient can also be visualized on horizontal sections of a *Netrin-1*$^{LacZ/+}$ E15.5 mouse embryo both at low (F) and high (G) magnification on horizontal sections immunostained for ß-galactosidase.

(**H**) This high-rostral to low-caudal gradient of *Netrin-1* expression coincides spatially with thalamocortical axons in the internal capsule in the VTel as visualized by this double immunofluorescence for the cell adhesion molecule L1 (green) and ß-galactosidase (red).

(**I**) Quantification of the gradient of Netrin-1 mRNA expression inside the VTel at E14.5 (red), E15.5 (green) and ß-galactosidase immunofluorescence in a *Netrin-1*$^{LacZ/+}$ E15.5 mouse (blue) using normalized optical density measurement in 30 vertical bins oriented along the rostro-caudal axis on horizontal sections. 'n' indicates the number of sections used to measure the normalized optical density values along the rostro-caudal axis. In panels B, D and G, arrowheads point to the rostro-caudal and dorso-ventral width of the internal capsule within the ventral telencephalon.

Scale bars values: A, 800 microns; B, 250 microns; C, 1 mm; D, 250 microns; E, 80 microns; F, 600 microns; G-H, 200 microns.

Netrin-1 is necessary for the establishment of the topography of thalamocortical projections in the ganglionic eminence.

Inspection of the internal capsule of wild-type or Netrin-1 knockout embryos at E18.5 using anti-L1 staining (which labels both thalamocortical and callosal but not corticothalamic axons (Ohyama et al. 2004)) failed to reveal any major axon outgrowth defect (see **Suppl. Fig. 4**): horizontal sections of E17.5 *Netrin-1* knockout embryos revealed no obvious decrease in the number of thalamic axons compared to wild-type littermate at the level of (i) the thalamic peduncle (axon bundle crossing the diencephalic to telencephalic boundary), (ii) the internal capsule or (iii) the corticostriatal boundary compared to wild-type embryos (**Suppl. Fig. 4**). This qualitative analysis suggested that Netrin-1 is not simply required *in vivo* for proper outgrowth of thalamic axon into the internal capsule as suggested previously (Braisted et al. 2000). As shown in Figure 5 below, wild-type DTR or DTC axons growing in the ventral telencephalon of Netrin-1-deficient embryos confirms quantitatively the absence of axon outgrowth defect compared to control wild-type telencephalon (quantified in **Suppl. Fig. 7**). Therefore, we conclude that Netrin-1 expression is not required for extension of thalamic axons in the ventral telencephalon.

In order to test if Netrin-1 controls the *guidance* of thalamocortical (TC) projections in the ventral telencephalon, we performed BDA microinjections in the dorsal thalamus (DTh) of both wild-type (n=34) and *Netrin-1*$^{LacZ/LacZ}$ (*Netrin-1-/-*; n=17) E18.5 embryos. A qualitative illustration of the type of topographic projection defect observed in the Netrin-1 knockout is shown in **Fig. 4A-G** following a relatively large injection of BDA (more than 5% of DTh volume, injection not used for our quantitative analysis) in the rostral part of the DTh of a control (Netrin-1$^{+/-}$; **Fig. 4B-D**) or Netrin-1 knockout embryo (**Fig. 4E-G**). Using an oblique plane of section revealing the entire tract of thalamocortical projections from the DTh to the cortex (see **Fig. 4A**; (Agmon and Connors 1991)), we show that thalamic axons originating from the rostral DTh invade more caudal territories of the VTel of Netrin-1 knockout embryos (arrows in **Fig. 4E-G**) than in control embryos (**Fig. 4B-D**).

Our quantitative analysis of a large number of BDA injections in E18.5 embryos reveals a profound disruption of the topography of thalamocortical projections in the *Netrin-1* knockout mouse. When viewed as a whole, the topography of the Netrin-1-/- mouse is completely disrupted (**Suppl. Fig. 12**). In Netrin-1-/-, injections along the rostro-caudal or medio-lateral axis of the DTh do not appear to segregate at CSB, indicating a lack of topography in the system. In viewing the reverse anatomical map, the projection path of the Netrin-1-/- DTh appears to have little resemblance to that of the wild-type. To study this, we performed a statistical analysis to show differences in TCA trajectory between wild-type and mutant mice. The significance of the differences between each axon density map of TC projections is tested statistically using a two-way ANOVA test comparing Netrin-1+/+ and Netrin-1-/- embryos (**Suppl. Fig. 6**). First when clustered along the rostro-caudal axis of the DTh, the most significant differences in the pattern of TC projections concerns axons originating from the rostral thalamus which reach the dorsal telencephalon at significantly more caudo-ventral levels of the CSB. Thalamic axons originating from both the medial and caudal third of the DTh reach the CSB at a significantly more rostral level in the Netrin-1-/- embryos than in wild-type control (**Fig. 4J-K** and **Suppl. Fig 6B-D**).

Similar disruption of the topography of TC projections in the VTel is visible when examining the medio-lateral organization of thalamic projections (**Fig. 4L-O**): axons originating from the medial and central part of the DTh reach the CSB at more caudo-ventral levels in Netrin-1 knockout compared to wild-type mouse embryos. Additionally, axons originating from the lateral-most third of the DTh in Netrin-1 knockout embryos are significantly shifted caudo-ventrally at the level of the CSB compared to wild-type control (**Fig. 4O** and **Suppl. Fig. 6H**).

Using a reciprocal analysis, we confirmed these results by categorizing neuron position within the DTh based on the rostro-caudal level at which their axons cross the CSB (**Fig. 4P).** This analysis confirms the severe disruption of topographic outgrowth of thalamic axons characterizing the *Netrin-1* knockout embryos. Axons crossing the CSB at its rostral-most third originate from the rostro-medial part of the DTh in wild-type embryos (green in **Fig. 4Q** and **Suppl. Fig. 6J**) but in

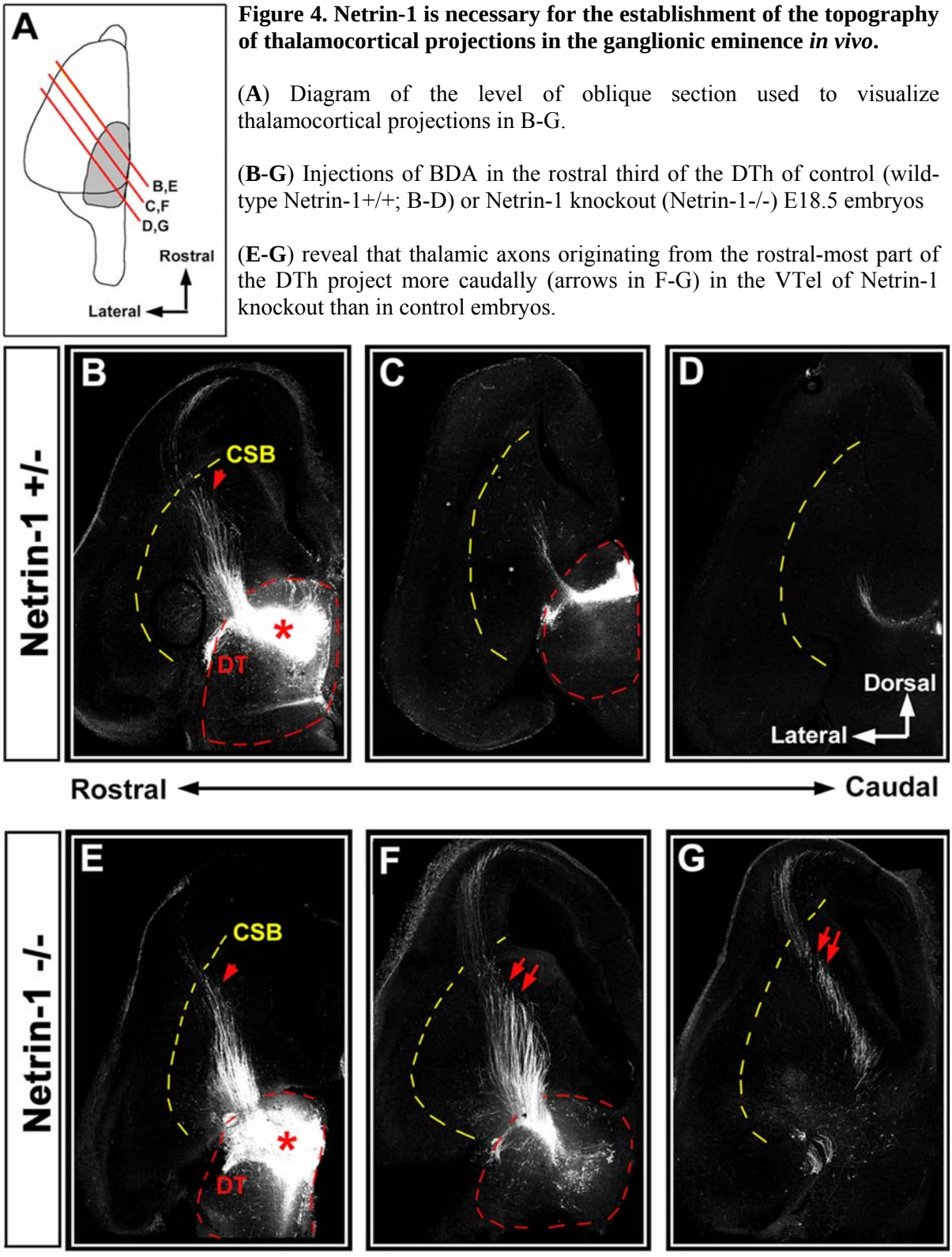

Figure 4. Netrin-1 is necessary for the establishment of the topography of thalamocortical projections in the ganglionic eminence *in vivo*.

(**A**) Diagram of the level of oblique section used to visualize thalamocortical projections in B-G.

(**B-G**) Injections of BDA in the rostral third of the DTh of control (wild-type Netrin-1+/+; B-D) or Netrin-1 knockout (Netrin-1-/-) E18.5 embryos

(**E-G**) reveal that thalamic axons originating from the rostral-most part of the DTh project more caudally (arrows in F-G) in the VTel of Netrin-1 knockout than in control embryos.

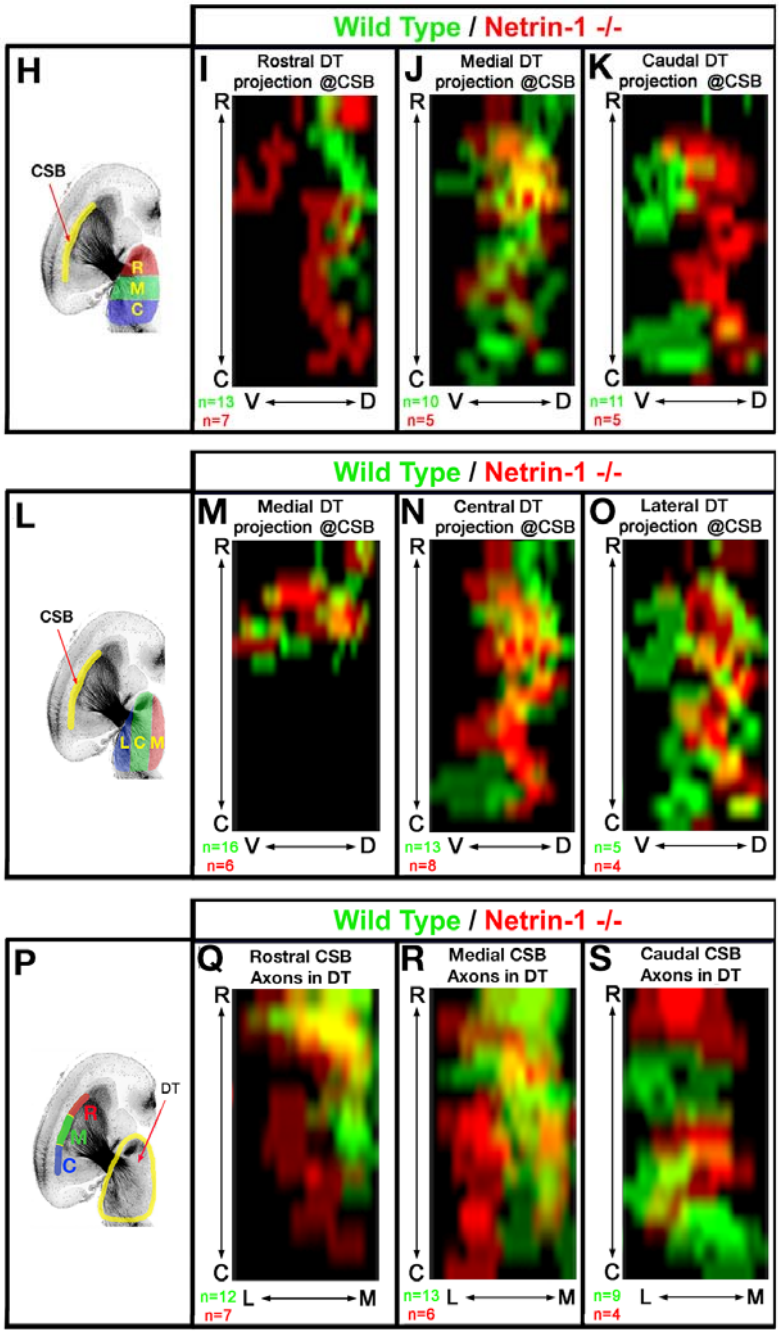

Figure 4. Netrin-1 is necessary for the establishment of the topography of thalamocortical projections in the ganglionic eminence *in vivo*. Cont.

(**H-O**) Averaged axon density maps showing the distribution of thalamic axons at the CSB of E18.5 wild-type (green) or Netrin-1-/- embryos (red) for thalamic injections clustered along the rostro-medial axis (I-K; as depicted in H) or the medio-lateral axis (M-O; as depicted in L).

(**P-S**) Averaged density maps of injection sites in the DTh leading to thalamic axons crossing the CSB at the rostral (Q), medial (R) or caudal (S) most thirds of the CSB in the wild-type control mice (green) or Netrin-1-/- at E18.5. For statistical analysis of these density maps, see **Supplementary Figure 6.**

contrast originate from a more widespread area of the DTh in the *Netrin-1* knockout, including the extreme caudo-lateral territories of the DTh (**Fig. 4Q** and **Suppl. Fig. 6J**). Axons crossing the CSB along its medial third originate from a more caudo-lateral domain of the DTh in *Netrin-1* knockout compared to wild-type littermates (**Fig. 4R** and **Suppl. Fig. 6K**). Strikingly, the reverse is found for thalamic axons crossing the CSB along its caudal third, where cell bodies are found in a more rostro-medial position of the DTh in *Netrin-1* knockout than in wild-type littermates (**Fig. 4S** and **Suppl. Fig. 6L**).

These results are surprising because they suggest that Netrin-1 gradient in the ventral telencephalon is not only attracting rostro-medial thalamic axons in the rostral part of the ventral telencephalon but might also act as a repulsive cue for caudo-lateral thalamic axons. In other words, in the absence of Netrin-1, rostral thalamic axons are shifted caudally according to their responsiveness to Netrin-1 (compatible with the removal of a rostral attractant in the VTel) but at the same time caudal thalamic axons are shifted rostrally according to their responsiveness to Netrin-1 (compatible with the removal of a rostral repulsive cue in the VTel).

However, there is a potential caveat with this interpretation: Netrin-1 is not only expressed in the VTel, it is also expressed in the dorsal thalamus itself (see arrowheads in **Fig. 3A** and **3C**). Therefore, at this point, we could not exclude that some of the topographic defects of thalamocortical axon outgrowth observed *in vivo* in the *Netrin-1* knockout embryos could be due to *Netrin-1* expression in the DTh itself.

Graded Netrin-1 expression in the ventral telencephalon is required for proper topographic sorting of thalamocortical projections.

In order to test whether the graded expression of Netrin-1 in the VTel is required for the establishment of the topography of TC projections, we took advantage of our wholemount telencephalic co-culture assay in order to uncouple the genotype of the dorsal thalamus and the telencephalon (see (Dufour et al. 2003; Seibt et al. 2003)). As shown in **Fig. 5A** and **5E**, we performed wholemount co-cultures between wild-type E14.5 EGFP-expressing dorsal thalamic explants (rostral DTh **Fig. 5A-D** or caudal DTh **Fig. 5E-H**) with telencephalic vesicles isolated from isochronic wild-type (**Fig. 5B and F**) or *Netrin-1*-/- embryos (**Fig. 5C** and **5G**).

Our results show that in the absence of Netrin-1 in the ventral telencephalon, a significant proportion of axons originating from the rostral part of the DT are shifted caudally (red arrow in **Fig. 5C**) compared to control co-cultures (arrow in **Fig. 5B**). However, a contingent of rostral thalamic axons is still projecting to the rostral third of the VTel (arrowheads in **Fig. 5C**). The quantification of these co-cultures (**Fig. 5D**) demonstrates that axons originating from the rostral DTh and growing in Netrin-1-deficient telencephalon can be sub-divided in two sub-populations that are both significantly shifted caudally (two peaks in **Fig. 5D**) compared to control co-cultures (green arrow in **Fig. 5D**).

Next we performed wholemount telencephalic co-cultures using axons originating from the caudal part of the DTh (DTC). As shown previously (Seibt et al. 2003) DTC axons diffusely invade caudal territories of the VTel (**Fig. 5F** and **H**). However, caudal DTh axons growing in a Netrin-1-deficient telencephalon do not show a preferential caudal outgrowth (arrowhead in **Fig. 5G**) and instead display a more random distribution in the ventral telencephalon (**Fig. 5H;** see also **Suppl. Fig. 7**). Taken together, these results demonstrate that the high-rostral to low-caudal gradient of Netrin-1 expression in the VTel is required for the differential topographic mapping of thalamic axons before they reach the cortex. These results also suggest that the function of Netrin-1 in the topographic sorting of TC axons in the VTel requires both its attractive and repulsive properties.

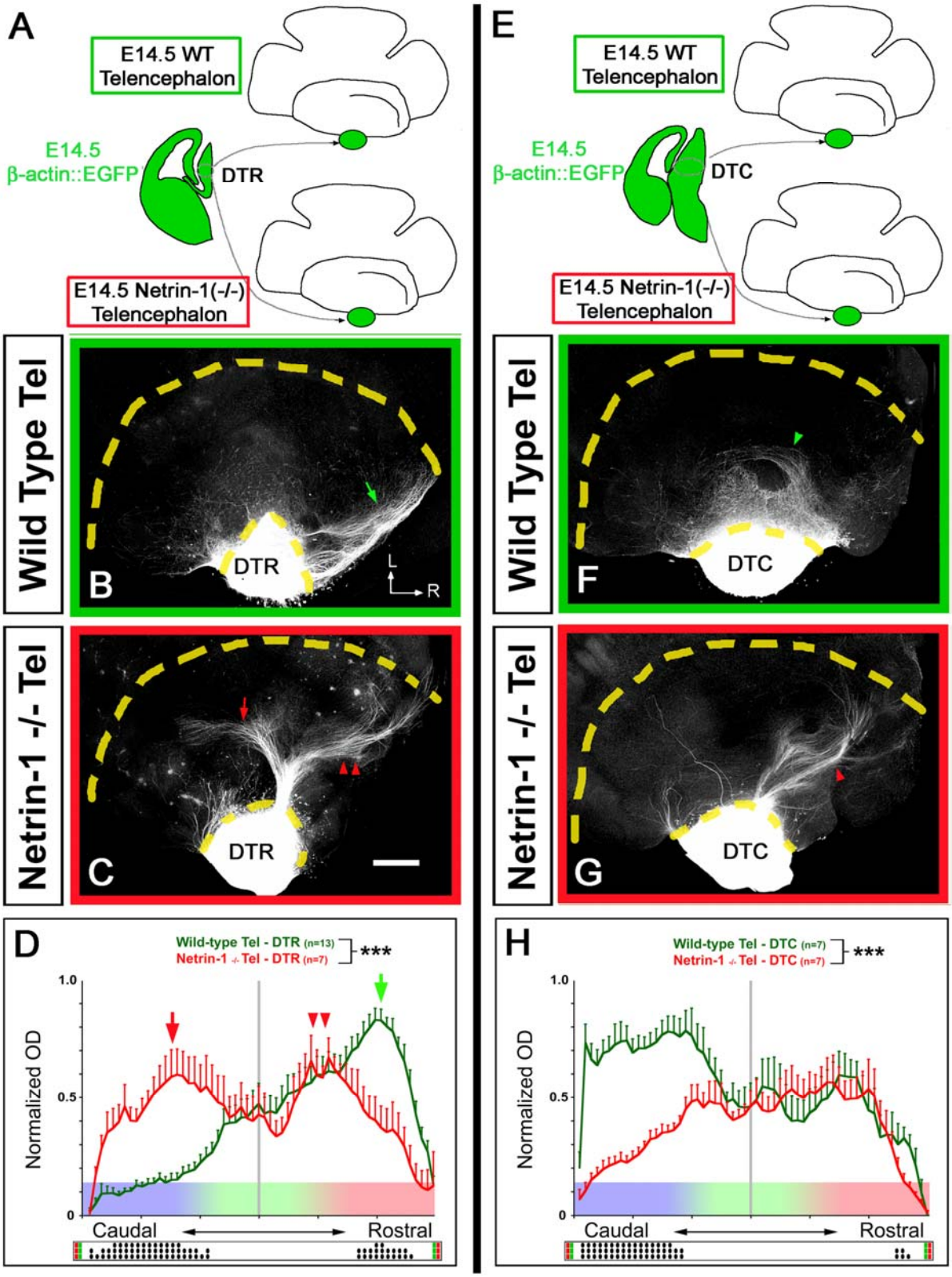

Figure 5. Netrin-1 is required in the ventral telencephalon to specify the topography of projection of both rostral and caudal thalamic axons.

Figure 5. Netrin-1 is required in the ventral telencephalon to specify the topography of projection of both rostral and caudal thalamic axons. Cont.

(**A** and **E**) Schema of the experimental paradigm: rostral (DTR; A-D) or caudal (DTC; E-H) thalamic explants isolated from ß-actin::EGFP E14.5 embryos were co-cultured with E14.5 wholemount telencephalon from either wild-type isochronic embryos (B and F) or Netrin-1 knockout isochronic embryos (C and G) in order to test for the requirement of Netrin-1 specifically in the VTel.

(**B-C**) DTR axons show a strong preferential outgrowth in the rostral part of the wild-type VTel (green arrow in B). A contingent of wild-type DTR axons grow significantly more caudally in a Netrin-1-deficient VTel (red arrow in C) whereas another contingent of TC axons maintains its projection to the rostral part of the VTel (double arrowheads in C).

(**D**) Quantification of normalized optical density (OD) of DTR-EGFP axons growing in wild-type (n=13, green) or Netrin-1 knockout (n=7, red) telencephalon. Significantly more EGFP-positive axons are growing in the caudal part of the VTel in the Netrin-1 knockout than in the wild-type telencephalon. *** $p<0.001$ ANOVA one-way test (bins *vs.* genotype).

(**F-G**) Axons originating from the caudal DTh preferentially grow in the caudal part of wild-type VTel (green arrow in F) but grow significantly more rostrally in the Netrin-1-deficient VTel (red arrowhead in G). (**H**) Quantification of normalized optical density (OD) of DTC-EGFP axons growing in wild-type (n=13, green) or Netrin-1 knockout (n=7, red) telencephalon.

The raster-like dot plots presented under each histogram (D and H) represents the significance of individual bin comparisons between the two experimental conditions according to a PLSD post-hoc test (• $p<0.05$; •• $p<0.01$ and ••• $p<0.001$). Scale bar values: B-C, F-G, 300 microns.

Netrin-1 is attractive for rostral thalamic axons and repulsive for caudal thalamic axons

We first tested whether *Netrin-1* differentially affects DTh axon populations through either attractive or repulsive activity, by testing directly if Netrin-1 has a differential effect on different TC axons using collagen co-cultures between E14.5 DTR or DTC explants and aggregates of HEK 293 that are stably expressing Netrin-1 (Keino-Masu et al. 1996) (**Suppl. Fig. 7**). These results show that DTR axons are significantly attracted by Netrin-1 (in accordance with (Braisted et al. 1999; Braisted et al. 2000)) but at the same time that DTC axons are not attracted but rather moderately repulsed by Netrin-1 *in vitro*. One of the drawback of this collagen co-culture assay is that TC axons are not growing through their 'natural' environment and therefore, axon responsiveness to specific axon guidance cue could be biased because axons do not express the right complement of axon guidance receptors. A precedent for this has been well-documented in the developing spinal cord where commissural axons only upregulate surface expression of Robo receptors after crossing the midline and therefore are not responding to the midline repellent Slits before they reach the midline (Zou et al. 2000).

In order to better test the differential effects of Netrin-1 on the response of thalamic axons originating from the rostral and caudal thalamus in a contextual environment, we performed wholemount telencephalic co-cultures where a source of Netrin-1 (using HEK293 cells stably expressing Netrin-1 and embedded in collagen (Metin et al. 1997)) is ectopically placed in the caudal VTel (see **Fig. 6A** and **E**). Axons originating from the rostral thalamus now invade more caudal territories of the VTel, overriding the repulsive effect of ephrinA5/EphA4 activity (Dufour et al. 2003), suggesting that they are attracted towards a caudal source of Netrin-1 (arrows in **Fig. 6C**) whereas control 293 cells graft has no effect (**Fig. 6B**).

Interestingly, the reverse is found for caudal thalamic axons, which are significantly shifted rostrally when confronted with a caudal source of Netrin-1 (**Fig. 6G** and **6H**) as compared to control grafts (**Fig. 6F** and **6H**). Note that this caudal source of Netrin-1 imposed experimentally is likely to disrupt the endogenous gradient of Netrin-1 still present at high levels in the rostral part of the ventral telencephalon (see **Fig. 3**). These results strongly suggest that in the ventral telencephalon, Netrin-1 functions as a chemorepulsive cue for caudal thalamic axons and a chemoattractive cue for rostral thalamic axons.

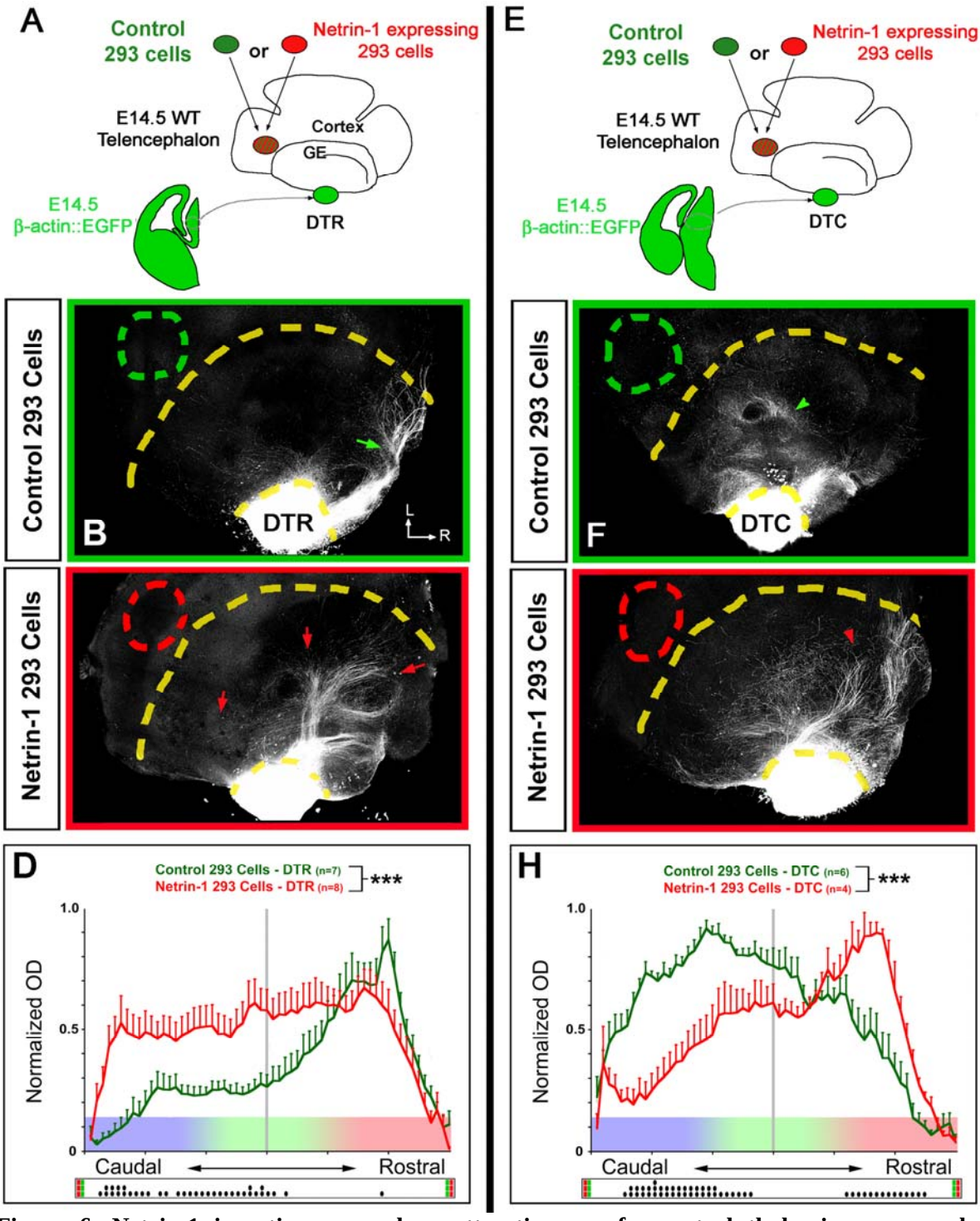

Figure 6. Netrin-1 is acting as a chemoattractive cue for rostral thalamic axons and a chemorepulsive cue for caudal thalamic axons.

Figure 6. Netrin-1 is acting as a chemoattractive cue for rostral thalamic axons and a chemorepulsive cue for caudal thalamic axons. Cont.

(**A** and **E**) Experimental paradigm: control 293 cells (B and F) or 293 cells stably expressing Netrin-1 and embedded in collagen (C and G) were grafted in proximity of the caudal part of the VTel of E14.5 wild-type wholemount telencephalon co-cultured with EGFP-expressing explants isolated from isochronic rostral DTh (DTR; B-C) or caudal DTh (DTC; F-G).

(**B-C**) Axons originating from the rostral DTh grow rostrally in the VTel of telencephalic wholemount grafted with control 293 cells in the caudal VTel (green arrow in B). In contrast, a significant proportion of DTR axons project caudally when Netrin-1 expressing cells are grafted in the caudal VTel (red arrows in C).

(**D**) Quantification of normalized optical density (OD) of DTR-EGFP axons growing in VTel grafted caudally with control 293 cells (green) or VTel grafted caudally with Netrin-1 expressing 293 cells (red).

(**F-G**) Axons originating from the caudal DTh grow caudally in the VTel of a telencephalic wholemount with control 293 cells grafted in the caudal VTel (green arrowheads in F). In contrast, a significant proportion of DTC axons grow rostrally when Netrin-1 expressing cells are grafted in the caudal VTel (red arrowhead in G).

(**H**) Quantification of normalized optical density (OD) of DTC-EGFP axons growing in VTel with control 293 cells grafted caudally (green) or VTel with Netrin-1 expressing 293 cells grafted caudally (red). Significantly more DTC axons grow to the rostral part of the VTel grafted with Netrin-1 expressing cells than in control-graft. *** $p<0.001$ ANOVA one-way test (overall effect: bins versus experimental conditions).

The raster-like dot plot presented under each histogram (D and H) represents the significance of individual bins comparisons performed between the two experimental conditions according to a PLSD-post-hoc test (• $p<0.05$; •• $p<0.01$ and ••• $p<0.001$).

Scale bar values: B-C, F-G, 150 microns.

Netrin-1 receptors are expressed in complementary domains in the dorsal thalamus

So far, our results imply that dorsal thalamic neurons express different Netrin-1 receptors conferring attractive (for rostral DTh axons) or repulsive (for caudal DTh axons) responses to Netrin-1. In order to substantiate this hypothesis, we examined the pattern of expression of several transmembrane receptors known to mediate Netrin-1 responsiveness: *Deleted in Colorectal Cancer* (*DCC*) known to mediate chemoattraction to Netrin-1 (Keino-Masu et al. 1996) and homologs of the *C.elegans Unc5* receptor called *Unc5A-C* (also called *Unc5H1-3*) known to mediate chemorepulsion to Netrin-1 upon heterodimerization with DCC (Ackerman et al. 1997; Leonardo et al. 1997). A fourth mammalian ortholog of *Unc5* has been recently identified but its affinity for Netrin-1 has not been assessed yet (Zhong et al. 2004). We performed *in situ* hybridization for *DCC* and *Unc5A, Unc5B* and *Unc5C* (**Fig. 7**) on serial horizontal sections of E14.5 mouse embryos in order to best visualize differences of Netrin-1 receptor expression along the rostro-medial and caudo-lateral axis of the dorsal thalamus.

First, we wanted to define accurately the caudal extent of the DTh on horizontal sections from E14.5 mouse embryos. To do this we used two markers: first the transcription factor *Gbx2* which is a reliable marker of the dorsal thalamus at E14.5 (Bulfone et al. 1993; Nakagawa et al. 1999) and the transcription factor *bHLHB4* which has been recently identified as a marker of the pretectum which is immediately caudal to the dorsal thalamus during embryogenesis (Bramblett et al. 2002). Our results show that these two markers reliably identify the caudal limit of the dorsal thalamus on horizontal sections of E14.5 mouse embryos along the dorso-ventral axis of the diencephalic-mesencephalic boundary (**Fig. 7C-K**). Therefore, in the rest of our analysis, we used the caudal limit of *Gbx2* expression as a marker of the caudal limit of the DTh (see lines in **Fig. 7N, Q, T, W**).

We found that *DCC* mRNA is expressed at high level in the rostro-medial part of the DTh (**Fig. 7L-Q** and **Suppl. Fig. 9A-B**) but is also expressed at lower levels in more caudo-lateral territories of the DTh (arrows in **Fig. 7U** and **Suppl. Fig. 9C**). In contrast, *Unc5A*, *Unc5B* and *Unc5C* are expressed in non-overlapping caudo-lateral domains of the DTh (**Fig. 7M-N, 7P-Q** and **7S-T** respectively). The star in **Fig.7N-Q-T-W** marks the peak of *Unc5A-C* expression. These complementary patterns of expression are compatible with our model suggesting that axons originating from the rostro-medial DTh (which are attracted by Netrin-1 in the rostral part of the VTel) express *DCC* only (**Fig. 11B**) whereas thalamic axons originating from the caudo-lateral domain of the DTh are repulsed by Netrin-1 in the rostral VTel and express *Unc5A-C* as well as low levels of *DCC* (**Fig. 11C**). Interestingly, *DCC* and *Unc5A-C* are highly expressed in other parts of the diencephalon including the epithalamus (**Suppl. Fig. 9B-C, E and H**), the ventral thalamus (**Suppl. Fig. 9B, E, K**) as well as in the pretectum (**Fig. 7L-W**) suggesting other functions during diencephalic/mesencephalic development.

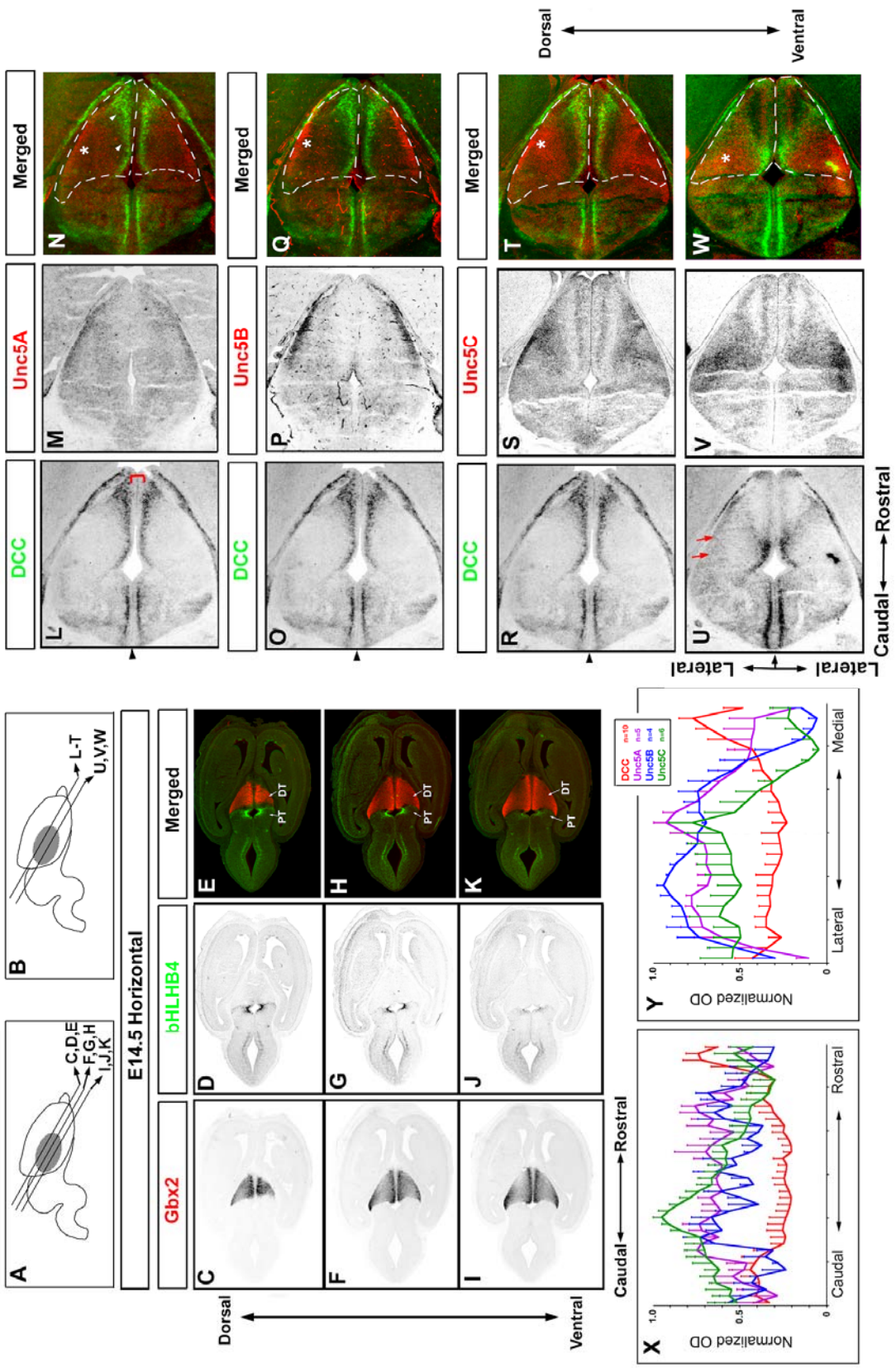

Figure 7. Patterns of expression of Netrin-1 receptors in the mouse dorsal thalamus.

Figure 7. Patterns of expression of Netrin-1 receptors in the mouse dorsal thalamus. Cont.

(**A, C-K**) At E14.5, mRNA *in situ* hybridization (ISH) for *Gbx2* delineates the dorsal thalamus (DTh) along its rostro-caudal axis on horizontal sections distributed along the dorso-ventral axis of the DTh (C-F-I; see levels of section in A). Expression of *bHLHB4* on adjacent sections delineates the pretectum (PT) (D-G-J). When merged (E-F-K), *Gbx2* and *bHLHB4* show non-overlapping and complementary expression at the diencephalic-mesencephalic boundary delineating the caudal limit of the dorsal thalamus on E14.5 horizontal sections.

(**B, L-W**) *In situ* hybridization for *DCC* (L-O-R-U, green in N-Q-T-W), *Unc5A* (M, red in N) and *Unc5B* (P, red in Q) and *Unc5C* (S and V, red in T and W) on adjacent horizontal sections of E14.5 mouse embryos isolated at two levels of sections along the dorso-ventral axis of the DTh (B). *DCC* is expressed most highly in a rostro-medial domain of the DTh in post-mitotic regions (data not shown) and is excluded from the thin ventricular zone left at this time (bracket in L). Conversely, *Unc5A*, *Unc5B* and *Unc5C* are all expressed in non-overlapping caudo-lateral domains of the DTh (stars in N-Q-T-W indicate the approximate peak of expression). The dashed line in panels N-Q-T-W corresponds to the actual limit of the dorsal thalamus as defined by *Gbx2* expression on adjacent sections (see I-K). Note that *DCC* is expressed at low but significant levels in the caudo-lateral domain of the DTh (red arrows in U) where it is co-expressed with *Unc5C* (star in V).

(**X-Y**) Quantification of the gradient of *DCC* (n=10), *Unc5A* (n= 5), *Unc5B* (n=4) and *Unc5C* (n=6 sections) mRNA expression along the rostro-caudal axis (X) and the medio-lateral axis (Y) of the dorsal thalamus at E14.5 as indicated by the lines in L. Gradients were measured by normalizing the optical density values on multiple adjacent sections (number indicated in Y) shown in L-W. Arrowhead in L-O-R-U indicates the midline.

Blocking DCC function impairs the ability of rostral DTh axons to grow rostrally in the VTel

We tested if DCC is required in the topographic projection of thalamic axons by using a well-characterized function-blocking anti-DCC antibody (clone AF5 (Keino-Masu et al. 1996)) in the wholemount telencephalic co-culture assay (**Fig. 8A** and **E**). Our results show that DTR axons specifically invade the rostral domain of the VTel when cultured in the presence of isotype-control mouse IgG (**Fig. 8B**) but in the presence of function-blocking anti-DCC antibodies, DTR axon outgrowth is significantly randomized (**Fig. 8C**) and grow significantly more caudally than in control co-cultures (**Fig. 8D**). Similarly, blocking DCC function tends to randomize the outgrowth of DTC axons, which invade significantly more rostral domains of the ventral telencephalon (arrow in **Fig. 8G** and **8H**) compared to DTC axons in control co-cultures (**Fig. 8F** and **8H**). Overall these results strongly suggest that DCC receptor function is required both for the attraction of DTR axons to rostral Netrin-1-rich territories of the ventral telencephalon and for the repulsion of DTC axons away from the same domain (see model in **Fig. 11B-C**).

Unc5A/C receptors are required for DTC axon repulsion away from rostral domain of the VTel.

We next tested if Unc5 receptor function is required for the topographic projections of DT axons in the ventral telencephalon. We used a commercially available polyclonal antibody initially raised against the extracellular domain of Unc5H1 (anti-rat Unc5H1, R&D Systems) and reported to act as a function-blocking reagent against both Unc5A and Unc5C (Unc5H1 and Unc5H3 respectively (Strizzi et al. 2005)). We verified the cross-reactivity of this anti-rat Unc5H1 antibody with mouse Unc5A, 5B and 5C proteins using a biochemical approach (see **Suppl. Figure 11**). Our results show that anti-rat Unc5H1 binds to mouse Unc5A and Unc5C but not Unc5B and that its relative affinity for Unc5C when standardized to anti-myc immunoreactivity is about a third of its affinity for Unc5A (**Suppl. Figure 11**). We used this reagent to block Unc5A/C receptor function in the wholemount telecenphalic assay using both DTR (**Fig. 9A-D**) and DTC (**Fig. 9E-H**). Our results show that blocking Unc5A/C receptors function does not have any significant effect on the guided outgrowth of DTR axons in the rostral domain of the VTel (**Fig. 9C** and **D**) compared to control (**Fig.9B** and **D**).

In contrast, blocking Unc5A/C receptors function had a highly significant effect on DTC outgrowth inducing a significant shift of DTC axons outgrowth into the rostral Netrin-1-rich domain of the VTel (**Fig. 9G-H**) compared to control (**Fig.9F-H**). These results suggest that Unc5A/C receptors are required for the repulsion of DTC axons away from the rostral Netrin-1-rich domain of the VTel but do not play any role in the attraction of DTR axons towards the same region.

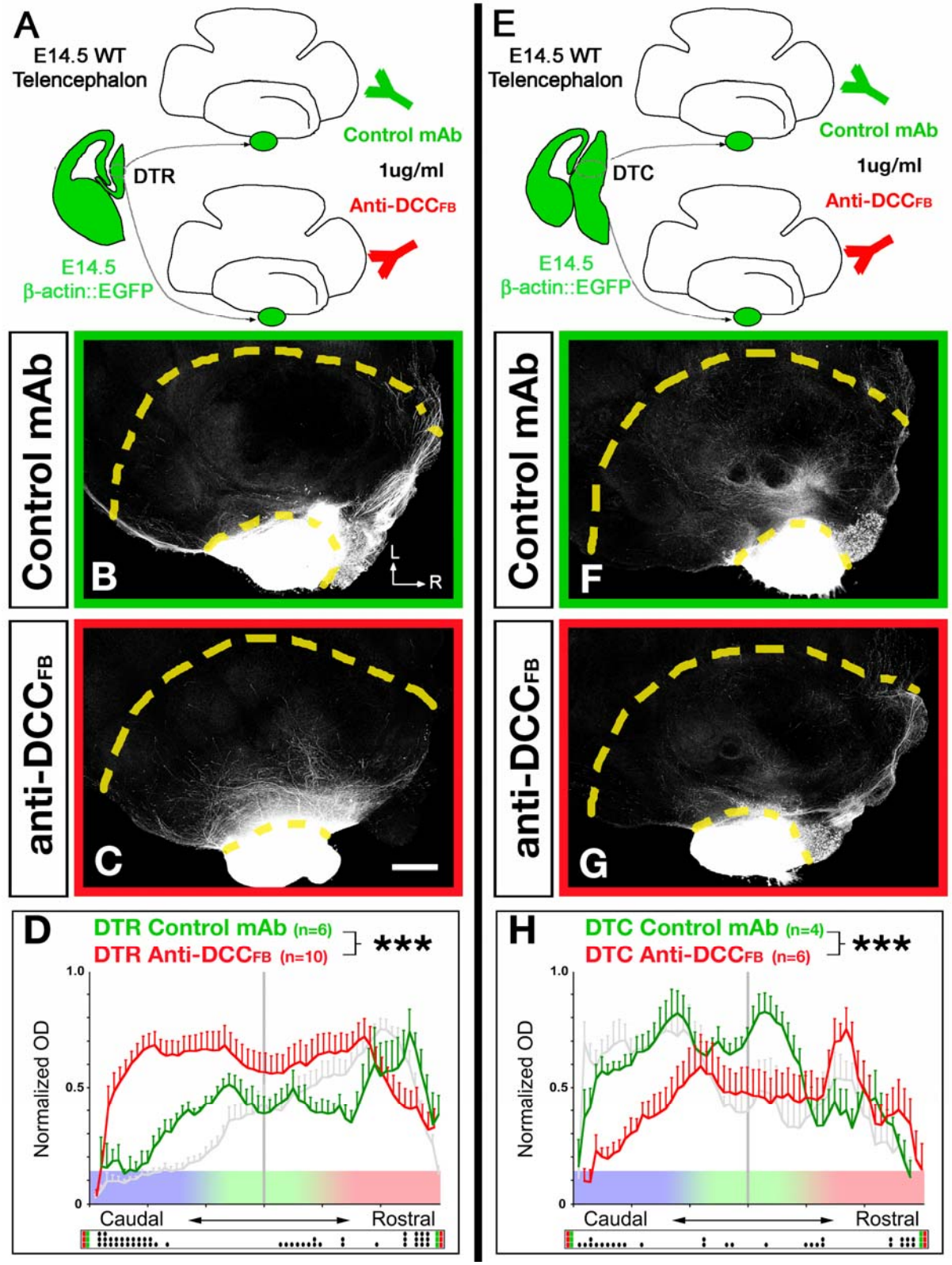

Figure 8. DCC is required for both attraction of rostral thalamic axons and repulsion of caudal thalamic axons from the Netrin-1-rich rostral domain of the ventral telencephalon.

Figure 8. DCC is required for both attraction of rostral thalamic axons and repulsion of caudal thalamic axons from the Netrin-1-rich rostral domain of the ventral telencephalon. Cont.

(**A** and **E**) Isochronic wholemount telencephalic co-cultures with EGFP-expressing rostral (B-D) or caudal (F-H)

(**B** and **F**) DTh explants were incubated either with control isotype mouse IgG.

(**C** and **G**). DTh explants incubated with function-blocking anti-DCC monoclonal antibody. Blocking DCC receptor function randomizes the outgrowth of both rostral and caudal DTh axons.

(**D** and **H**) Quantification of normalized optical density (OD) of DTR-EGFP axons (D) or DTC-EGFP axons (H) growing in VTel with function-blocking anti-DCC antibodies (red curves) or control mouse anti-IgG antibodies (green curves). *** $p<0.001$ ANOVA one-way test (overall effect: bins versus experimental conditions). For comparisons, the gray curves represent the distribution of control DTR axons (in D) and control DTC axons (in H) cultured without antibody as shown in Figure 5D and 5H.

The raster-like dot plot presented under each histogram represents the significance of individual bin comparisons performed between the two experimental conditions using a PLSD-post-hoc test (• $p<0.05$; •• $p<0.01$ and ••• $p<0.001$).

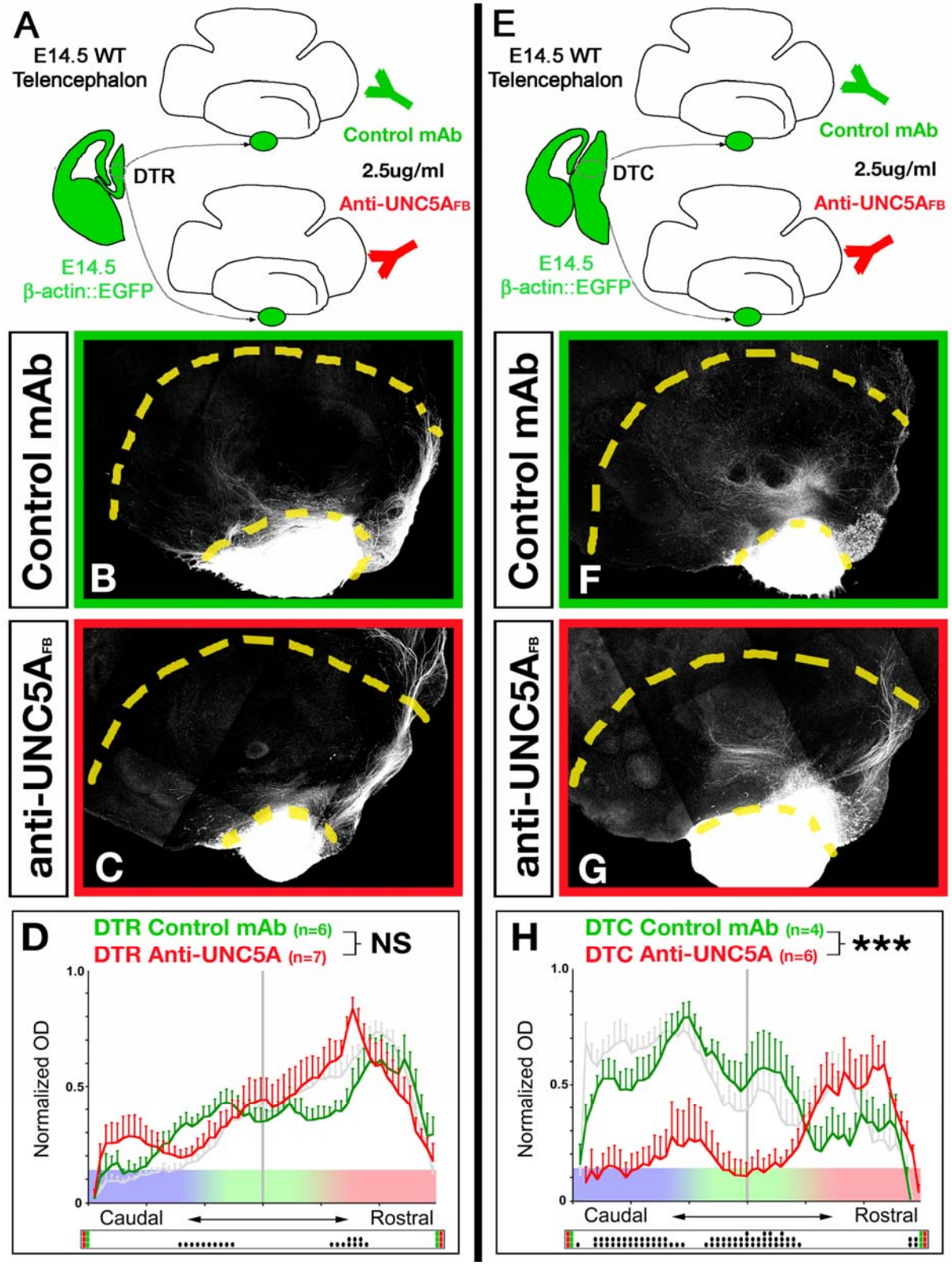

Figure 9. Unc5A and 5C receptors are required for the repulsion of caudal DT axons from the Netrin-1-rich rostral domain of the ventral telencephalon.

Figure 9. Unc5A and 5C receptors are required for the repulsion of caudal DT axons from the Netrin-1-rich rostral domain of the ventral telencephalon. Cont.

(**A** and **E**) Isochronic wholemount telencephalic co-cultures with EGFP-expressing rostral (B-D) or caudal (F-H)

(**B** and **F**) DTh explants were incubated with control isotype mouse IgG.

(**C** and **G**) DTh explants were incubated with function-blocking anti-Unc5A/C polyclonal antibody Blocking the function of Unc5A/C receptors does not affect the rostral outgrowth of DTR axons but induces a significantly more rostral outgrowth of DTC axons in the VTel

(**H**) Quantification of normalized optical density (OD) of DTR-EGFP axons (D) or DTC-EGFP axons (H) growing in VTel with function-blocking anti-Unc5A/C antibodies (red curves) or control mouse anti-IgG antibodies (green curves). NS, non-significant ($p>0.05$); *** $p<0.001$ ANOVA one-way test (overall effect: bins versus experimental conditions). For comparisons, the gray curves represent the distribution of control DTR axons (in D) and control DTC axons (in H) cultured without antibody as shown in Figure 5D and 5H.

The raster-like dot plot presented under each histogram represents the significance of individual bin comparisons performed between the two experimental conditions using a PLSD-post-hoc test (• $p<0.05$; •• $p<0.01$ and ••• $p<0.001$).

Unc5 receptor over-expression in rostral thalamic neurons is sufficient to induce caudal outgrowth of their axons into the ventral telencephalon

We tested if Unc5 receptor expression is the critical determinant of the difference between DTR and DTC axons towards Netrin-1 in the ventral telencephalon. To do this, we over-expressed the Unc5C receptor in rostral thalamic neurons where it is normally expressed at low levels. We implemented an *ex vivo* slice electroporation technique developed recently by Cobos et al. (Cobos et al. 2007). Following focal microinjection of plasmid expressing myristoylated-(m)Venus or Unc5C-IRES-mVenus in the DTh and slice electroporation, explants corresponding to DTR or DTC were co-cultured for 4 days *in vitro* with isochronic wholemount telencephalon (**Fig. 10A**). This technique results in clear visualization of single thalamic axons or small axon fascicles that were traced individually in ImageJ and plotted on a common reference for quantification (**Fig. 10A**). Our results show that over-expression of Unc5C (but also Unc5A or B –data not shown) is sufficient to convert the preferential outgrowth of DTR axons in the rostral domain of the VTel (**Fig. 10B**) into outgrowth in the caudal domain of the VTel (**Fig. 10C**) as observed with DTC axons (**Fig. 10D**). The quantification (**Fig. 10E**) demonstrates that the topography of DTR axons outgrowth over-expressing Unc5C does not differ from DTC axons but is significantly different from control DTR axons in the VTel. These results show that differential Unc5 receptor expression is a critical determinant in the topographic outgrowth of thalamic axons originating from the rostro-medial compared to the caudo-lateral part of the thalamus in response to Netrin-1 in the VTel.

DISCUSSION

Our results provide novel insights into the molecular mechanisms patterning the topography of thalamocortical projections to specific cortical domains by controlling their guidance at the level of their main intermediate target, the ventral telencephalon. We show that *Netrin-1* is expressed in a high-rostral to low-caudal gradient in the VTel and demonstrate that the graded expression of *Netrin-1* in the ventral telencephalon is required cell non-autonomously for (i) attracting rostral thalamic axons in a DCC-dependent manner and (ii) repulsing caudal thalamic axons in a DCC-Unc5 receptor-dependent manner. Our results show that the long-range gradient of Netrin-1 expression in the ventral telencephalon confers a novel function to this well-characterized axon guidance cue: controlling the topographic mapping of large ensembles of axons, a function largely attributed to the ephrin/Eph signaling system and more recently to the Wnt/Ryk signaling (Luo 2006).

The topography of thalamocortical projections is initiated in the ventral telencephalon

Recent studies provided evidence showing that thalamocortical axons are topographically organized in response to axon guidance cues located in the ventral telencephalon (Garel et al. 2002; Dufour et al. 2003; Seibt et al. 2003). However, the exact three-dimensional organization of thalamocortical axons in ventral telencephalon where they form the internal capsule with descending corticofugal axons has remained elusive because of the lack of quantitative analysis. Qualitative analysis based on carbocyanine injections in single brains suggested that thalamocortical axons are segregated according to their origin in the dorsal thalamus along the latero-medial axis (Molnar and Blakemore 1995; Molnar et al. 1998a; Bonnin et al. 2007) as well as the rostro-caudal axis (Seibt et al. 2003). Our quantitative analysis demonstrate that both axes are equally important and we demonstrate that at the level of the corticostriatal boundary i.e. before invading the cortex, thalamic

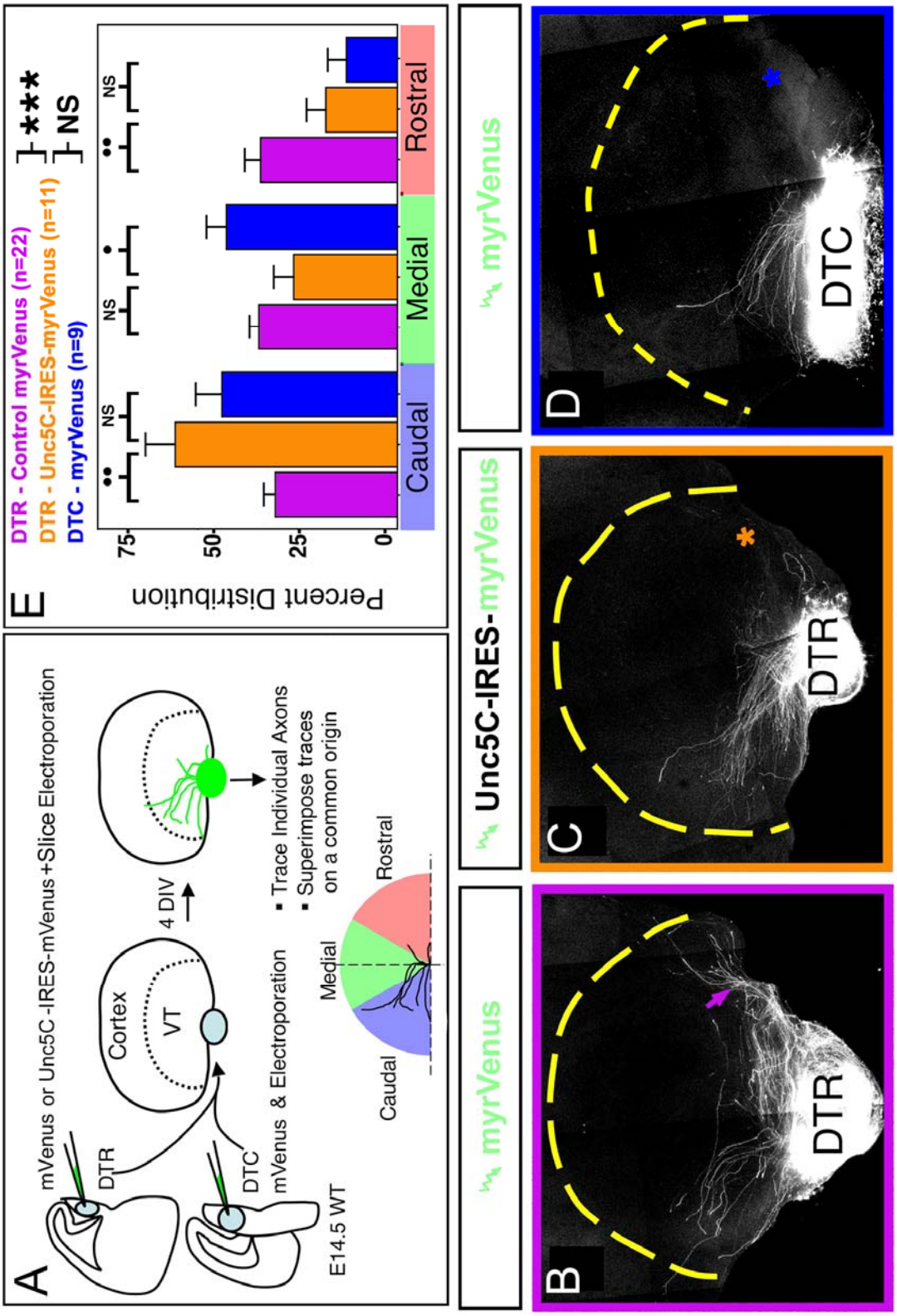

Figure 10. Expression of Unc5C in the rostral part of the dorsal thalamus is sufficient to induce repulsion of DTR axons from Netrin-1-rich rostral domain of the ventral telencephalon.

Figure 10. Expression of Unc5C in the rostral part of the dorsal thalamus is sufficient to induce repulsion of DTR axons from Netrin-1-rich rostral domain of the ventral telencephalon. Cont.

(**A**) Experimental approach: E14.5 250 micron-thick slices containing the rostral or caudal domain of the DTh were microinjected and electroporated using a control IRES-myristoylated (m)Venus or a Unc5C-IRES-mVenus expression plasmid. Immediately following electroporation, DTR or DTC explants were isolated and co-cultured with a wholemount telencephalon for 4 days *in vitro*. Following fixation and staining with anti-EGFP antibodies, individual DTR or DTC fluorescent axons or fascicles were traced and superimposed on a referenced-plot that was then quantified using ImageJ for optical density distribution in three radial bins.

(**B-D**) DTR (B) and DTC (D) axons electroporated with control mVenus-expression plasmid grow preferentially to the rostral and caudal domain of the VTel respectively. However, DTR axons over-expressing Unc5C grow significantly more caudally than control DTR axons (B) in the VTel suggesting that Unc5C expression is sufficient to convert DTR into DTC pattern of axon growth in the VTel.

(**E**) Quantification of the results shown in B-D analyzing the percentage of fluorescent axons located in caudal, medial and rostral bins of the VTel.

*** $p<0.001$ ANOVA one-way test (overall effect: bins versus experimental conditions). NS, non-significant ($p>0.05$); • $p<0.05$; •• $p<0.01$: significance of individual bin comparisons performed between the two experimental conditions using a PLSD-post-hoc test.

projections are highly organized along a *rostro-medial* to *caudo-lateral* axis (**Fig. 1**). Therefore, there is a precise 'blueprint' of the topography of TC projections generated before entering the cortex as suggested previously (Vanderhaeghen and Polleux 2004).

Where exactly is this topography initiated within the ventral telencephalon? Axons entering the ventral telencephalon show a loose degree of organization when pioneering the internal capsule and axons originating from different regions of the thalamus have to redistribute or 'fan-out' over a large area: at E14/15 thalamic axons pioneer the internal capsule as a bundle referred to as the thalamic peduncle, roughly 100-200 microns wide along its rostro-caudal axis. These axons will redistribute over approximately 2-3 millimeters when they reach the cortico-striatal boundary and enter the cortex. Based on previous and present results, we proposed that TC axon sorting occurs progressively as they grow along the medio-lateral axis of the ventral telencephalon (Vanderhaeghen and Polleux 2004) (**Fig. 11**). Interestingly, the only two axon guidance molecules (ephrin-A5; (Dufour et al. 2003) and Netrin-1; present study) identified so far as playing a significant role in this topographic sorting of TC axons in the ventral telencephalon are both expressed in the most lateral part of the mantle region of the ventral telencephalon and are therefore likely expressed by postmitotic neurons forming the striatum. Future studies will address how opposing gradients of ephrin-A5 and Netrin-1 are generated. Two interesting possibilities come to mind: first this gradient is the result of patterning cues such as Shh or FGFs specifying the rostro-caudal identity of ventral telencephalic regions and/or second, this graded expression of Netrin-1 is the result of a graded density of cells migrating rostro-caudally within the ventral telencephalon.

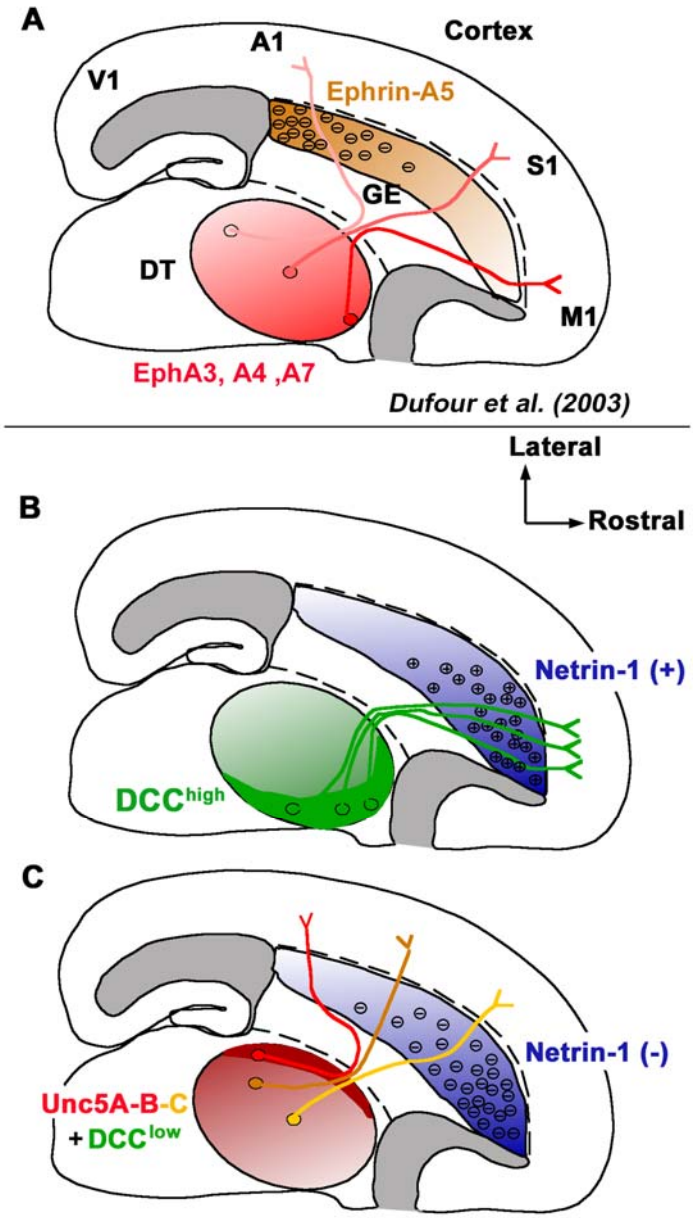

Figure 11. Model of the role of Netrin-1 signaling in the topography of thalamocortical projections in the ventral telencephalon.

Schemas summarizing previous (Dufour et al. 2003) and present findings regarding the axon guidance cues controlling the topographic sorting of TC axons in the ventral telencephalon.

(**A**) High rostro-medial and low caudo-lateral gradient of EphA receptors (EphA3-4-7) mediate chemopulsion of rostro-medial DTh axons to the high-caudal to low-rostral gradient of ephrinA5 in the ventral telencephalon. Adapted from Dufour et al. (2005) as represented in Marin (2005)

(**B-C**) In the present study, we demonstrate that a high-rostral to low-caudal gradient of Netrin-1 in the ventral telencephalon plays a critical role in the topographic projection of DTh axons in the ventral telencephalon. We show that the rostro-medial domain of the DTh expresses high levels of DCC and that the caudo-lateral domain of the DTh expresses low levels of DCC, which is required both for the attraction of DTR axons and the repulsion of DTC axons to the Netrin-1-rich rostral domain of the VTel. We also show that Unc5A-B are expressed preferentially in the caudo-lateral domain of the DT and Unc5C is expressed in a high-caudo-lateral to low-rostro-medial gradient in the DTh. Finally we provide evidence that (1) Unc5A/C are required for the repulsion of caudal DTh axons from the Netrin-1-rich domain of the VTel but (2) does not play any significant role in the projection of rostro-medial DTh axons and (3) that ectopic over-expression of Unc5C in DTR axons is sufficient to convert their outgrowth into DTC ougrowth i.e. repulsion away from the Netrin-1-rich rostral domain of the VTel.

Critical role of Netrin-1 in the establishment of TC projections in the ventral telencepahlon

Recent evidence provided by Bonnin et al. (2007) suggested that thalamic axon responsiveness to Netrin-1 expressed in the ventral telencephalon is modulated by extracellular serotonin levels. Bonnin et al. reports that *in vitro*, in the absence of serotonin, Netrin-1 is repulsive to 'anterior' thalamic axons and attractive to 'posterior' thalamic axons which seems at odds with our present conclusions. However, the authors provide evidence that in the presence of high concentrations of serotonin (30mM), these responses are reversed and now Netrin-1 is attractive to anterior thalamic axons and repulsive to posterior thalamic axons. Considering serotonin levels are high in rodent embryos as it crosses the placental barrier and is present at very high levels in the maternal circulation (Lauder 1988; Yavarone et al. 1993), one would expect axons throughout an embryo to be exposed to high levels of extracellular serotonin. We did test the responsiveness of DTR or DTC explants to a source of Netrin1 in a collagen assay in the presence of horse serum-containing medium (presumably containing serotonin) and confirmed that DTR axons are attracted by Netrin-1 source but that DTC are either not responsive or repulsed by a source of Netrin-1 (**Suppl. Fig. 8**).

Our quantitative analysis of BDA tracing in wild-type and Netrin-1 knockout embryos (**Fig. 4**) provides unequivocal genetic evidence for the requirement of Netrin-1 *in vivo* for (1) the preferential growth of rostro-medial thalamic axons (expressing high levels of DCC and low or undetectable levels of Unc5A-B-C; **Figure 7**) into the rostro-dorsal part of the VTel and (2) for the preferential growth of caudo-lateral thalamic axons (expressing low levels of DCC but high levels of Unc5A-B-C) into the caudo-ventral part of the VTel. The fact that in the Netrin-1 knockout embryos (i) axons originating from the rostro-medial domains of the DT are significantly shifted caudo-ventrally compared to controls and (ii) axons originating from the caudo-lateral domains of the DT

are significantly shifted rostro-dorsally compared to control represents strong evidence in favor of our model suggesting that Netrin-1-rich rostral domain of the ventral telencephalon normally acts as an attractant for rostro-medial thalamic axons and a repulsive cue for caudo-lateral thalamic axons. This model is corroborated by our DCC and Unc5A-C expression data and more importantly by our function-blocking experiments demonstrating that high level of DCC receptor expression by rostro-medial thalamic axons mediates attraction towards the Netrin-1-rich domain of the VTel and that both DCC and Unc5-A-B-C expression are required for repulsion of axons originating from caudo-lateral domain of the DT away from the Netrin-1-rich rostral domain of the VTel.

Interestingly, Netrin-1 is also required for the organization of thalamic axons along the dorso-ventral axis of the developing DT (see **Suppl. Fig.5**), an axis that is not tigthly associated with differences of expression of DCC and/or Unc5A-C. Future experiments will explore if other Netrin-1 receptors such as Neogenin or recently identified Unc5D (Unc5H4) are differentially expressed along the dorso-ventral axis of the DT and mediate segregation of thalamic axons in the VTel.

Establishment of topographic maps: general requirement for several counter-balancing gradients?

In retinotectal projections, retinal ganglion cell (RGC) axons originating along the dorso-ventral axis of the retina project topographically along the medio-lateral axis of the tectum. Recent evidence demonstrates that the topography established along this axis of projection is regulated by EphB-ephrinB signaling (reviewed in (McLaughlin and O'Leary 2005)). However, mathematical modeling suggests that the graded expression of a single axon guidance cue is not sufficient for specifying a continuous topographic map in the tectum, at least one other gradient of an additional cue is necessary for proper topographic map formation in the retino-tectal system (Hindges et al. 2002). Recent evidence suggested that a gradient of Wnt3 along the medio-lateral axis of the tectum

counter-balances the attractive function of ephrinB1 (Schmahl 1983). These results have raised the possibility that in order to produce a continuous topographic map, sorting axons in a linear fashion, gradients of several axon guidance cues that are spatially or functionally complementary are required (Luo 2006).

Our results also suggest that a Netrin-1 gradient counter-balances the function of the ephrin-A5 gradient identified in the ventral telencephalon (Dufour et al. 2003) and that the combined expression of these two cues (possibly along with other graded cues) is required for the establishment of thalamocortical topography in the ventral telencephalon (**Fig. 11**). The main difference between the retino-tectal and the thalamocortical projections is that TC axons are first sorted in the VTel, their main intermediate target, before they reach their final target, the cortex. This reflects the 'nested' nature of thalamocortical projections: at embryonic stages, axons from distinct parts of the mouse thalamus (ultimately corresponding to different thalamic nuclei) are first sorted to different cortical domains in the intermediate target, the ventral telencephalon (*inter-areal* topography) but at early postnatal stages, neurons in each sensory thalamic nuclei are projecting topographically within each cortical area (*intra-areal* mapping i.e. sensory map formation) (Vanderhaeghen et al. 2000). Interestingly, the sorting of axons along the rostro-medial to caudo-lateral axis of the thalamus at the level of the internal capsule (i.e. before they reach the cortex) is perfectly conserved in humans as shown recently by tract tracing studies using diffusion tensor imaging (Behrens et al. 2003), which suggests that the establishment of thalamocortical topography in the ventral telenceaphalon is the result of an evolutionary conserved developmental mechanisms in mammals.

Regionalization of the dorsal thalamus and specification of the topography of TC projections

Importantly, the basic topography of thalamocortical projections is specified in the ventral telencephalon before individual thalamic nuclei can be identified cytoarchitecturally (Nakagawa and O'Leary 2001; Dufour et al. 2003; Seibt et al. 2003). Careful examination of the expression pattern of several transcription factors including *Ngn2*, *Lhx2*, *Lhx9* and *Gbx2* from E12 to P0 demonstrated that their expression is regionalized between E12 and E14, well before the appearance of distinct thalamic nuclei (E15-16) (Nakagawa and O'Leary 2001). These results suggested that phenotypic traits of thalamic neuron identity such as their patterns of axon projections are intrinsically specified by the combinatorial expression of transcription factors, a model based on specification of motor neurons identity in the developing spinal cord (Tanabe and Jessell 1996; Shirasaki and Pfaff 2002). Interestingly, an experimental validation of this model was provided recently by the analysis of the function of the bHLH transcription factor Ngn2, which specifies the topography of TC projections to the frontal cortex by controlling the responsiveness of thalamic axons to so-far unidentified intermediate axon guidance cues present in the ventral telencephalon (Seibt et al. 2003). Based on the present results, we can hypothesize that the caudal shift displayed by rostral thalamic axons of the Ngn2 knockout embryos in the ventral telencephalon could be due to down-regulation of Netrin-1, or ephrinA5 responsiveness. Further experiments will determine if Netrin-1 and ephrinA5 receptors examined in this and previous studies (*DCC*, *Unc5A-C, EphA4*) have altered expression profiles in the dorsal thalamus of Ngn2 knockout embryos.

Role of Netrin-1 as an intermediate axon guidance cue in the ventral telencephalon

Several studies have implicated Netrin-1 as an intermediate target cue for both corticofugal (Metin et al. 1997) and thalamocortical axons (Braisted et al. 2000; Bonnin et al. 2007). Netrin-1 was first shown to stimulate the outgrowth of descending corticofugal axons *in vitro* and attract these axons towards the internal capsule (Metin et al. 1997). Interestingly, Netrin-1 expression in the ventral telencephalon has also been proposed to stimulate thalamic axon outgrowth (Braisted et al. 2000). This study provided evidence for a decreased number of thalamic axons invading the ventral telencephalon as well as a disorganized internal capsule using DiI tracing and L1 staining. Despite careful examination, we did not find evidence of a significant decrease in the number of thalamic axons in the ventral telencephalon of Netrin-1-/- embryos compared to control (see **Suppl. Fig. 4**) and the longest DTh axons length was not significantly altered when axons were growing in Netrin-1-/- or control ventral telencephalon (**Suppl. Fig.7**). Furthermore, in our wholemount telencephalic assay, wild-type DTR axons grew equally well in a wild-type or a Netrin-1-deficient ventral telencephalon (**Fig. 5**), suggesting that Netrin-1 does not play a critical role in the stimulation of thalamic axon outgrowth *in vivo*. The potential discrepancies between our results and the study by Braisted et al. (2000) could be due to methodological differences or to differences in the genetic background of the *Netrin-1* knockout mice between the two studies. As a precedent, mice presenting a null mutation in the Netrin-1 receptor *Unc5C* on the inbred C57BL/6J (B6) genetic background display abnormal projections of both trochlear nerve and motor neuron axons, but these defects are greatly attenuated on a hybrid B6 x SJL background (Burgess et al. 2006). The authors have provided evidence for a locus representing a genetic suppressor of Unc5C function on mouse chromosome 17 (Burgess et al. 2006).

DCC and Unc5 receptors mediate the differential responsiveness to Netrin-1 in rostral and caudal thalamic axons

In mammals, there are six genes encoding transmembrane receptors for Netrin-1: DCC (Deleted in Colorectal Cancer) and Neogenin receptors mediate the attractive response elicited by Netrin-1, while Unc5A-C family members mediate repulsion elicited by Netrin-1 either as homodimers or heterodimers with DCC (Hong et al. 1999; Keleman and Dickson 2001). Our current results show an interesting regionalization of Netrin-1 receptors expression along the rostro-medial to caudo-lateral axis of the DTh. At E14.5 when the topography of TC axons is initiated in the ventral telencephalon but before individual thalamic nuclei are formed, *DCC* is expressed at high levels in a rostro-medial domain of the DTh whereas *Unc5A*, *Unc5B* and *Unc5C* are expressed in largely non-overlapping caudo-lateral domains of the DTh (see **Fig. 7**). Interestingly, *Unc5C* expression pattern is more widespread than Unc5A-B and seems to overlap at least partially with the rostro-medial domain of DCC expression (see **Fig. 7**). Our function-blocking experiments demonstrate that DCC is required for the guidance of rostral thalamic axons to the Netrin-1-rich, rostral domain of the ventral telencephalon, whereas DCC and Unc5C are required for the proper repulsion of caudal thalamic axons to the same Netrin-1-rich region.

A recent study has implicated ephrinA5-EphA4 signaling in the initiation of the topography of TC axon projection in the ventral telencephalon (Dufour et al. 2003). Three EphA receptors (*EphA4, A3 and A7*) were shown to be expressed in a high rostro-medial to low caudo-lateral gradients in the E14.5 DTh whereas the ephrinA5 ligand was found to be expressed in a high-caudal to low-rostral gradient in the ventral telencephalon (**Fig. 8C**). This study also provided in vivo and in vitro functional evidence demonstrating that both ephrinA5 expression in the ventral telencephalon and EphA4 expression in the DTh were required for the proper topographic projection of thalamic axons (Dufour et al. 2003). Taken together, our results and those of Dufour *et al.* (2003) suggest that

rostro-medial thalamic neurons express high levels of DCC and EphA receptors conferring to their axons both attractive and repulsive responses to rostral Netrin-1 and caudal ephrinA5 respectively, resulting in repulsion from the caudal domain and attraction to the rostral domain of the VTel. Our DCC function-blocking experiments demonstrate that DCC is required for the attraction of rostral thalamic axons to the rostral domain of the VTel. In contrast, progressively more caudo-lateral thalamic neurons express lower levels of EphA receptors and higher levels of Unc5A-C receptors, we demonstrate that this decreased sensitivity to the repulsive effect of ephrinA5 is accompanied by an increasing sensitivity to the repulsive action of rostral Netrin-1.

EXPERIMENTAL PROCEDURES

Animals

Mice were used according to a protocol approved by the Institutional Animal Care and Use Committee at the University of North Carolina-Chapel Hill, and in accordance with NIH guidelines. Time-pregnant females were maintained in a 12-hr light/dark cycle and obtained by overnight breeding with males of the same strain. Noon following breeding is considered as E0.5. Netrin-1 knockout mice (*Ntn1*$^{Gt(pGT1.8TM)629Wcs}$ abbreviated *Ntn1*^{LacZ}) were generated by crossing between heterozygous mice (Skarnes et al. 1995; Serafini et al. 1996). The initial line was on a mixed C57Bl6 and Sv129 background and was backcrossed for more than 10 generations on BALB/c background (Jackson Laboratories, Bar Harbor, ME). Genotyping of *Netrin-1*^{LacZ} mice was performed by the University of North Carolina genotyping core facility using quantitative PCR detecting the presence of 0, 1 or 2 copies of the lacZ transgene. The genotype of embryos heterozygote or homozygote for the *Netrin-1* transgene was confirmed by anatomical defects described previously (absence of callosal and anterior commissure projections) (Serafini et al. 1996). Transgenic mice expressing EGFP under the control of CMV enhancer/chicken ß̃actin promoter were maintained by heterozygous crossing on a Balb/C background for more than 10 generations (Okabe et al. 1997).

Biotinylated Dextran Amine (BDA) anterograde axon tracing

in live mouse embryos.

BDA Injections

This process is diagrammed in **Supplemental Figure 1**. Pregnant females, E15 or E18 are cervically dislocated in accordance with DLAM protocols and embryos removed via caesarian section. All dissections are performed on ice in HBSS. Brains are removed from the skulls, hemisected and positioned to reveal the dorsal thalamus. A solution of 10% Biotinylated Dextran Amine (BDA-MW 3000kd Molecular Probes) and 1% Fast Green in 0.1M PBS is microinjected into the dorsal thalamus from a medial approach (PicoSpritzer III, General Valve Corp). Injections sizes are limited to the smallest amount visible through the dissecting scope as uptake of BDA is unpredictable. Injection size will be calculated during analysis. Brains are then placed in oxygenated (95/5% O2/CO2) aCSF at 37˚ C for 5 hours. Upon removal, brains are immersion fixed in 4% PFA and placed overnight at room temperature.

Samples are washed in PBS, embedded in 3% agarose and vibratome sectioned coronally in 100um intervals (LEICA VTel 1000S). Every section is collected serially in 6 wells of a standard 24 well plate containing PBS. This leaves 5-6 anatomically distinguishable sections in each well. Once sections are in 24 well plates, all removal of solutions is performed manually with transfer pipettes. PBS is removed and replaced with 250ul PBST (5% goat serum, 3% BSA, 3% Triton, 0.01% NaH3 in PBS) to block and permeabilized the tissue. After shaking at 4˚ C overnight, 250ul of 1:1K AlexaFlour 546 conjugated Streptavidin and 1:10K Hoescht are added to each well and the samples are again left to shake overnight at 4˚ C. Slices are washed 3x with PBS and quantified.

Creation of Scoring Sheets

To quantify BDA labeled neurons, a Scoring Sheet of a "model brain" is made for every anatomically distinguishable brain studied. For this study, the only Scoring sheets required were for E15 and E18 brains as Netrin-1 hypomorphs do not have anatomical abnormalities drastic enough to affect this analysis. To create the Scoring Sheet, an entire series of 100uM coronal sections is stained with Hoescht and mounted on slides. Each section is imaged by digital camera on a Leica binocular dissecting scope through a UV single pass filter. Special care is made to ensure zoom is identical between images. Images are taken in black and white. The series of images are imported into ImageJ as an image sequence, aligned using the StackReg plugin, and exported as a 6x6 montage with visible, 1 pixel borders between the sections. The montage is printed and used as the Scoring Sheet for the location of BDA labeled axons and cell bodies.

Creation of Anatomical Masks

In order to measure relative BDA locations within specific structures, i.e. injection location inside the thalamus, Anatomical Masks corresponding to the scoring sheets are created to define the boundaries of all relevant anatomy. In Photoshop, each Anatomical Mask is drawn as a layer over the Scoring Sheet according to known anatomical record. The following masks are created: dorsal thalamus, ventral telencephalon, dorsal telencephalon, cortico-striatal boundary, septum, hippocampus, and hypothalamus. A final mask, referred to as the Grid Reference, is made consisting of 36 black rectangles separated by the borders between each coronal section in the original montage. All masks and score sheets are converted to grayscale and the levels are appropriately adjusted to have the background as white, and the mask as a series of solid black blobs.

Scoring of Traces

Injections are quantified by precisely drawing axons and cell body positions on Scoring Sheets using a red fine tip marker. The scorer is blinded to any information regarding the sample, including genotype, relative location of the injection, and size of the injection. Samples found to be inadequate for quantification due to missing sections or a plane of section that is not coronal are immediately discarded from analysis. Score sheets are digitized using a standard tabletop scanner. Score Sheets and all Anatomical Masks are imported into ImageJ as an image sequence and aligned using the StackReg plugin.

Isolation of Traces

The aligned Score Sheets are exported and opened in Photoshop where the Select Color Range Tool is used to highlight the red injection traces. All information outside of the red traces is then deleted. The file is converted to grayscale and made binary, so that all information is either 100% black or white. This leaves a series of black traces surrounded by a white background. These are the Cleaned Traces.

Masking of Traces

All Cleaned Traces and Anatomical Masks are imported into ImageJ as a stack. For a given Anatomical Mask to be quantified, the magic wand tool is used to select every part of the mask. The selection is inverted and all data located outside the designated mask is erased for every Cleaned Trace in the stack. This leaves only information regarding the relative position of an axon tracing inside the structure being masked. These are referred to as Masked Traces, with the individual remnant of each trace referred to as a Segment. For analysis of injection location, portions of the trace not corresponding to cell bodies in the thalamus are erased before applying the Dorsal Thalamus mask.

Collection of Raw Segment Data

The Masked Traces are then quantified using the Analyze Particles tool. This individually collects the area, center of mass, and XY bounding coordinates (minimums and maximums) for every Segment of a Masked Trace. Each data point contains information regarding which sample it is from so that analysis of multiple Masked Traces can be associated with each other and classifications based upon genotype or other factors can be made. The data are exported to Excel.

Calculating XYZ Positioning of Segments Inside the Model Brain

Upon collection, the raw XY coordinates correspond to the relative position of a Segment on the entire Scoring Sheet. However these need to be adjusted to reflect their XY coordinates inside the appropriate 100uM section. To do this the raw XY coordinates collected from the 36 rectangles of the Grid Reference are used to establish the selection criteria for each 100uM section. Each Grid Rectangle is assigned a Z coordinate corresponding to the rostral to caudal position in the brain (Rostral=1, Caudal=36). Mask and Trace Segments are assigned the appropriate Z coordinate based upon where they are located in comparison to the Grid Reference. The minimum X and Y values of the assigned grid rectangle is then subtracted from the raw XY coordinates of a Segment, leaving the relative position of the Segment inside the Grid Rectangle. These are the Adjusted XY Coordinates. Three axes are now adjusted for each Segment with value from low to high being: X=Lateral to Medial, Y=Dorsal to Ventral, Z=Rostral to Caudal.

Calculating Relative Segment Position Inside a Structure

In order to determine the relative position of a trace inside a structure, it is necessary to normalize the X and Y components of the Segment to those of the Anatomical Mask of the same Z position. To do this, the minimum Adjusted XY Coordinates of an Anatomical Mask are subtracted from the Adjusted XY Coordinates of a Segment. These are now divided by the maximum Adjusted

XY Coordinates minus the minimum of the masks, a standard normalization. The resulting number is a normalized, relative position inside a specific structure.

Classification Criteria for an Entire Trace

The position of all the Segments of a trace inside a single structure can be used to categorize the entire trace. For instance, the relative position of the injection site can be classified along the rostral-caudal axis based upon the average Z position of all Segments of the injection trace. For this study, all injections larger that 5% of the total area of the dorsal thalamus mask are discarded from analysis.

Entire Trace Overlay Graphs

Cleaned Traces of a single given criteria are imported into ImageJ as a stack. An average projection of the stack is made, revealing the density of a population of traces. Up to 3 criteria are combined as RGB images, each channel representing one criterion.

Structural Overlay Graphs

In order to display the path of axons through a structure such as the CSB, it is necessary to display it in a 2 dimensional plane. After creating an Entire Trace Overlay, the Anatomical Mask used for the CSB is applied to the overlay. The remaining Segments of the overlay are aligned, rotated horizontally, and made into a stack of images. Using the reslice and maximum projection tools in ImageJ, a topographic map of axons crossing the CSB is created.

RNA in situ hybridization

Sense and antisense probes for mouse *Netrin-1, DCC, Unc5A, Unc5B* (Serafini et al. 1994; Keino-Masu et al. 1996) and *Unc5C* (Ackerman et al. 1997; Engelkamp 2002) were generated as described previously. In situ hybridizations were performed as previously described using DIG-labeled probes (Dufour et al. 2003). All in situ hybridization experiments were performed by Dr. Yongqin Wu.

Immunofluorescent staining

Wholemount telencephalon/dorsal thalamic co-cultures were maintained on organotypic slice culture inserts, fixed and stained for immunofluorescence as previously described (Polleux and Ghosh 2002; Seibt et al. 2003). The following primary antibodies were used: polyclonal rabbit anti-ß-galactosidase (Molecular Probes; 1:1000), monoclonal anti-neurofilament 165kD (clone 2H3; Developmental Hybridoma Bank; 1:2000), polyclonal rat anti-L1 cell adhesion molecule (Chemicon; 1:1000) as well as polyclonal chicken and rabbit anti-GFP (Molecular Probes, 1:2000). The following secondary antibodies were used: Alexa-488, -546 and -647 conjugated goat anti-chicken, anti-rabbit or anti-mouse IgG (Molecular Probes; 1:2000).

Construction of Myc-tagged Unc5 cDNAs

Full-length cDNA clones of mouse Unc5A, Unc5B and Unc5C (Image ID: Unc5A, 6813463; Unc5B, 6417563; Unc5C, 40085998) were purchased from Open Biosystems. Open reading frame of each clone was amplified by PCR using LA Taq polymerase (TAKARA BIO) and cloned with a Myc-tag at the carboxy-terminus into a modified pCIG2 vector, which drives expression of cloned cDNA from chicken ß-actin promoter and CMV-enhancer. All constructs were confirmed by DNA sequencing. This work was completed by Dr. Takayuki Sassa.

Western Analysis

COS7 cells were transfected with GFP and Unc5A-Myc, Unc5B-Myc or Unc5C-Myc expression vectors using Lipofectamine 2000 (Invitrogen). Cells were lysed in RIPA buffer (50 mM Tris-Hcl (pH 7.5), 150 mM NaCl, 1% Triton X-100, 0.1% SDS) supplemented with protease inhibitors (Complete protease inhibitors cocktail tablets, Roche) 48 hours after transfection. Protein samples (20 μg each) were run on 4-12% gradient SDS-PAGE gels (Invitrogen) and transferred to Hybond-P membranes (Amersham). Membranes were pre-incubated in 5% nonfat dry milk and 0.1% Tween-20 in Tris-buffered saline and incubated with the primary antibodies in the same solution. The primary antibodies used were; mouse anti-Myc antibody (clone 9B11, Cell Signaling Technology, 1:2000), goat anti-Unc5A antibody (anti-rat Unc5h1, R&D Systems, 1:200) and rabbit anti-GFP antibody (IgG fraction, Molecular Probes, 1:2000). The fluorescent signals were generated using corresponding HRP-conjugated secondary antibodies and ECL-Plus Western Blotting Detection Reagents (Amersham), and were detected using Typhoon 9400 image scanner (Amersham). This experiment was completed by Dr. Takayuki Sassa.

Electroporation of plasmids into thalamic slices, axonal tracing and quantification

To visualize axons of dorsal thalamic neurons, we transfected myristoylated-Venus (mVenus) plasmid (pCX-myrVenus, kindly provided by Anna-Katerina Hadjantonakis, 1 μg/μl). For Unc5 overexpression, the mixture (0.5 μg/μl each) of Unc5A-Myc, Unc5B-Myc and Unc5C-Myc (data not shown) or Unc5C-Myc alone (1 μg/μl) was transfected together with mVenus plasmid (1 μg/μl). Control experiments included transfection of mVenus plasmid alone or the mixture of mVenus and Myc-tag empty plasmids. These two conditions gave similar results and therefore we combined them as control.

Electroporation into slices was performed essentially as described previously (Cobos et al. 2007). Briefly, coronal slices (250 μm) of E14.5 wild-type brains were prepared using a Leica VTel

1000S vibratome and plasmid solution was pressure injected through a glass pipette into the rostral or caudal dorsal thalamus (DTR or DTC; See Fig. 10) using a Picrospritzer III (General Valve) microinjector. Electroporations were performed with gold-coated electrodes (GenePads 5 x 7 mm, BTX) using an ECM 830 electroporator (BTX) and the following parameters: five 5 ms long pulses separated by 500 ms intervals at 100 V. After electroporation, the dorsal thalamus was dissected and co-cultured with E14.5 wild-type wholemount telencephalon for 4 days, followed by fixation and immunostaining for GFP as described previously (Seibt et al. 2003).

To identify GFP-positive axons, we used either of the two methods based on the axon density in each sample. When the number of axons in the sample was small as shown in Fig. 10D, we identified axons by single axon tracing using NeuronJ plug-in for ImageJ. Traced axons were superimposed on a reference framework with common origin and the percent of pixels in caudal, medial or rostral 60-degree radial bin was quantified. When axon density in the sample was too high to identify individual axons, we quantified the percent of EGFP-pixel distribution in the same way as in single axon tracing. Thus, the two methods utilize essentially identical quantification analysis and we combined the results obtained by using these two methods. This experiment was completed by Dr. Takayuki Sassa.

Confocal microscopy

Fluorescent immunostaining was observed using a LEICA TCS-SL laser scanning confocal microscope equipped with an Argon laser (488 nm), green Helium-Neon laser (546nm) and red Helium-Neon laser line (633nm) mounted on an inverted DM-IRE2 microscope equipped with a Marzhauzer X-Y motorized stage allowing large scale tiling of wholemount telencephalic co-cultures obtained by scanning multiple fields using a long-working distance 10x objective followed by an automatic tiling function available from the LEICA confocal software.

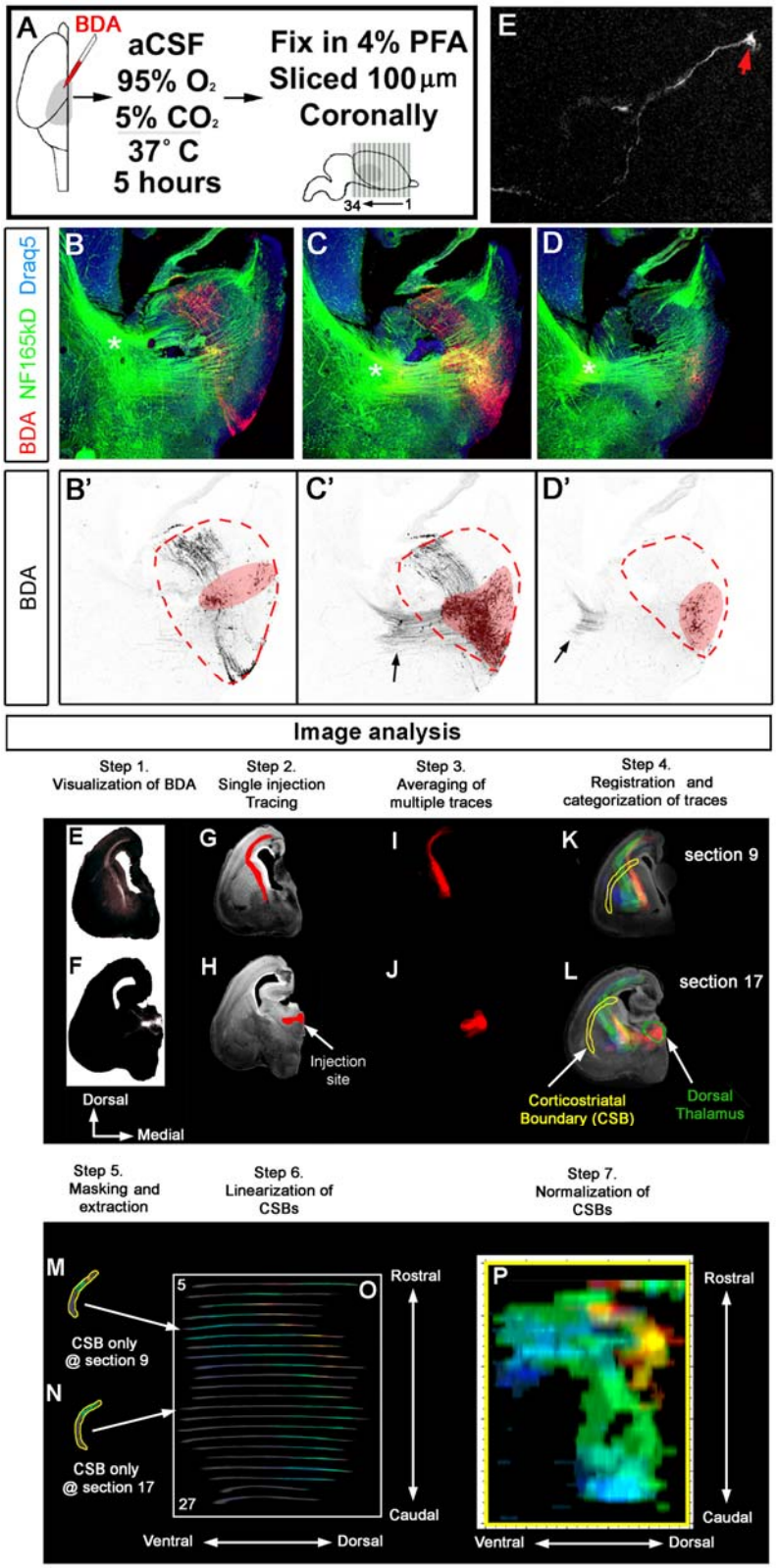

Supplementary Figure 1. Biotinylated Dextran Amine (BDA) axon tracing and reconstruction of the topography of thalamocortical projections in embryonic mouse brain.

Supplementary Figure 1. Biotinylated Dextran Amine (BDA) axon tracing and reconstruction of the topography of thalamocortical projections in embryonic mouse brain. Cont.

(**A**) Experimental paradigm underlying BDA anterograde tracing in live mouse embryonic dorsal thalamus.

(**B-D'**) This method allows the labeling of small numbers of thalamic neurons as visualized on these three confocal micrographs taken of adjacent 100-microns thick vibratome sections of the anterior portion of the thalamus of an E14.5 hemisphere (injection site delineated by red shaded area in B'-D').

(**E**) This method allows the full anterograde labeling of thalamic axons (red arrow points to growth cone in the internal capsule shown in E) and is compatible with immunofluorescent staining (neurofilament 165kD staining in green in B-D). Panels in B-D are counterstained with the axonal marker neurofilament 165kD (green) and nucleic acid staining Draq5 (blue).

(**F-S**) Image analysis involved in the reconstruction of the topography of thalamocortical projections at the level of the cortico-striatal boundary (CSB).

Steps 1 and 2: Individual BDA microinjections in the dorsal thalamus of single E18.5 mouse hemisphere (F) and its resulting axon projection (E) are traced onto corresponding Draq-5-counterstained coronal sections (G-H see also **Suppl. Figure 2** for the entire 'model' coronal section series).

Steps 3-4: Extraction of the X-Y coordinates of the injection site (K) and the axon tracts (J) on a mask of model sections.

Step 4: Averaging of the traces of multiple axon projections (L) resulting from multiple injections sites (M; see **Figure 2** for different categorization of injection sites). This is performed in coronal sections where anatomical regions such as the dorsal thalamus (green outline in L) or the cortico-striatal boundary (CSB, yellow outline in K-L) correspond to individual masks (see also **Suppl. Figure 2**).

Steps 5-6: Categorized and averaged axon traces crossing the CSB at each section are masked (M-N), linearized and aligned (O) in a frame organized along the rostro-caudal (R-C) axis (vertical) and the dorso-ventral (D-V) axis (horizontal).

Steps 7 and 8: The individual CSB frames are assembled in a common referenced space (R) and then normalized along the R-C and the D-V axis (S). (**T**) Schematic representation of the position of the CSB reconstructions shown in S on a horizontal section of the mouse brain.

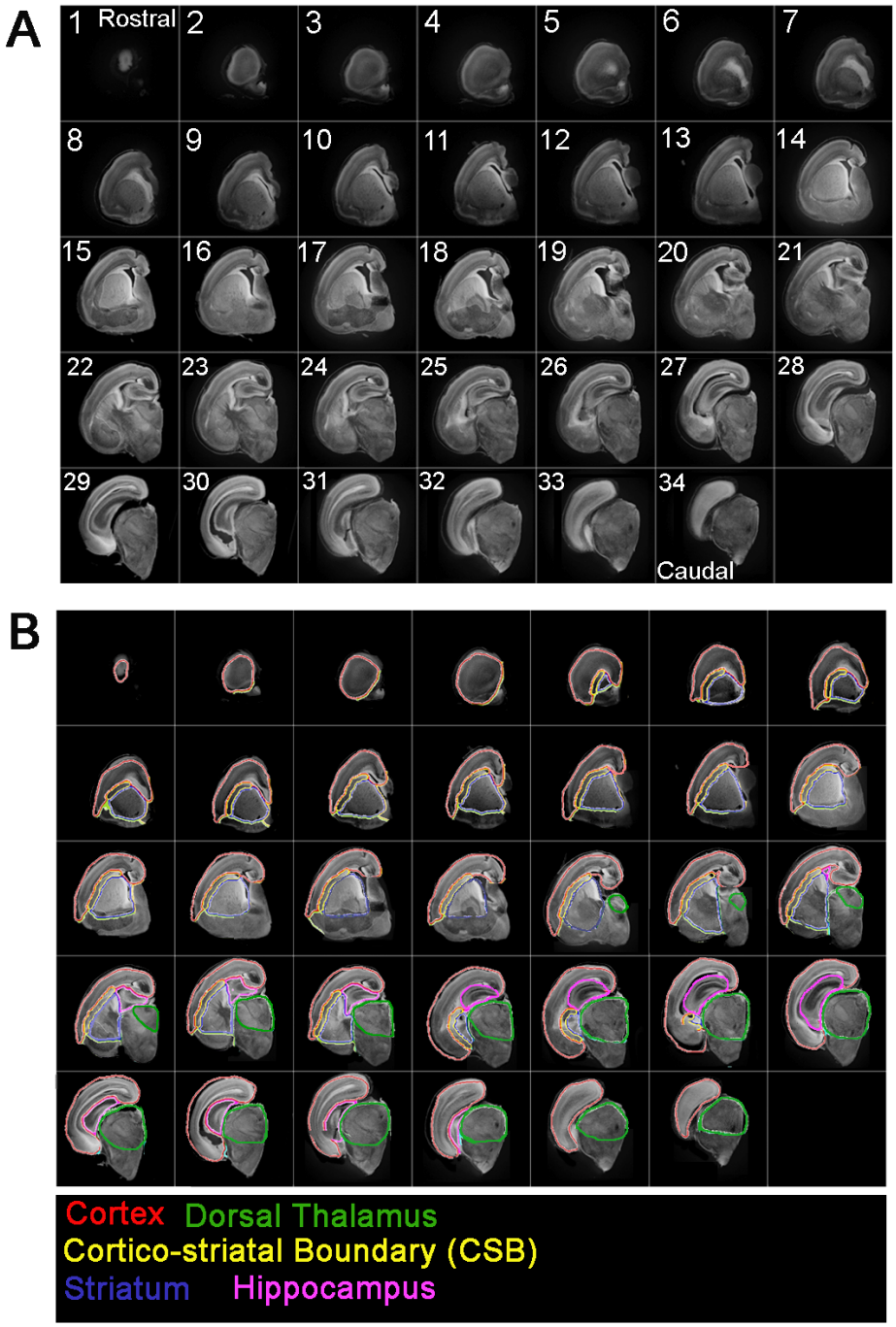

Supplementary Figure 2. Regional segmentation of E18.5 mouse brain used for reconstruction of BDA axon tracing.

(**A**) Series of adjacent 100 micron thick coronal sections of an E18.5 mouse brain used as a model for BDA axon tracing and injection site reconstruction. Sections numbered from 1 to 34 (rostral to caudal) were counterstained with Draq-5 revealing the cytoarchitecture of distinct regions outlined in B.

(**B**) Segmentation of distinct regions used for reconstructions as shown in Figure 1. Red: cortex, yellow: corticostriatal boundary, green: dorsal thalamus, blue: ganglionic eminence (ventral telencephalon), pink: hippocampus.

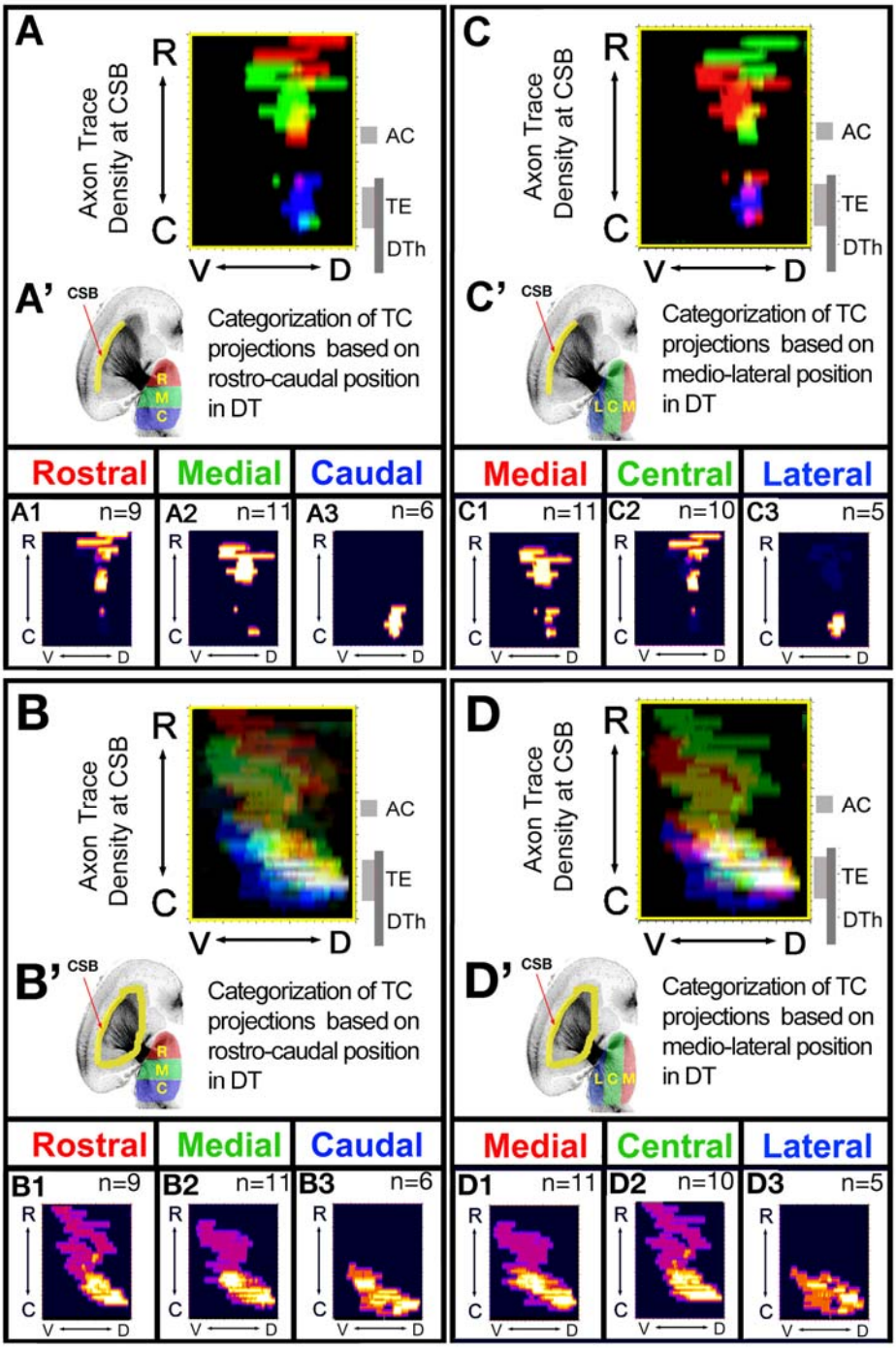

Supplementary Figure 3. The topography of TC axon projections is established at E15 in the mouse ventral telencephalon.

BDA microinjection were performed in the dorsal thalamus of multiple E15.5 mouse embryos and axon tracing analysis were performed as in Figure 1.

(**A-A'**) Axon density maps of TC projections at the cortico-striatal boundary for axons originating along the rostro-caudal axis of the dorsal thalamus (A'). Color code corresponds to injections performed in three third of the dorsal thalamus along the rostro-caudal axis of the DTh shown individually in A1-3.

(**B-B'**) Same analysis as in A-A' but along the medio-lateral axis of the dorsal thalamus at E15.5.

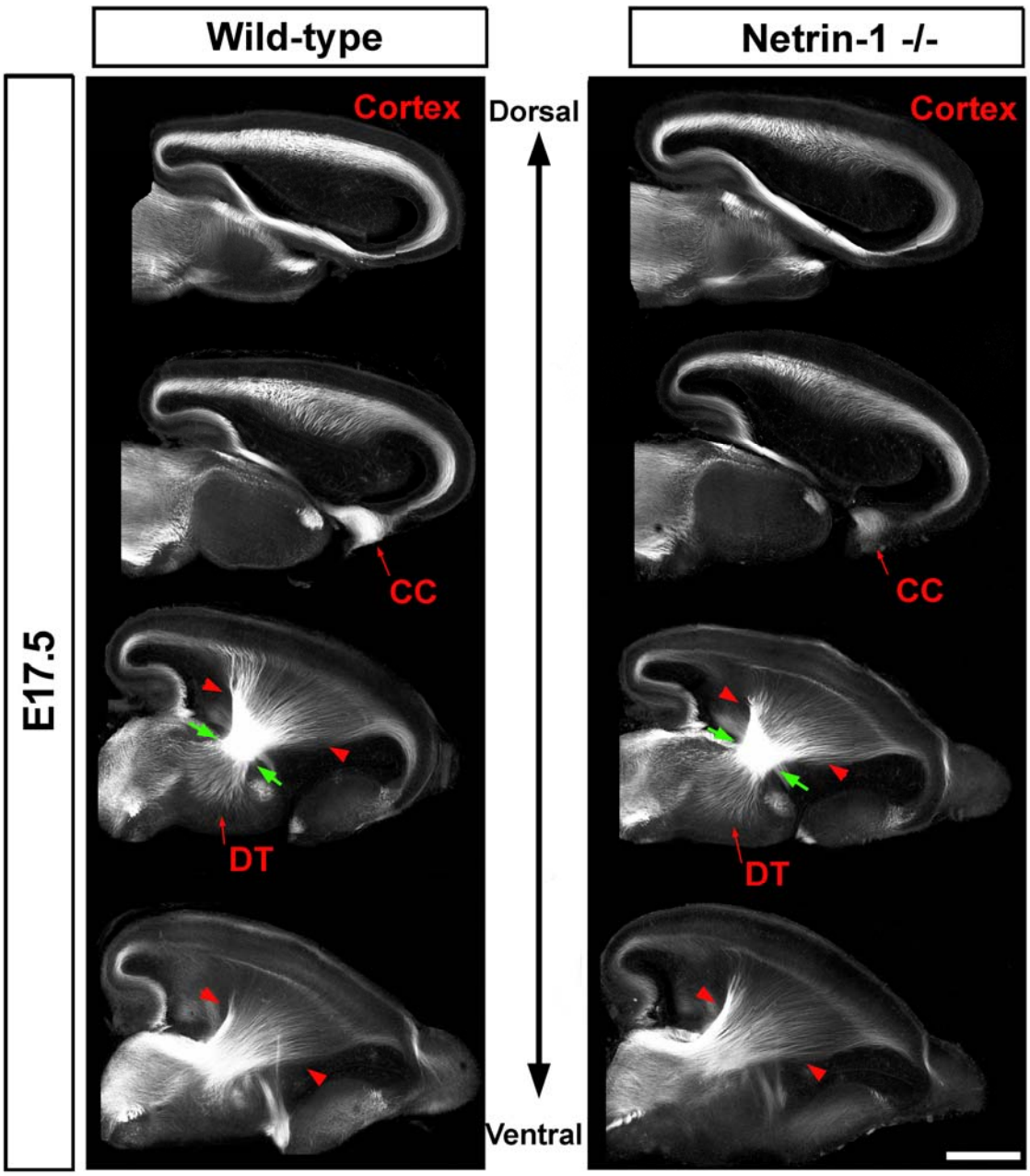

Supplementary Figure 4. Absence of obvious TC axon pathfinding defect in the internal capsule of the Netrin-1 knockout mouse at E18.5.

Confocal reconstruction of immunofluorescent staining for the axonal marker L1 on 100 microns-thick horizontal sections taken at 400 microns intervals of a wild-type (**A-D**) and a Netrin-1 knockout (**E-H**) E17.5 mouse embryos. L1 stains both thalamocortical axons as well as other axon tracts such as the corpus callosum (CC) but not other corticofugal axons ((Ohyama et al. 2004); AP and FP unpublished observations). Red arrowheads indicate the internal capsule, green arrows indicate the thalamic peduncle. CC and anterior commissure projection defects can be observed in the Netrin-1 knockout embryos as described previously (Keino-Masu et al. 1996). However, no gross thalamocortical axon pathfinding defect can be detected at this level. Abbreviations: DTh, dorsal thalamus; VTh , ventral thalamus; CC: corpus callosum. Scale bar value: A-H, 1 mm.

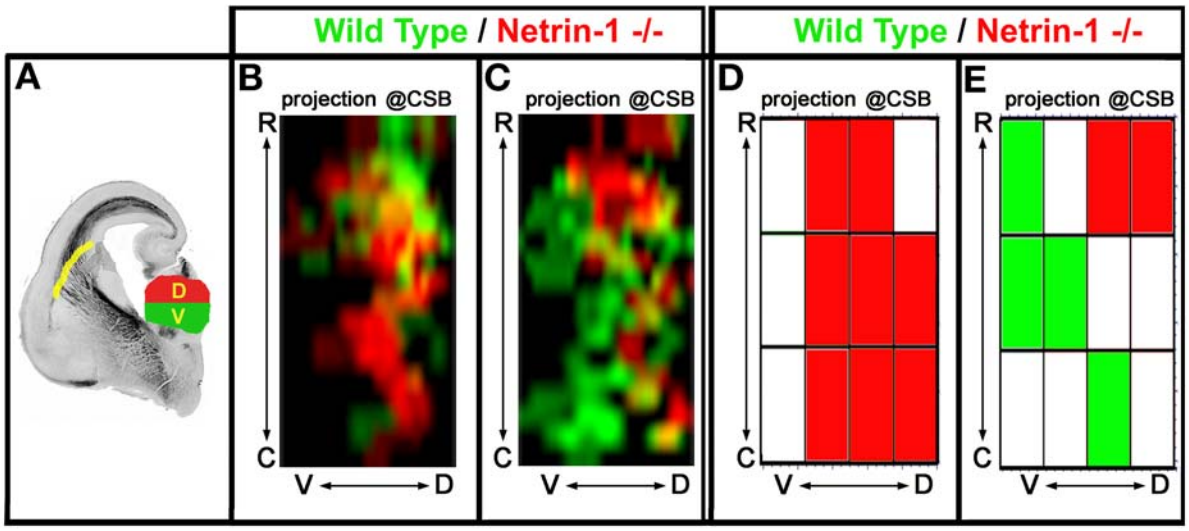

Supplementary Figure 5. Differences of TC projections along the dorso-ventral axis of the ventral telencephalon between wild-type and Netrin-1 knockout embryos.

(**A-C**) Superimposition of the averaged injection site position in the dorsal thalamus of wild-type (green) and Netrin-1-/- (red) embryos for thalamic axons crossing the CSB along its dorsal (B) or ventral (C) halves as shown in A.

(**D-E**) Statistical analysis of the differences of averaged density maps using a two-way ANOVA test to determine the significance of the axon density maps between wild-type and Netrin-1 knockout embryos.

Significance was arbitrarily set at $p<0.001$ with green representing bins where the averaged density observed in WT is superior to Netrin-1-/- and vice versa for red bins. Any comparison with $p>0.001$ was considered non-significant and shown in white.

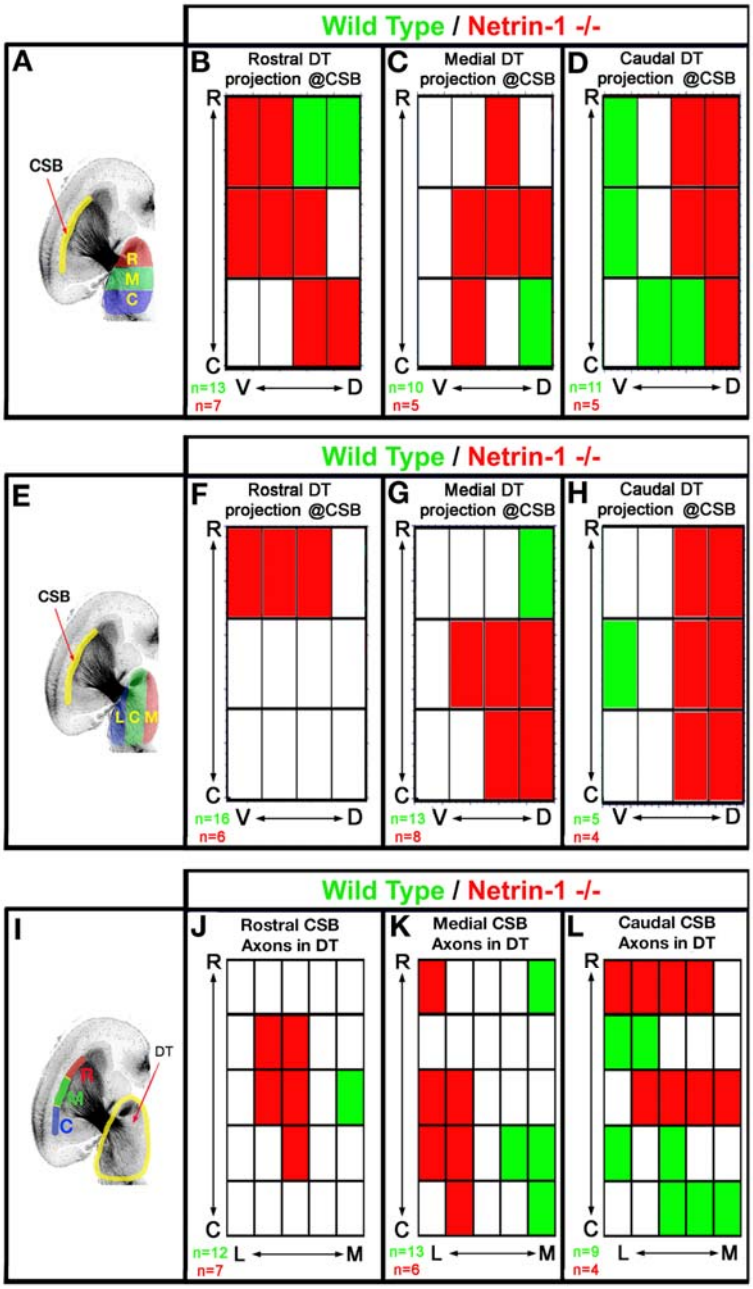

Supplementary Figure 6. Statistical analysis of the differences in the averaged axon density maps of thalamocortical projections between wild-type and Netrin-1 knockout embryos.
Each map shown in Figure 4I-S comparing the distribution of TC projections at the CSB between wild-type and Netrin-1-/- embryos have been divided into twelve bins along the rostro-caudal and dorso-ventral axis of the cortico-striatal boundary (**A-H**) or 25 bins in the dorsal thalamus (**I-L**). Within each bin, two-way ANOVA test was used to determine the significance of the axon density maps between wild-type and Netrin-1 knockout embryos. Significance was arbitrarily set at $p<0.001$ with green representing bins where the averaged density observed in WT is superior to Netrin-1-/- and vice versa for red bins. Any comparison with $p>0.001$ was considered non-significant and shown in white.

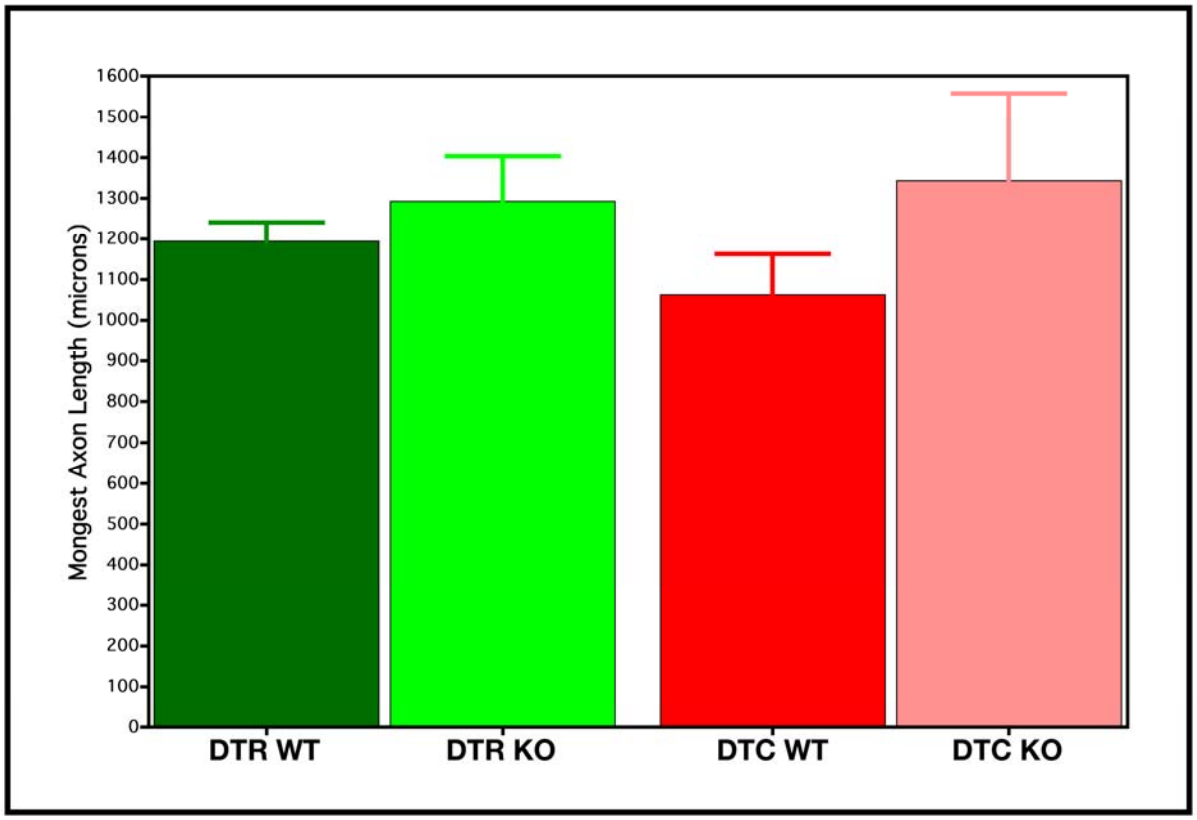

Supplementary Figure 7. Analysis of the length of the longest axon projecting in telencephalic wholemount reveals that Netrin-1 is not required for DTh axon outgrowth.

The length of the longest thalamic axon was measured in wholemount co-cultures shown in Figure 5 between wild-type EGFP+ DTR or DTC explants and either wild-type (WT-VTel) or Netrin-1-/- (Netrin1-/- VTel) telencephalon.

This analysis reveals no significant differences ($p>0.05$ according to non-parametric Mann-Whitney test) between the length of the longest DTR or DTC axon growing in wild-type or Netrin-1 deficient ventral telencephalon suggesting that Netrin-1 is not required *in vivo* for DTh axon extension.

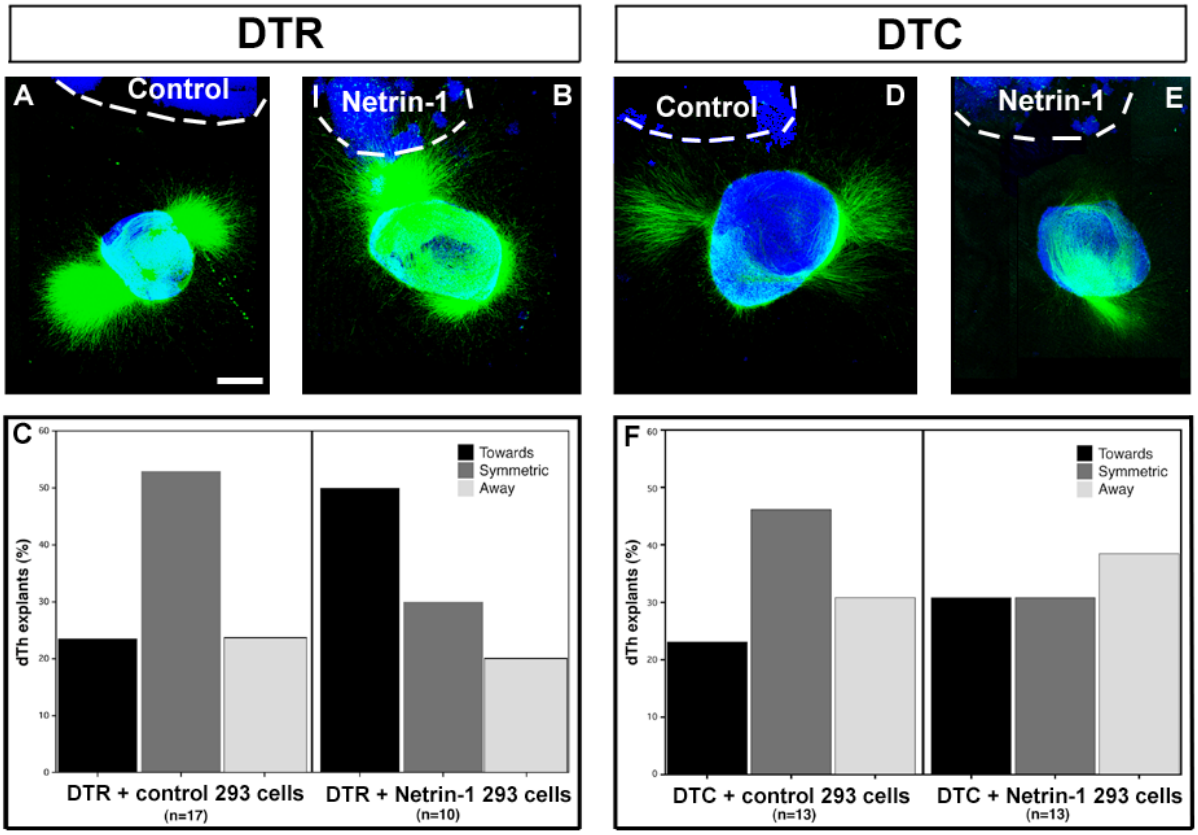

Supplementary Figure 8. Differential effect of Netrin-1 on the guidance of rostro-medial and caudo-lateral thalamic axons *in vitro*.

Collagen co-cultures of DTR axons (**A-B**) and DTC axons (**D-E**) with either control HEK 293 (**A** and **D**) or 293 cells stably expressing Netrin-1 (**B** and **E**).

Axons are visualized using anti-Neurofilament 165kD immunofluorescence (green). Blue is Draq-5 nuclear staining.

Quantification of the orientation of axon outgrowth categorized as growing towards, symmetrically or away from the 293 cell aggregates as described in (Braisted et al. 2000). DTR axons show a strong attraction towards Netrin-1-expressing cells but not control HEK cells whereas DTC axons show a modest (but significantly different from control) repulsion from Netrin-1-expressing cell aggregates.

Chi-square analysis: DTR – Control 293 cells vs Netrin-1 cells 293 $p<0.001$; DTC – Control 293 cells vs Netrin-1 293 cells $p<0.01$; DTR vs DTC to Netrin-1 293 cells $p<0.001$.

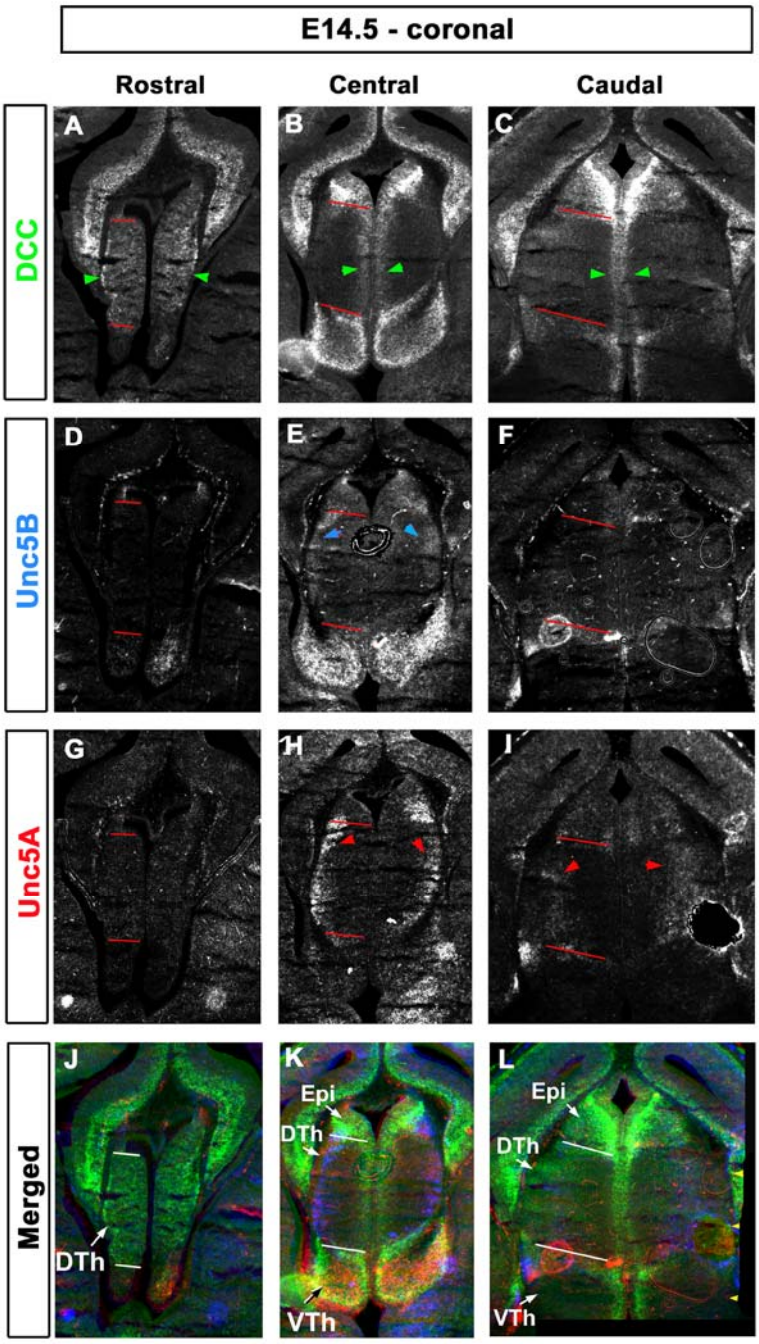

Supplementary Figure 9. Complementary expression patterns of *DCC* and *Unc5A-B* receptors in the dorsal thalamus, ventral thalamus and epithalamus of E14.5 mouse embryos.
(**A-L**) mRNA *in situ* hybridization for *DCC* (A-C), *Unc5B* (D-F), *Unc5A* (G-I) performed on coronal sections of E14.5 mouse embryos reveals that in addition to their expression in the dorsal thalamus, DCC and Unc5B are also expressed at high levels in the ventral thalamus (B, E and K) and the epithalamus (B-C, K-L) respectively. Each individual panel performed on adjacent 20 microns-thick coronal sections were merged in Adobe Photoshop (version 9.0) using a pseudo-coloring RGB function.

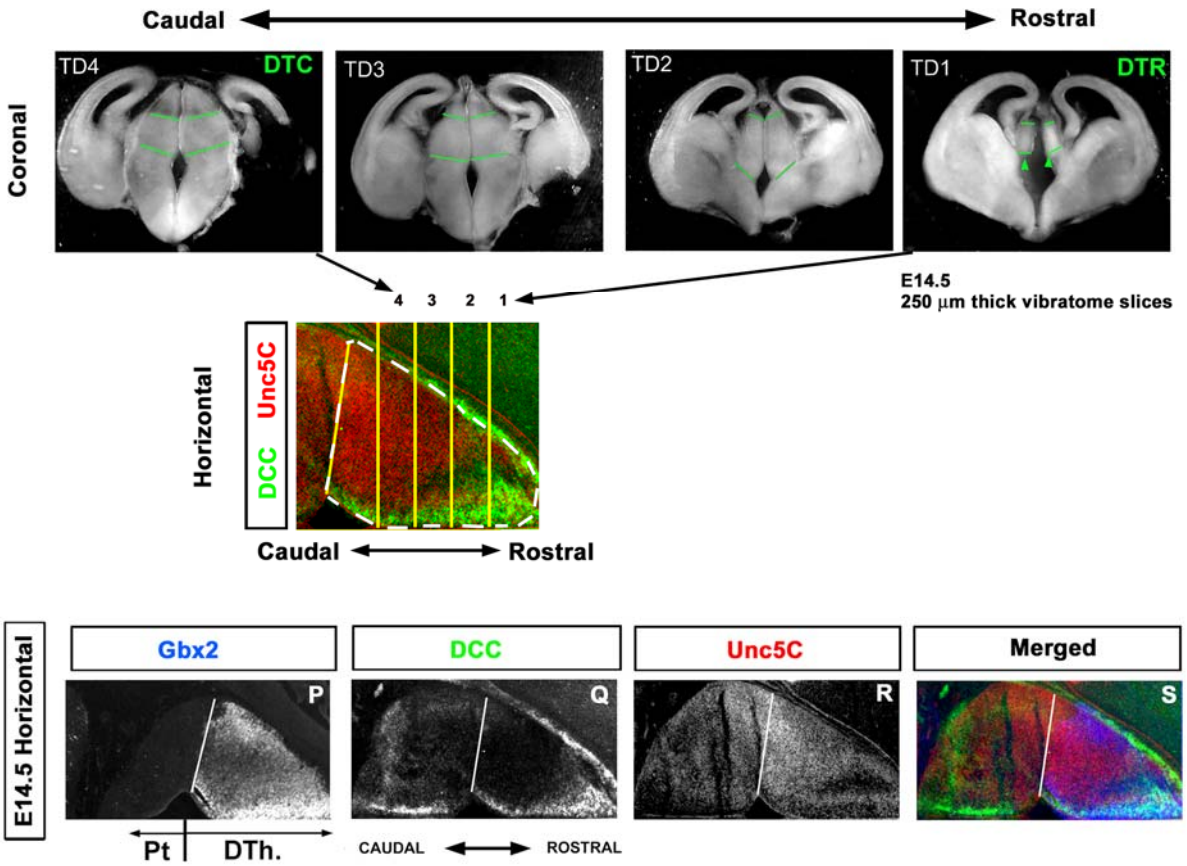

Supplementary Figure 10. Microdissection of thalamic explants and their relationship to Netrin-1-receptors expression patterns.

Dorsal thalamic explants are isolated on adjacent 250-microns thick vibratome sections performed on E14.5 EGFP+ mouse embryos (top panel ordered from rostral to more caudal levels going from left to right).

Expression patterns of *DCC* and *Unc5C* receptors (bottom panel as shown in **Figure 7** and **Suppl. Figure 9**) suggest that section 1 (systematically used for DTR explants (Seibt et al. 2003)) expresses high levels of DCC receptor whereas section 4 (systematically used for DTC explants (Seibt et al. 2003)) expresses low level of *DCC* and high levels of *Unc5A-C*.

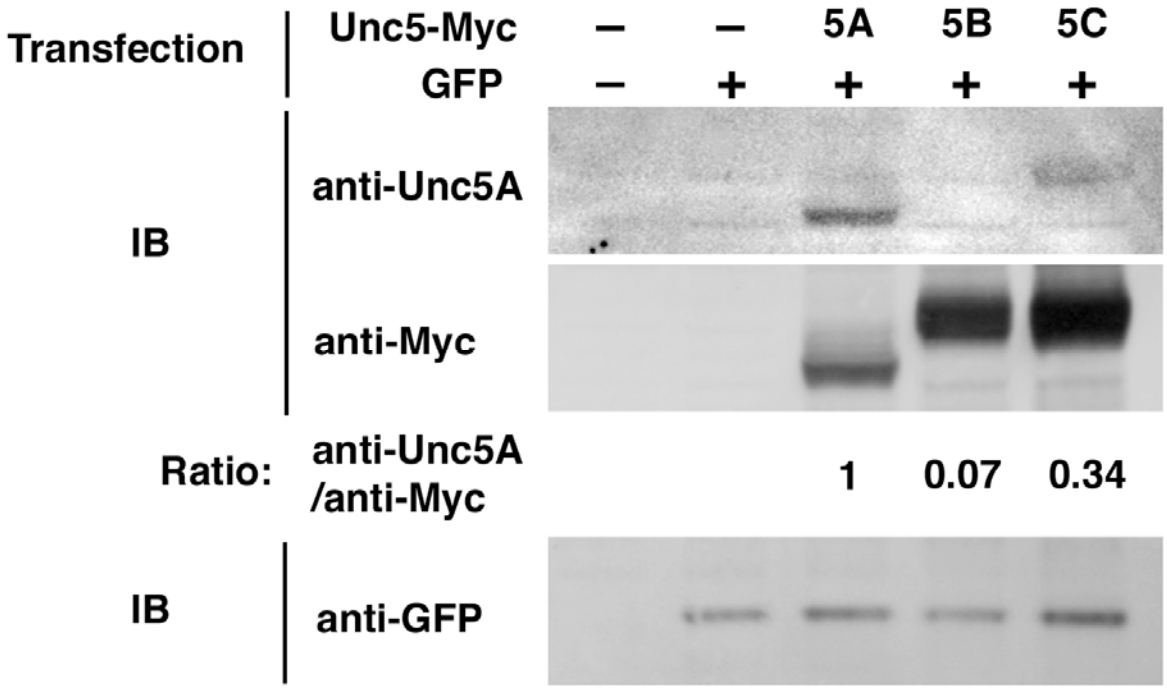

Supplementary Figure 11. Biochemical analysis of the reactivity of function-blocking anti-Unc5A.

COS7 cells were transfected with myc-tagged Unc5A, Unc5B or Unc5C expressed under chicken beta-actin promoter (pCIG2) followed by IRES-mVenus. Two days after transfection, cells were lysed and lysates subjected to SDS-PAGE and probed with mouse anti-Myc antibody (clone 9B11, Cell Signaling Technology, 1:2000), goat anti-Unc5A antibody (anti-rat Unc5H1, R&D Systems, 1:200) and rabbit anti-GFP antibody (IgG fraction, Molecular Probes, 1:2000). The fluorescent signals were detected using Typhoon 9400 image scanner (Amersham) in the linear range. Ratios indicate the relative fluorescence obtained with anti-Unc5A (H1) and anti-myc (control for amount of recombinant Unc5A-B-C protein present in lysate). This analysis demonstrates that the commercially available anti-Unc5A cross-reacts with Unc5C (but not Unc5B) and has approximately 3 times more affinity for Unc5A than for Unc5C.

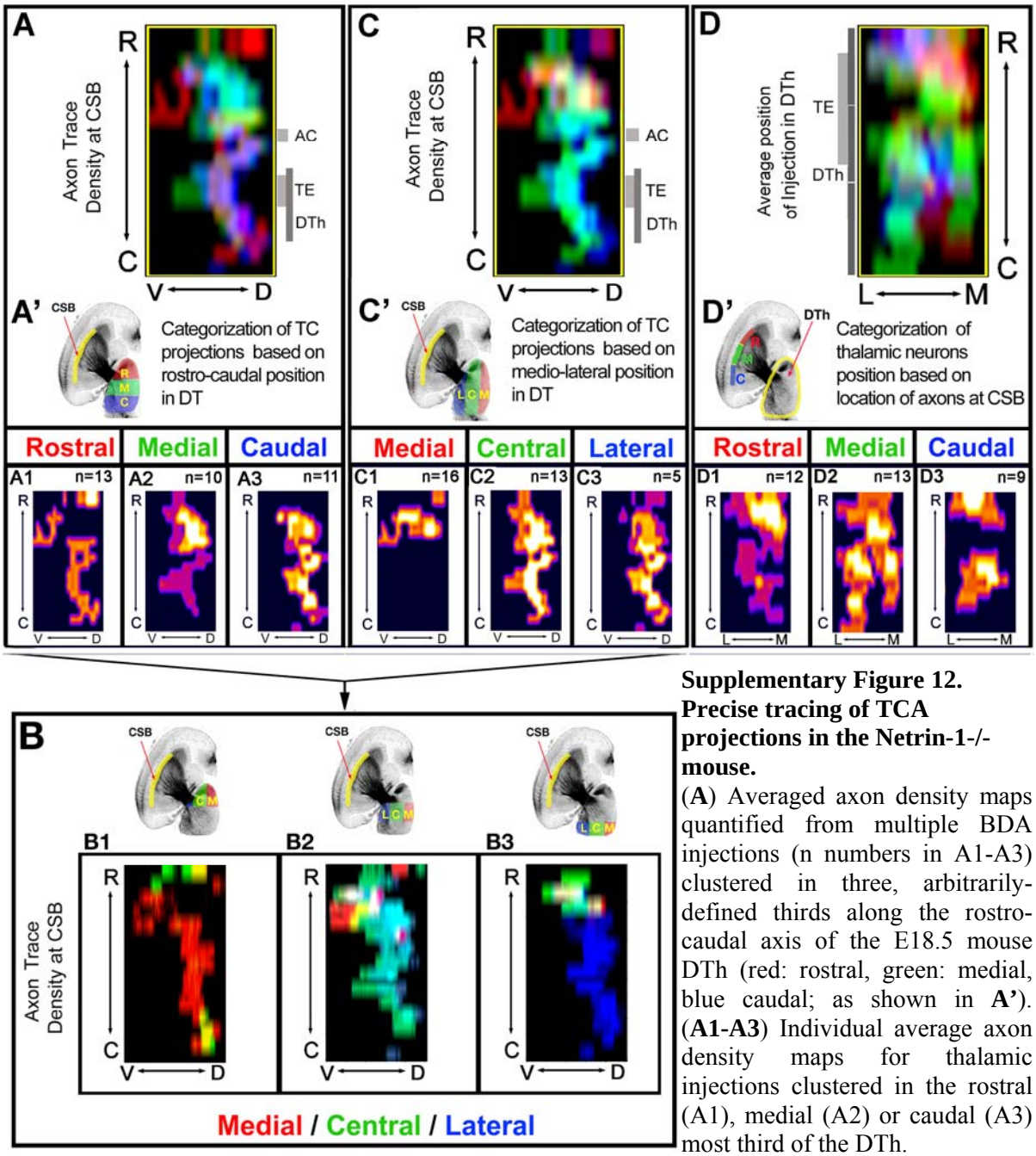

Supplementary Figure 12. Precise tracing of TCA projections in the Netrin-1-/- mouse.

(**A**) Averaged axon density maps quantified from multiple BDA injections (n numbers in A1-A3) clustered in three, arbitrarily-defined thirds along the rostro-caudal axis of the E18.5 mouse DTh (red: rostral, green: medial, blue caudal; as shown in **A'**). (**A1-A3**) Individual average axon density maps for thalamic injections clustered in the rostral (A1), medial (A2) or caudal (A3) most third of the DTh.

(**B**) Averaged axon density maps quantified from multiple BDA injections clustered along the medio-lateral axis of the DTh (red: medial, green: central, blue: lateral; as shown in **B'**).

(**C**) Averaged axon density maps shown in A1 (rostral third along rostro-caudal extent), A2 (medial third along rostro-caudal extent), and A3 (caudal third along rostro-caudal extent) were further subdivided into three thirds along the medio-lateral axis (C1-C3respectively).

(**D-D'**) Averaged position of BDA injection sites in the DTh leading to axons crossing CSB at its most rostral (red), medial (green) or caudal-most (blue) third. (**D1-D3**) Individual averaged density maps of thalamic injection sites leading to axons crossing the CSB at its rostral (D1), medial (D2) or caudal-most (D3) third.

ACKNOWLEDGMENTS

We would like to thank Dr Y. Nakagawa for his insightful advice on thalamic and pretectal markers and for providing us with the *bHLHB4* probe. We would like to thank Dante Bortone for his initial help with Macro programming in Excel as well as all members of the Polleux laboratory for fruitful discussions. The anti-neurofilament 165kD (2H3) monoclonal antibody developed by Tom Jessell was obtained through the Developmental Studies Hybridoma Bank (NICHD -University of Iowa, Dept of Biol. Sciences). We are grateful to Dr Susan Ackerman for providing the mouse *Unc5C* in situ hybridization probe. We would like to thank Quita Earl for her help with creature care and handling. This project was funded by the NIH-National Institute of Neurological Disorders and Stroke (NS047701-01) (FP) and by the March of Dimes Foundation for Birth Defects (FP). This work benefited from the UNC-CH Confocal and Multiphoton Imaging Core facility and the In Situ Hybridization Core facility supported by the NINDS Institutional Center Core Grant to Support Neuroscience Research (P30 NS45892-01).

References

Ackerman SL, Kozak LP, Przyborski SA, Rund LA, Boyer BB et al. (1997) The mouse rostral cerebellar malformation gene encodes an UNC-5-like protein. Nature 386(6627): 838-842.

Agmon A, Connors BW (1991) Thalamocortical responses of mouse somatosensory (barrel) cortex in vitro. Neuroscience 41(2-3): 365-379.

Behrens TE, Johansen-Berg H, Woolrich MW, Smith SM, Wheeler-Kingshott CA et al. (2003) Non-invasive mapping of connections between human thalamus and cortex using diffusion imaging. Nat Neurosci 6(7): 750-757.

Bonnin A, Torii M, Wang L, Rakic P, Levitt P (2007) Serotonin modulates the response of embryonic thalamocortical axons to netrin-1. Nat Neurosci 10(5): 588-597.

Braisted JE, Tuttle R, O'Leary D D (1999) Thalamocortical axons are influenced by chemorepellent and chemoattractant activities localized to decision points along their path. Dev Biol 208(2): 430-440.

Braisted JE, Catalano SM, Stimac R, Kennedy TE, Tessier-Lavigne M et al. (2000) Netrin-1 promotes thalamic axon growth and is required for proper development of the thalamocortical projection. J Neurosci 20(15): 5792-5801.

Bramblett DE, Copeland NG, Jenkins NA, Tsai MJ (2002) BHLHB4 is a bHLH transcriptional regulator in pancreas and brain that marks the dimesencephalic boundary. Genomics 79(3): 402-412.

Bulfone A, Puelles L, Porteus MH, Frohman MA, Martin GR et al. (1993) Spatially restricted expression of Dlx-1, Dlx-2 (Tes-1), Gbx-2, and Wnt-3 in the embryonic day 12.5 mouse forebrain defines potential transverse and longitudinal segmental boundaries. J Neurosci 13(7): 3155-3172.

Burgess RW, Jucius TJ, Ackerman SL (2006) Motor axon guidance of the mammalian trochlear and phrenic nerves: dependence on the netrin receptor Unc5c and modifier loci. J Neurosci 26(21): 5756-5766.

Caviness VS, Jr., Frost DO (1980) Tangential organization of thalamic projections to the neocortex in the mouse. J Comp Neurol 194(2): 335-367.

Chang SL, LoTurco JJ, Nisenbaum LK (2000) In vitro biocytin injection into perinatal mouse brain: a method for tract tracing in developing tissue. J Neurosci Methods 97(1): 1-6.

Cobos I, Borello U, Rubenstein JL (2007) Dlx transcription factors promote migration through repression of axon and dendrite growth. Neuron 54(6): 873-888.

Crandall JE, Caviness VS, Jr. (1984) Thalamocortical connections in newborn mice. J Comp Neurol 228(4): 542-556.

Dufour A, Seibt J, Passante L, Depaepe V, Ciossek T et al. (2003) Area specificity and topography of thalamocortical projections are controlled by ephrin/Eph genes. Neuron 39(3): 453-465.

Engelkamp D (2002) Cloning of three mouse Unc5 genes and their expression patterns at mid-gestation. Mech Dev 118(1-2): 191-197.

Frappe I, Gaillard A, Roger M (2001) Attraction exerted in vivo by grafts of embryonic neocortex on developing thalamic axons. Exp Neurol 169(2): 264-275.

Fritzsch B (1993) Fast axonal diffusion of 3000 molecular weight dextran amines. J Neurosci Methods 50(1): 95-103.

Frost DO, Caviness VS, Jr. (1980) Radial organization of thalamic projections to the neocortex in the mouse. J Comp Neurol 194(2): 369-393.

Garel S, Rubenstein JL (2004) Intermediate targets in formation of topographic projections: inputs from the thalamocortical system. Trends Neurosci 27(9): 533-539.

Garel S, Huffman KJ, Rubenstein JL (2003) Molecular regionalization of the neocortex is disrupted in Fgf8 hypomorphic mutants. Development 130(9): 1903-1914.

Garel S, Yun K, Grosschedl R, Rubenstein JL (2002) The early topography of thalamocortical projections is shifted in Ebf1 and Dlx1/2 mutant mice. Development 129(24): 5621-5634.

Godement P, Vanselow J, Thanos S, Bonhoeffer F (1987) A study in developing visual systems with a new method of staining neurones and their processes in fixed tissue. Development 101(4): 697-713.

Hindges R, McLaughlin T, Genoud N, Henkemeyer M, O'Leary DD (2002) EphB forward signaling controls directional branch extension and arborization required for dorsal-ventral retinotopic mapping. Neuron 35(3): 475-487.

Hohl-Abrahao JC, Creutzfeldt OD (1991) Topographical mapping of the thalamocortical projections in rodents and comparison with that in primates. Exp Brain Res 87(2): 283-294.

Hong K, Hinck L, Nishiyama M, Poo MM, Tessier-Lavigne M et al. (1999) A ligand-gated association between cytoplasmic domains of UNC5 and DCC family receptors converts netrin-induced growth cone attraction to repulsion [see comments]. Cell 97(7): 927-941.

Keino-Masu K, Masu M, Hinck L, Leonardo ED, Chan SS et al. (1996) Deleted in Colorectal Cancer (DCC) encodes a netrin receptor. Cell 87(2): 175-185.

Keleman K, Dickson BJ (2001) Short- and long-range repulsion by the Drosophila Unc5 netrin receptor. Neuron 32(4): 605-617.

Lauder GV (1988) Vertebrate Phylogeny: The Biology and Evolution of Lungfishes. Science 239(4847): 1547-1548.

Leonardo ED, Hinck L, Masu M, Keino-Masu K, Ackerman SL et al. (1997) Vertebrate homologues of C. elegans UNC-5 are candidate netrin receptors. Nature 386(6627): 833-838.

Luo L (2006) Developmental neuroscience: two gradients are better than one. Nature 439(7072): 23-24.

McLaughlin T, O'Leary DD (2005) Molecular gradients and development of retinotopic maps. Annu Rev Neurosci 28: 327-355.

Metin C, Deleglise D, Serafini T, Kennedy TE, Tessier-Lavigne M (1997) A role for netrin-1 in the guidance of cortical efferents. Development 124(24): 5063-5074.

Molnar Z, Blakemore C (1995) How do thalamic axons find their way to the cortex? Trends Neurosci 18(9): 389-397.

Molnar Z, Adams R, Blakemore C (1998a) Mechanisms underlying the early establishment of thalamocortical connections in the rat. Journal of Neuroscience 18(15): 5723-5745.

Molnar Z, Adams R, Goffinet AM, Blakemore C (1998b) The role of the first postmitotic cortical cells in the development of thalamocortical innervation in the reeler mouse. Journal of Neuroscience 18(15): 5746-5765.

Nakagawa Y, O'Leary DD (2001) Combinatorial expression patterns of LIM-homeodomain and other regulatory genes parcellate developing thalamus. J Neurosci 21(8): 2711-2725.

Nakagawa Y, Johnson JE, O'Leary DD (1999) Graded and areal expression patterns of regulatory genes and cadherins in embryonic neocortex independent of thalamocortical input. J Neurosci 19(24): 10877-10885.

Ohyama K, Tan-Takeuchi K, Kutsche M, Schachner M, Uyemura K et al. (2004) Neural cell adhesion molecule L1 is required for fasciculation and routing of thalamocortical fibres and corticothalamic fibres. Neurosci Res 48(4): 471-475.

Okabe M, Ikawa M, Kominami K, Nakanishi T, Nishimune Y (1997) 'Green mice' as a source of ubiquitous green cells. FEBS Lett 407(3): 313-319.

Polleux F, Ghosh A (2002) The slice overlay assay: a versatile tool to study the influence of extracellular signals on neuronal development. Sci STKE 2002(136): PL9.

Schmahl W (1983) Developmental gradient of cell cycle in the telencephalic roof of the fetal NMRI-mouse. Anat Embryol 167: 355-364.

Seibt J, Schuurmans C, Gradwhol G, Dehay C, Vanderhaeghen P et al. (2003) Neurogenin2 specifies the connectivity of thalamic neurons by controlling axon responsiveness to intermediate target cues. Neuron 39(3): 439-452.

Serafini T, Kennedy TE, Galko MJ, Mirzayan C, Jessell TM et al. (1994) The netrins define a family of axon outgrowth-promoting proteins homologous to C. elegans UNC-6. Cell 78(3): 409-424.

Serafini T, Colamarino SA, Leonardo ED, Wang H, Beddington R et al. (1996) Netrin-1 is required for commissural axon guidance in the developing vertebrate nervous system. Cell 87(6): 1001-1014.

Shimogori T, Grove EA (2005) Fibroblast growth factor 8 regulates neocortical guidance of area-specific thalamic innervation. J Neurosci 25(28): 6550-6560.

Shirasaki R, Pfaff SL (2002) Transcriptional codes and the control of neuronal identity. Annu Rev Neurosci 25: 251-281.

Skarnes WC, Moss JE, Hurtley SM, Beddington RS (1995) Capturing genes encoding membrane and secreted proteins important for mouse development. Proceedings of the National Academy of Sciences of the United States of America 92(14): 6592-6596.

Strizzi L, Bianco C, Raafat A, Abdallah W, Chang C et al. (2005) Netrin-1 regulates invasion and migration of mouse mammary epithelial cells overexpressing Cripto-1 in vitro and in vivo. J Cell Sci 118(Pt 20): 4633-4643.

Tanabe Y, Jessell TM (1996) Diversity and pattern in the developing spinal cord. Science 274(5290): 1115-1123.

Tuttle R, Nakagawa Y, Johnson JE, O'Leary DD (1999) Defects in thalamocortical axon pathfinding correlate with altered cell domains in Mash-1-deficient mice. Development 126(9): 1903-1916.

Vanderhaeghen P, Polleux F (2004) Developmental mechanisms patterning thalamocortical projections: intrinsic, extrinsic and in between. Trends Neurosci 27(7): 384-391.

Vanderhaeghen P, Lu Q, Prakash N, Frisen J, Walsh CA et al. (2000) A mapping label required for normal scale of body representation in the cortex. Nat Neurosci 3(4): 358-365.

Yavarone MS, Shuey DL, Sadler TW, Lauder JM (1993) Serotonin uptake in the ectoplacental cone and placenta of the mouse. Placenta 14(2): 149-161.

Zhong Y, Takemoto M, Fukuda T, Hattori Y, Murakami F et al. (2004) Identification of the genes that are expressed in the upper layers of the neocortex. Cereb Cortex 14(10): 1144-1152.

Zou Y, Stoeckli E, Chen H, Tessier-Lavigne M (2000) Squeezing axons out of the gray matter: a role for slit and semaphorin proteins from midline and ventral spinal cord. Cell 102(3): 363-375.

CHAPTER THREE

Cellular and molecular mechanisms underlying the 'handshake' between thalamocortical and corticothalamic axons in the ventral telencephalon

Ashton Powell [1, 2], Amanda G. Wright [3], Anthony Paul Barnes [1], Patricia F. Maness [3] and Franck Polleux [1#]

[1] University of North Carolina, Neuroscience Center, Department of Pharmacology, Chapel Hill, NC 27599-7250, USA
[2] Curriculum in Neuroscience, UNC Chapel Hill, NC 27599, USA
[3] Department of Biochemistry, UNC Chapel Hill, NC 27599, USA

[#] Address correspondence to: polleux@med.unc.edu

Franck POLLEUX
University of North Carolina
Neuroscience Center - Dept of Pharmacology
115 mason farm road –CB#7250
Chapel Hill, NC 27599 -7250
USA

Tel: 919-966-1449

Fax: 919-966-9605

SUMMARY

Thalamocortical (TC) axons fasciculate with corticofugal (CF) axons in the internal capsule during embryonic development which has led to the 'handshake' hypothesis postulating that CF axons play an instructive role in the guidance of TC axons towards their appropriate cortical target. Recent results demonstrate that several axon guidance cues expressed in gradient along the rostro-caudal axis of the ventral telecenphalon (including ephrinA5, Netrin-1 and Sema3A) and play a critical role in the guidance of TC axons towards their appropriate cortical domain. In the present study, we provide *ex vivo* and *in vivo* evidence showing that CF axons are specifically required for the proper guidance of TC axons originating from the caudal but not the rostral thalamus. We also show that Close Homolog of L1 (CHL1) is required on both caudal CF axons and TC axons for proper guidance of caudal thalamic axons to the caudal part of the ventral telencephalon. Our results suggest that CHL1 expression along caudal CF axons silences Sema3A-mediated chemorepulsion of caudal TC axons allowing these axons to grow in the Sema3A-rich, caudal part of the VTel. Taken together, we propose that CHL1 represents one of the functional molecular substrates for the 'handshake' between TC and CF axons in the ventral telencephalon.

INTRODUCTION

The dorsal thalamus is a pivotal forebrain structure, receiving sensory inputs from the periphery and communicating with the cerebral cortex via thalamocortical (TC) axons. Each thalamic nucleus projects topographically to a unique set of cortical areas. This *inter-areal* topography of TC projections is organized so that rostro-medial thalamic neurons project to more rostral cortical areas than caudo-lateral nuclei which tend to project to more caudal cortical areas (Caviness and Frost 1980; Crandall and Caviness 1984; Hohl-Abrahao and Creutzfeldt 1991). Several line of evidence have demonstrated that the ventral telencephalon (VTel) is an important intermediate target for TC axons where they fasciculate with corticofugal (CF) axons (Molnar et al. 1998) and interact with various cell populations present in the mantle region of the VTel (Molnar and Cordery 1999). Several lines of evidence suggested that the VTel contained important cues participating to the guidance of different subsets TC axons to their appropriate cortical targets (Metin et al. 1997; Garel et al. 2002; Garel et al. 2003; Seibt et al. 2003). Recent results have identified several of these axon guidance cues including ephrinA5 (Dupont et al. 1983), Sema3A (Gates et al. 2007) and Netrin-1 (Powell et al. 2007) which display graded expression along the rostro-caudal axis of the VTel and play critical and complementary roles in the guidance of TC axons to their appropriate cortical domain (Garel et al. 2003; Garel and Rubenstein 2004; Vanderhaeghen and Polleux 2004).

However, another mechanism has been proposed to play a role in guiding TC axons to their appropriate cortical target. The 'handshake' model has been proposed based on the fact that TC axons fasciculate with corticofugal axons (CF) of the preplate cells which first pioneer the internal capsule (Molnar and Blakemore 1995). The functional relevance of the 'handshake' model has been supported by the analysis of knockout mice for genes expressed predominantly in the cortex and affecting axon pathfinding of preplate and layer 6a axon projections (*Tbr1*) or the dorsal thalamus (*Gbx2*) expressed predominantly in the dorsal thalamus (DT) displaying guidance defects of TC axons in the internal capsule (Hevner et al. 2002). Both of these mutant mice show reciprocal axon

guidance defects for TC axons (*Tbr1* knockout) and corticofugal axons (*Gbx2* knockout) suggesting that TC and CF axons are mutually guiding each other in the internal capsule (Hevner et al. 2002). However, the interpretation of the phenotype characterizing these knockout mice is obscured by the fact that these genes are not exclusively expressed in the dorsal thalamus (*Gbx2*) or the cortex (*Tbr1*): *Gbx2* is also expressed in the mantle region of the ventral telencephalon (data not shown; (Grigoriou et al. 1998)) and *Tbr1* is expressed in the ventral thalamus (data not shown; (Bulfone et al. 1995)). Therefore, the indirect effect of *Tbr1* mutation on TC axon pathfinding might be due to either the reported abnormal cortical axon projections in the internal capsule and/or to a more direct mispatterning of putative axon guidance cues present in the ventral thalamus which has been shown to play an important role in the guidance of TC axons (Braisted et al. 1999).

In the present study, we have tested directly the role of corticofugal projections in the establishment of the topography of TC axons projections in the VTel using combinations of *ex vivo* co-culture assays as well as conditional genetic manipulation leading to the absence of corticofugal axons *ex vivo* and *in vivo* respectively. Our results demonstrate that the absence of CF axons in the internal capsule affects the pathfinding of axons originating from the caudal but not the rostral part of the DT. Our results also show that in the absence of CF axons, both thalamic axons originating from both rostral and caudal thalamus exhibit defects in their ability to cross the cortico-striatal boundary (CSB). Finally, we show that Close Homolog of L1 (CHL1), a membrane-bound cell adhesion molecule expressed along both thalamic and caudal cortical axons is required for proper guidance of TC axons originating from caudal but not rostral thalamus. Our results suggest that CHL1 expression along caudal CF axons silences Sema3A-mediated chemorepulsion of caudal TC axons allowing these axons to grow in the Sema3A-rich caudal part of the VTel. Taken together, we propose that CHL1 represents one of the functional molecular substrates for the 'handshake' between TC and CF axons in the ventral telencephalon.

RESULTS

Corticofugal axons are required for proper guidance of caudal but not rostral thalamic axons *in vitro*

We first tested the function of corticofugal axons for the proper guidance of thalamocortical axons in the ventral telencephalon (VTel) by performing co-cultures of E14.5 DTR (**Fig. 1A-D**) or DTC explants (**Fig. 1E-H**) with intact wholemount telencephalic vesicles (**Fig. 1B and F**) or telencephalic vesicles where the cortex had been dissected out (**Fig. 1C and G**). The results show that DTR axons are not affected by the absence of corticofugal axons from the telencephalic vesicles (**Fig. 1D**) but DTC axons display a significant rostral shift in the absence of corticofugal axons in the VTel (**Fig. 1H**). These results suggest an unexpected difference in the mechanisms guiding axons originating from the rostral versus caudal thalamus in the VTel.

Abnormal topography of caudal thalamocortical projections in the absence of corticofugal axons in the ventral telencephalon *in vivo*

We next took advantage of a recent observation showing that the tumor suppressor LKB1 specifically controls the polarized outgrowth of axons in cortical neurons (Barnes et al. 2007). We have previously shown that a cortex-specific conditional LKB1 knockout (obtained by crossing the $Emx1^{Cre}$ driver mouse line (Gorski et al. 2002) with a conditional allele of LKB1 (Bardeesy et al. 2002)) is characterized by a nearly complete ablation of corticofugal axons (Barnes et al. 2007).

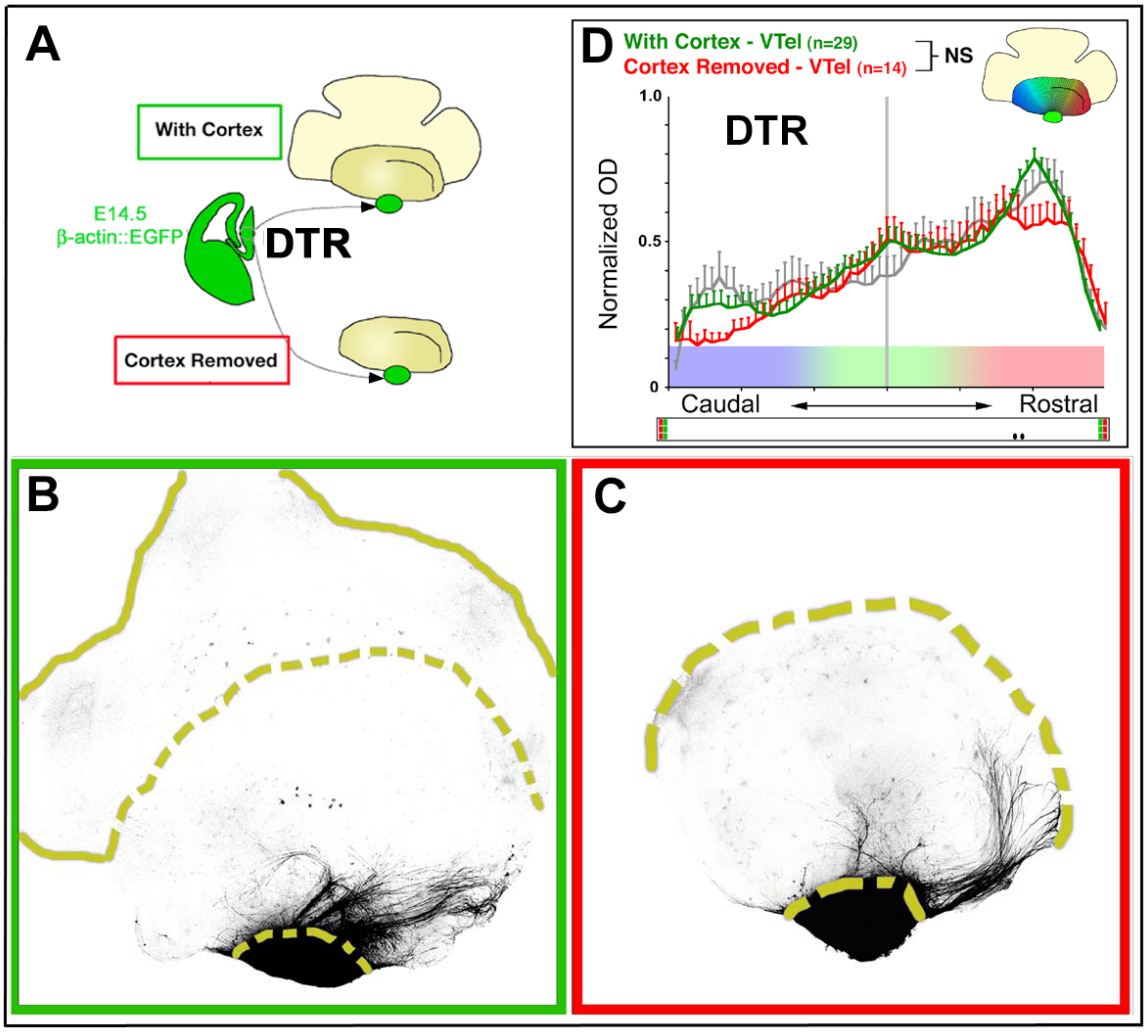

Figure 1. The absence of corticofugal axons in the ventral telencephalon leads to misguidance of axons originating from the caudal but not the rostral thalamus.

(**A**) Schematic of the experimental paradigm: isochronic wholemount telencephalic co-cultures were performed using EGFP-expressing explants isolated at E14.5 from the rostral part of the dorsal thalamus and telencephalic vesicles with (top) or without (bottom) the dorsal telencephalon.

(**B-C**) Wholemount telencephalic co-cultures showing that removal of the dorsal telencephalon (C) does not affect the outgrowth of DTR axons towards the rostral domain of the ventral telencephalon (arrowhead) compared to control co-cultures (B).

(**D**) Quantification of the topography of rostral thalamic axon outgrowth in the VTel in control co-cultures containing the cortex (green) or with cortex removed (red). Each histogram represents the average normalized optical density (OD) from the EGFP signal measured in 60 radial bins centered on the thalamic explant.

(**E**) Schematic of the experimental paradigm: isochronic wholemount telencephalic co-cultures were performed using EGFP-expressing explants isolated at E14.5 from the caudal part of the dorsal thalamus and telencephalic vesicles with (top) or without (bottom) the dorsal telencephalon.

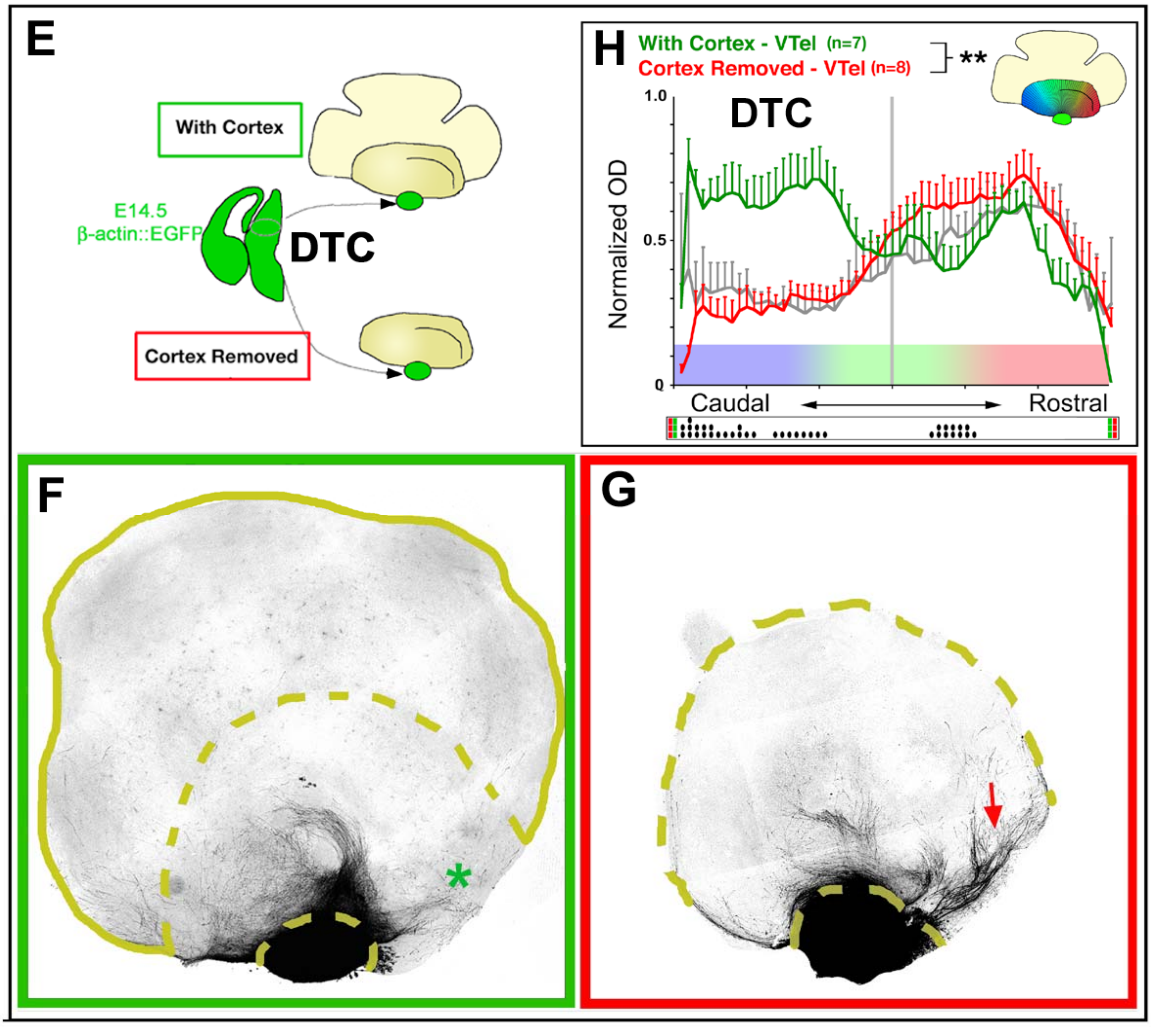

Figure 1. The absence of corticofugal axons in the ventral telencephalon leads to misguidance of axons originating from the caudal but not the rostral thalamus. Cont.

(**F-G**) Wholemount telencephalic co-cultures showing that removal of the dorsal telencephalon (C) induces a significant rostral shift of caudal TC axons towards the rostral domain of the VTel (arrow in G) compared to control co-cultures where DTC axons specifically avoid the rostral domain of the VTel (star in F) and grow preferentially towards the caudal domain of the VTel (arrowhead in F).

(**D**) Quantification of the topography of caudal thalamic axon outgrowth in the VTel in control co-cultures containing the cortex (green) or with cortex removed (red). Each histogram represents the average normalized optical density (OD) from the EGFP signal measured in 60 radial bins centered on the thalamic explant. Statistical analysis:

*** $p<0.001$ ANOVA one-way test (overall effect: bins versus experimental conditions). The raster-like dot plot presented under the histograms represents the significance of individual bin comparisons between the two experimental conditions according to a PLSD-post-hoc test (• $p<0.05$; •• $p<0.01$ and ••• $p<0.001$). Scale bar value: B-C, 250 microns.

We used this specific genetic model of cortical axon ablation in order to test the function of corticofugal axons in the guidance of TC axons within the VTel. As shown in **Figure 2A** and **2D**, the cortex of $Emx1^{Cre/+}$;$LKB1^{F/F}$ embryos at E14.5 does not contain any detectable number of TAG1+ corticofugal axons compared to control $Emx1^{Cre/+}$;$LKB1^{F/+}$ littermates. Interestingly, the number of L1-positive thalamic axons successfully entering the cortex of $Emx1^{Cre/+}$;$LKB1^{F/F}$ embryos at E16.5 is significantly lower than in control mice (compare **Fig. 2 B-C** and **2E-F**).

One potential caveat identifying thalamic axons using L1 staining is that L1 is also expressed in callosally projecting axons (star in Figure 2B). Therefore, the axons remaining in the cortex of the $Emx1^{Cre/+}$;$LKB1^{F/F}$ knockout embryos (Fig. 1E) could be callosally projecting axons rather than thalamic axons which could lead to an underestimation of the consequence of the absence of corticofugal axons in the ventral telencephalon on TC axons pathfinding. In order to confirm the results obtained using axonal staining, we traced TC axons using the anterograde tracer Biotinylated Dextran Amine injected in the dorsal thalamus of control $Emx1^{Cre/+}$;$LKB1^{F/+}$ embryos at E18.5 (**Fig. 2 G-J**) or $Emx1^{Cre/+}$;$LKB1^{F/F}$ embryos (**Fig. 2 K-N**). This revealed that the absence of corticofugal axons from the ventral telencephalon characterizing the conditional LKB1 knockout leads to defective cortical entry of TC axons at the level of the corticostriatal boundary.

Our quantification of the topography of TC axon projections in the ventral telencephalon containing corticofugal axons ($Emx1^{Cre/+}$;$LKB1^{F/+}$ embryos) or not containing corticofugal axons ($Emx1^{Cre/+}$;$LKB1^{F/F}$ embryos) demonstrate that a contingent of TC axons originating from the caudal thalamus are projecting significantly more rostrally in the VTel of cortex-specific LKB1 conditional knockout (**Fig. 3I**) than in control (**Fig. 3D**).

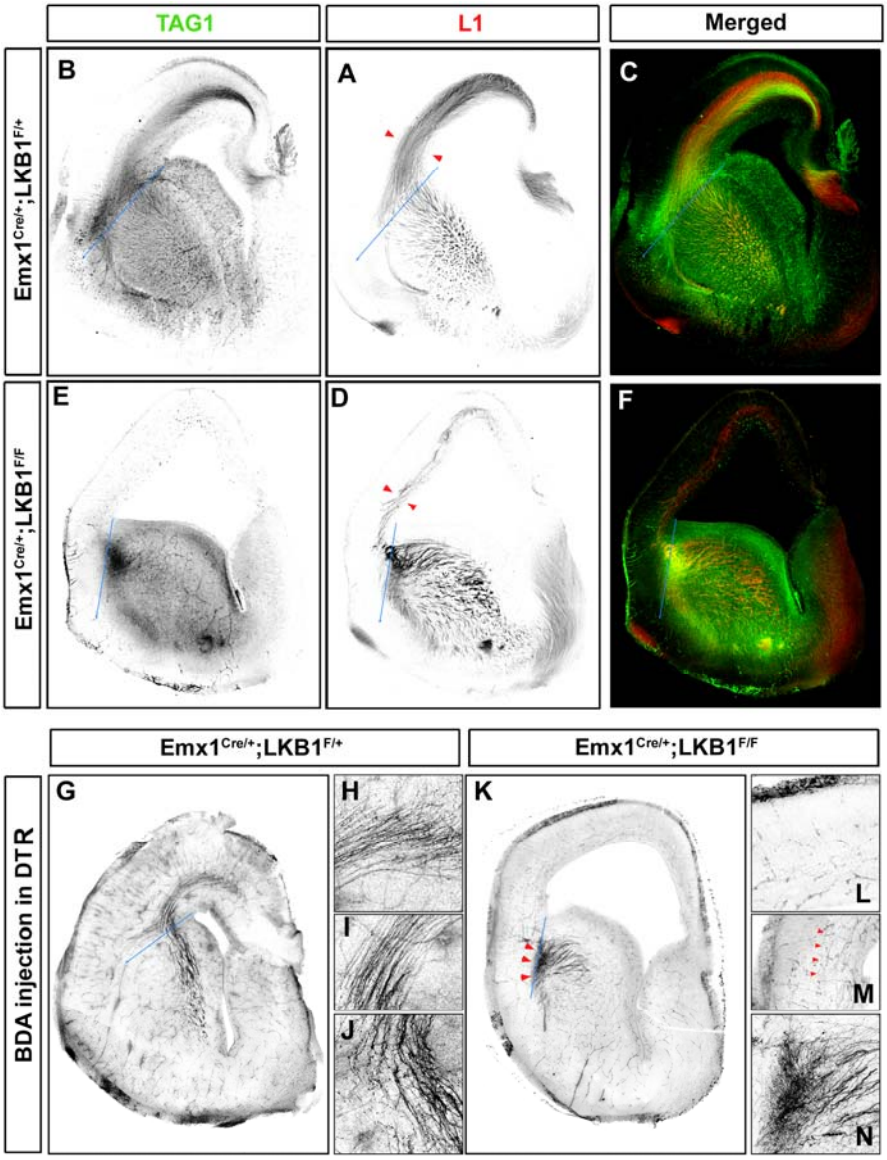

Figure 2. Absence of cortical projections *in vivo* prevents thalamocortical axons to cross the corticostriatal boundary (CSB).

(**A-F**) TAG1-positive corticofugal axons are projecting towards the internal capsule in control $Emx1^{Cre/+};LKB1^{F/+}$ embryos at E16.5 (A; green in C) but are absent from the cortex of littermate cortex-specific LKB1 conditional knockout ($Emx1^{Cre/+};LKB1^{F/F}$) (D; green in F). Interestingly, only a limited subset of L1-positive thalamocortical axons (B; red in C) cross the corticostriatal boundary (CSB; blue line in A-F) in conditional LKB1 knockout E16.5 embryos (arrowheads in E) compared to control littermate (arrowheads in B). Note that L1 also stains callosally projecting axons in control embryos (star in B) which are absent from the conditional LKB1 embryos (Star in E).

(**G-N**) Anterograde tracing of axons originating from the rostral part of the dorsal thalamus using biotinylated Dextran Amine (BDA; 3000 MW) reveals the stalling of TC axons at the CSB of conditional LKB1 embryos (arrowheads in K) compared to control littermates (G). Panels H-J and L-N represents high magnification of BDA-positive axons in the internal capsule (H and L), intermediate zone of the lateral (I and M) and medial cortex (J and N). Note that few TC axons are found in the lateral cortex of LKB1 conditional knockout embryos. Scale bar values: A-F and G and K: 300 microns; H-I-J and L-M-N: 100 microns.

In contrast, the topographic outgrowth of axons originating from the rostral DTh is not affected by the absence of corticofugal axons characterizing the cortex-specific LKB1 conditional knockout embryos (**Fig. 3B-C** and **3G-H**). All the axon projections quantified in Fig.3B-D and 3G-H had successfully reached the CSB by E18.5. However, a significant contingent of thalamic axons originating from the caudal thalamus do not even reach the CSB and are stalled in the caudal part of the VTel (**Fig. 3 L**).

In order to confirm the role of corticofugal axons in the guidance of caudal but not rostral TC axons in the ventral telencephalon, we performed co-cultures of DTR or DTC axons with telecenphalic vesicles isolated from control ($Emx1^{Cre/+}$;$LKB1^{F/+}$) embryos or cortex-specific LKB1 knockout ($Emx1^{Cre/+}$;$LKB1^{F/F}$) embryos at E14.5. Our results show that the absence of corticofugal axons from the ventral telencephalon characterizing the cortex-specific conditional LKB1 knockout embryos has no detectable effect on the guidance of rostral thalamic axons to the rostral domain of the VTel (**Fig. 4A-D**). However, the absence of corticofugal axons from the ventral telencephalon has a pronounced effect on the guidance of caudal TC axons (**Fig. 4F-I**), which are significantly shifted rostrally in the co-cultures with $Emx1^{Cre/+}$;$LKB1^{F/F}$ telencephalon (**Fig. 4H** and **4I**) compared to control co-cultures with $Emx1^{Cre/+}$;$LKB1^{F/+}$ telencephalon (**Fig. 4G** and **4I**).

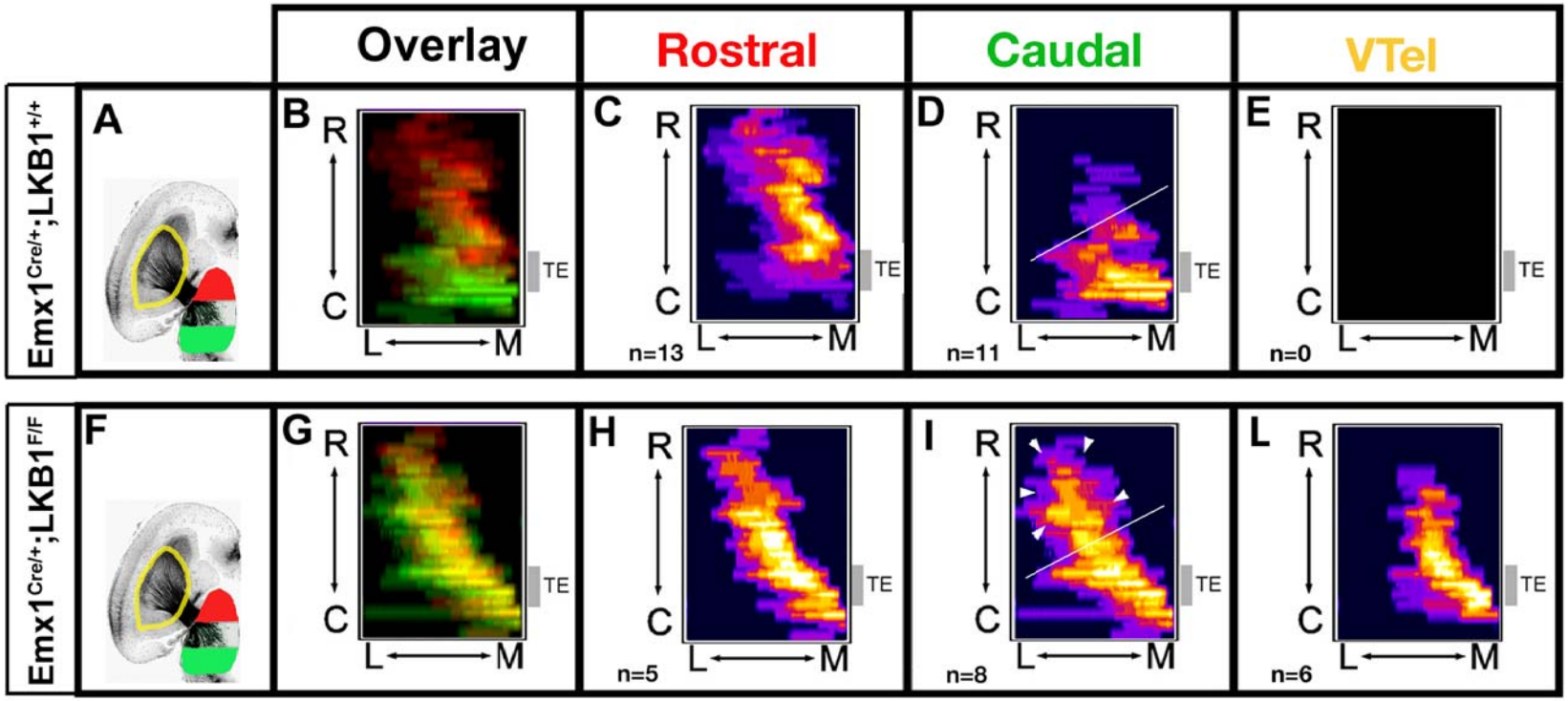

Figure 3. Quantitative analysis of the topography of thalamocortical projections in cortex-specific LKB1 knockout embryos *in vivo*. (**A-D**) Averaged axon density maps showing the distribution of BDA-positive axons originating from the rostral (C; red in B) or caudal (D; green in B) thalamus of E18.5 control $Emx1^{Cre/+};LKB1^{F/+}$ embryos in the ventral telencephalon (as shown by yellow circle area on schematic horizontal section in A). Note that axons originating from the rostral thalamus project to more rostro-medial domain of the VTel (green in B) than axons originating from the caudal thalamus (red in B). (**F-I**) Averaged axon density maps showing the distribution of BDA-positive axons originating from the rostral (C; red in B) or caudal (D; green in B) thalamus of E18.5 cortex-specific LKB1 conditional knockout ($Emx1^{Cre/+};LKB1^{F/F}$) embryos in the ventral telencephalon (as shown by yellow circle area on schematic horizontal section in F). The line in D and I represents the rostral-most limit of caudal thalamic projection in the VTel in control brains. The area delineated by arrowheads in I represents the contingent of axons originating from the caudal thalamus that project abnormally rostrally in the cortex-specific LKB1 knockout embryos at E18.5. (**E** and **L**) Average axon density maps showing the distribution of BDA-positive thalamic axons that do not reach the corticostriatal boundary in control $Emx1^{Cre/+};LKB1^{F/+}$ embryos (E-none) and $Emx1^{Cre/+};LKB1^{F/F}$ embryos (L). Note that a significant contingent of thalamic axons projecting to the caudal part of the VTel do not reach the CSB in the cortex-specific LKB1 conditional knockout embryos.

Abbreviations: TE: indicates the position of the thalamic eminence, the exit point of thalamic axons transiting from the diencephalon into the ventral telencephalon.

The absence of corticofugal axons leads to deflection of thalamocortical axons at the corticostriatal boundary

The absence of corticofugal axons in the ventral telencephalon has another more general effect on TC axon guidance at the level of the CSB. Both rostral (**Fig. 4E**) and caudal (**Fig. 4J**) thalamic axons display significant shifts in their projections upon reaching the CSB. This result is confirmed by an analysis of the angle of deflection of rostral or caudal TC axons at the corticostriatal boundary of control $Emx1^{Cre/+}$;$LKB1^{F/+}$ telencephalon or $Emx1^{Cre/+}$;$LKB1^{F/F}$ telencephalon lacking corticofugal axons (**Fig. 5**). These results suggest that corticofugal axons are required for the general ability of TC axons to cross the CSB and to grow directionally (dorsally) once in the dorsal telencephalon.

CHL1 is required both on corticofugal and thalamocortical axons for proper guidance of TC axons inside the ventral telencephalon

We explored the function of CHL1 as a candidate molecular substrate for the 'handshake' model. CHL1 is expressed on corticofugal axons originating from the caudal but not the more rostral cortical areas (Liu et al. 2000; Demyanenko et al. 2004; Gates et al. 2007). CHL1 is also expressed in the vast majority of thalamocortical axons (Gates et al. 2007). The diffusible class 3 Semaphorin, Sema3A is expressed in a high-caudal to low-rostral gradient in the ventral telencephalon and recent evidence shows that CHL1 is functionally required for Sema3A-mediated chemorepulsion (Gates et al. 2007). We hypothesized that caudal thalamic axons (which express the high-affinity Sema3A transmembrane receptor Neuropilin1; Npn1) are not repulsed from the caudal domain of the ventral telencephalon because CHL1, expressed along caudal corticofugal axons, could silence, in *trans,* the function of CHL1-mediated chemorepulsion evoked by Sema3A. In order to test this hypothesis, we

performed wholemount co-cultures between DTR and DTC axons and wholemount telencephalon, all expressing or not CHL1 (**Fig. 6A-H**). Our results show that removing CHL1 simultaneously from thalamic axons and the telencephalon is sufficient to significantly shift the projection of caudal TC axons into the rostral part of the ventral telencephalon (**Fig. 6J**) but has little effect on the projection of rostral TC axons (**Fig. 6I**).

Interestingly, removing CHL1 from either CF axons or TC axons alone had a comparatively modest but significant effect on caudal TC projections compared to control conditions (compare blue and purple graphs to the red one in **Fig. 6L**). Interestingly, removal of CHL1 from both TC and CF axons simultaneously shows an additive effect (green curve in Fig, 6L) and results in a very significant shift of the of caudal TC axon projections towards rostral territories of the VTel. Again, we observed only modest effect of removing CHL1 from either the CF axons or TC axons on the topographic projections of rostral DT, with no rostral condition having a statistically significant difference from controls (**Fig. 6K**).

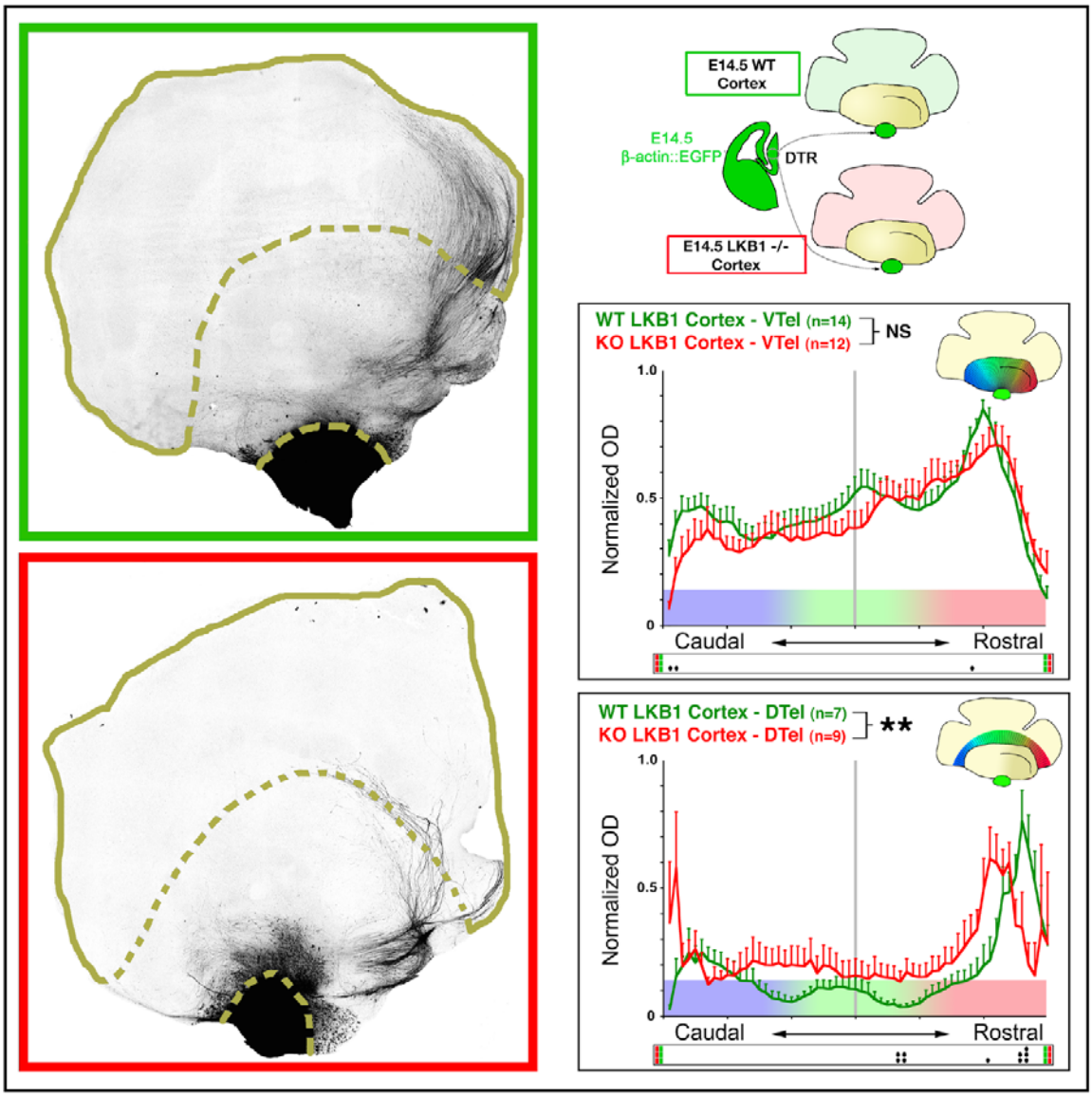

Figure 4. Genetic removal of corticofugal axons in the ventral telencephalon affect the topographic projection of axons originating from the caudal but not the rostral thalamus.

(**A-D**) Experimental paradigm is same than in Figure 1 expect that the wholemount co-cultures are performed using wild-type EGFP-expressing DTR explants and wholemount telencephalic vesicles isolated from either control ($Emx1^{Cre/+}$;$LKB1^{F/+}$) E14.5 embryos or cortex-specific LKB1 knockout embryos ($Emx1^{Cre/+}$;$LKB1^{F/F}$). Note that in the absence of corticofugal axons in the ventral telencephalon, rostral thalamic axons project to the rostral part of the VTel (C; quantified in D) as observed in control co-cultures (B; quantified in D).

(**E**) Quantification of the distribution of EGFP+ DTR axons at a level just dorsal of the CSB in control co-cultures (green) and co-cultures with telencephalic vesicles isolated from cortex-specific LKB1 conditional knockout embryos (red).

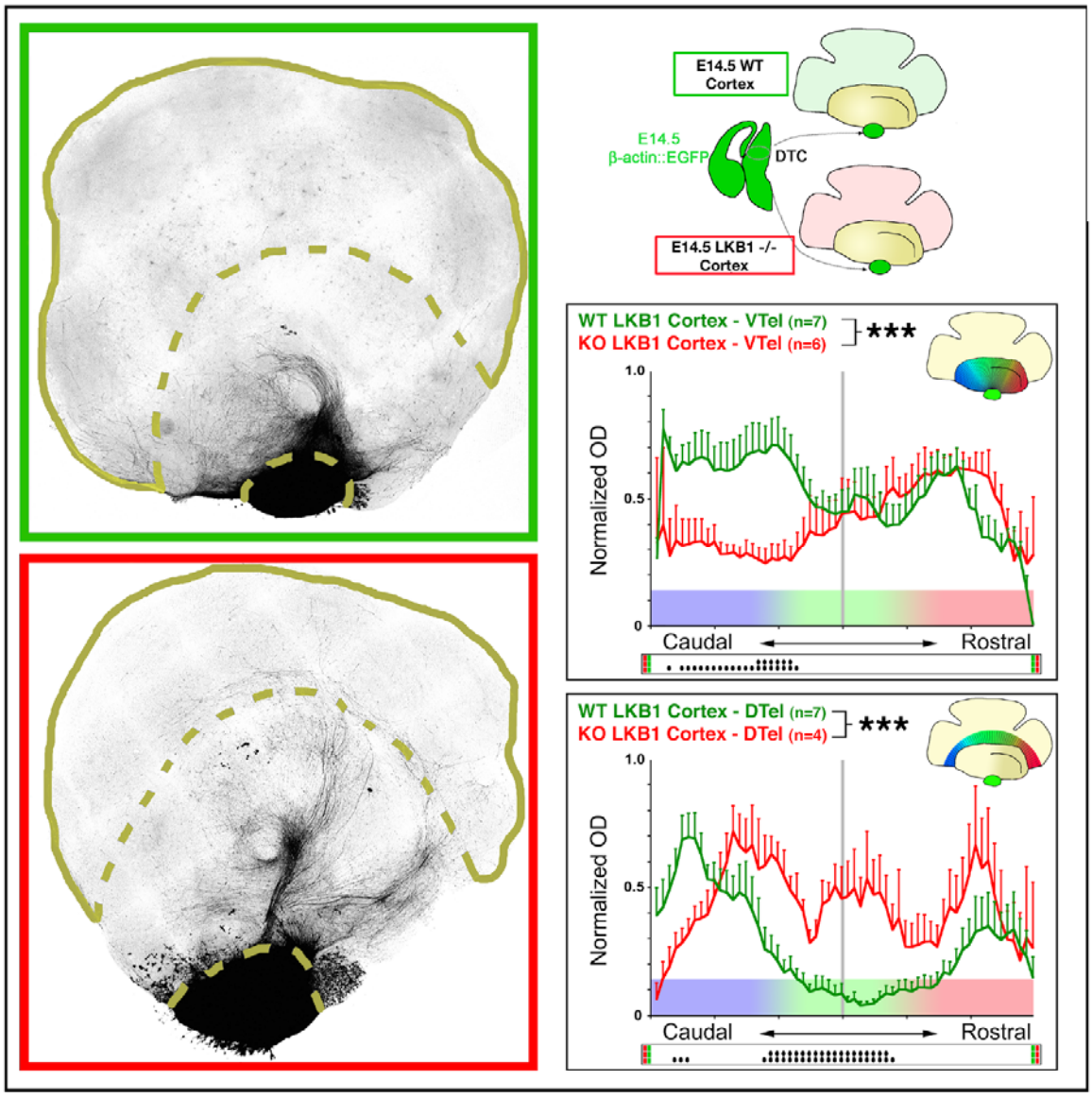

Figure 4. Genetic removal of corticofugal axons in the ventral telencephalon affect the topographic projection of axons originating from the caudal but not the rostral thalamus. Cont. Note that after crossing the CSB, DTR axons are projecting slightly more caudally when growing in the absence of corticofugal axons than in control cases.

(**F-I**) Same as in A-D but for wholemount co-cultures with DTC explants. Note that DTC axons are significantly shifted rostrally when growing in a LKB1-deficient telencephalon (arrow in H) compared to control co-cultures where DTC specifically avoid the rostral domain of the VTel (star G). Statistical analysis as in Figure 1.

(**J**) Quantification of DTC axon distribution after crossing the CSB reveals a pronounced randomization of projection suggesting that corticofugal axons are necessary for the proper guidance of DTC axons in the cortex. Statistical analysis as in Figure 1.

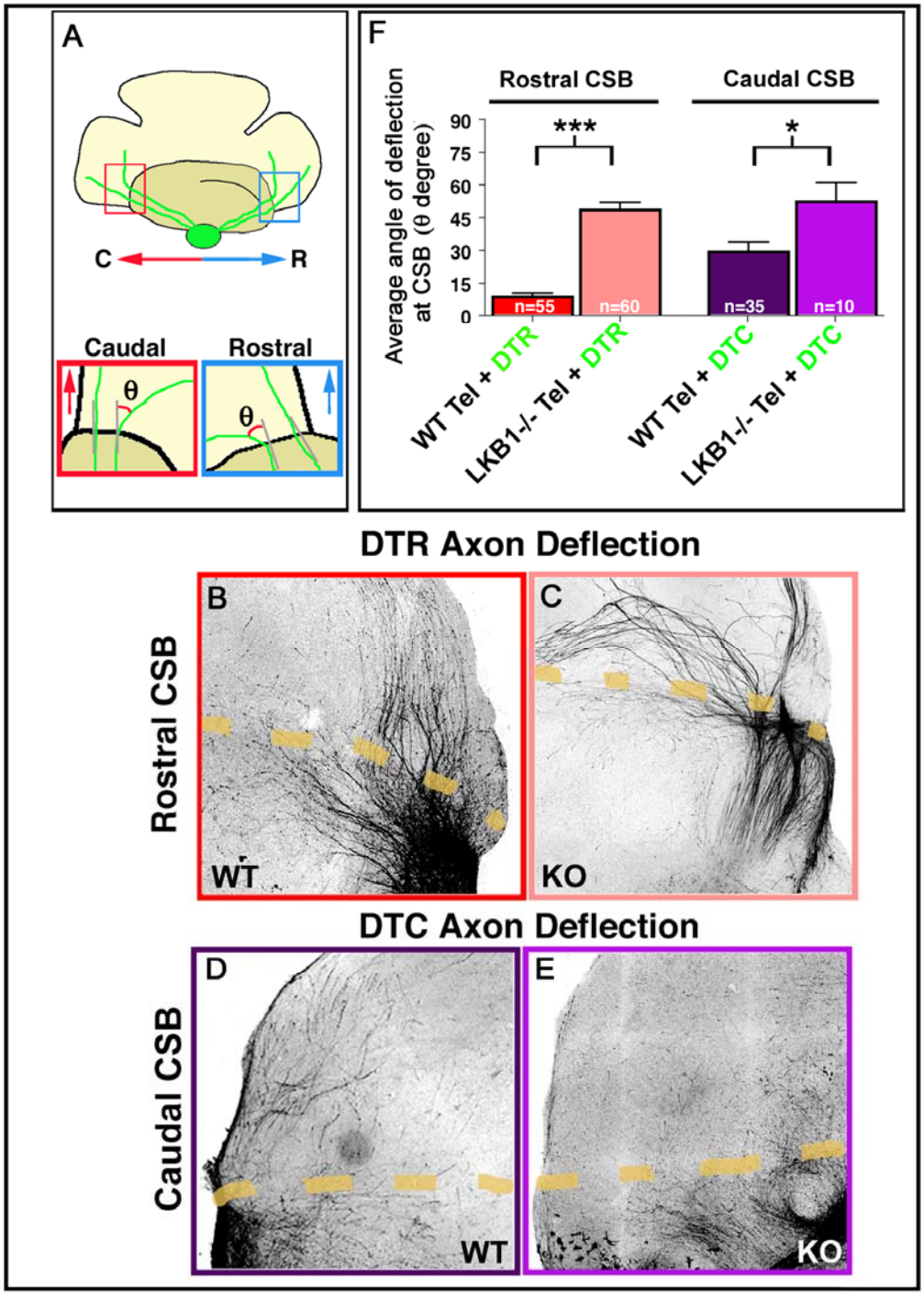

Figure 5. Corticofugal axons are necessary for proper crossing of the corticostriatal boundary by thalamic axons. (**A**) The angle of deflection (Ø) is defined as the angle difference between an axis perpendicular to the CSB and individual thalamic axons or thalamic axon fascicles. (**B-E**) Confocal micrograph illustrating the behavior of EGFP+ DTR axons (B-C) or DTC axons (D-E) crossing the CSB of control ($Emx1^{Cre/+}$;$LKB1^{F/+}$; B and D) or cortex-specific LKB1 knockout ($Emx1^{Cre/+}$;$LKB1^{F/F}$; C and E) wholemount telencephalon. (**F**) Quantification of the deflection angle displayed by DTR (red histograms) or DTC axons (purple histograms) at the CSB of control or cortex-specific LKB1 conditional knockout telencephalon. Statistical analysis as in Figure 1.

CHL1 silences the Sema3A-mediated chemorepulsion of axons

In order to test more directly our hypothesis that caudal thalamic axons are not repulsed from the caudal domain of the ventral telencephalon because CHL1 expressed along caudal corticofugal axons could silence, in *trans,* the function of CHL1-mediated chemorepulsion evoked by Sema3A, we performed growth cone (GC) collapse assays of TC axons using Sema3A and soluble CHL1. Our results show that incubation of TC growth cones with Sema3A induces the collapse of close to 90% of CHL1-expressing GC, but only half of them are repulsed when Sema3A is co-incubated with a soluble form of CHL1 (**Figure 7**). These results demonstrate that CHL1 expression along corticofugal axons might mimic the application of the ectodomain of CHL1 and prevent the Sema3A-mediated collapse of thalamic axons from the caudal domain of the VTel.

DISCUSSION

Overall, the results presented in this study demonstrate (1) that corticofugal axons are required for proper guidance of caudal but not rostral thalamic axons towards the appropriate domain of the VTel and (2) that CHL1 is required on both thalamocortical axons and corticofugal axons for the proper guidance of caudal but not rostral thalamic projections in the ventral telencephalon (see model in **Figure 8**).

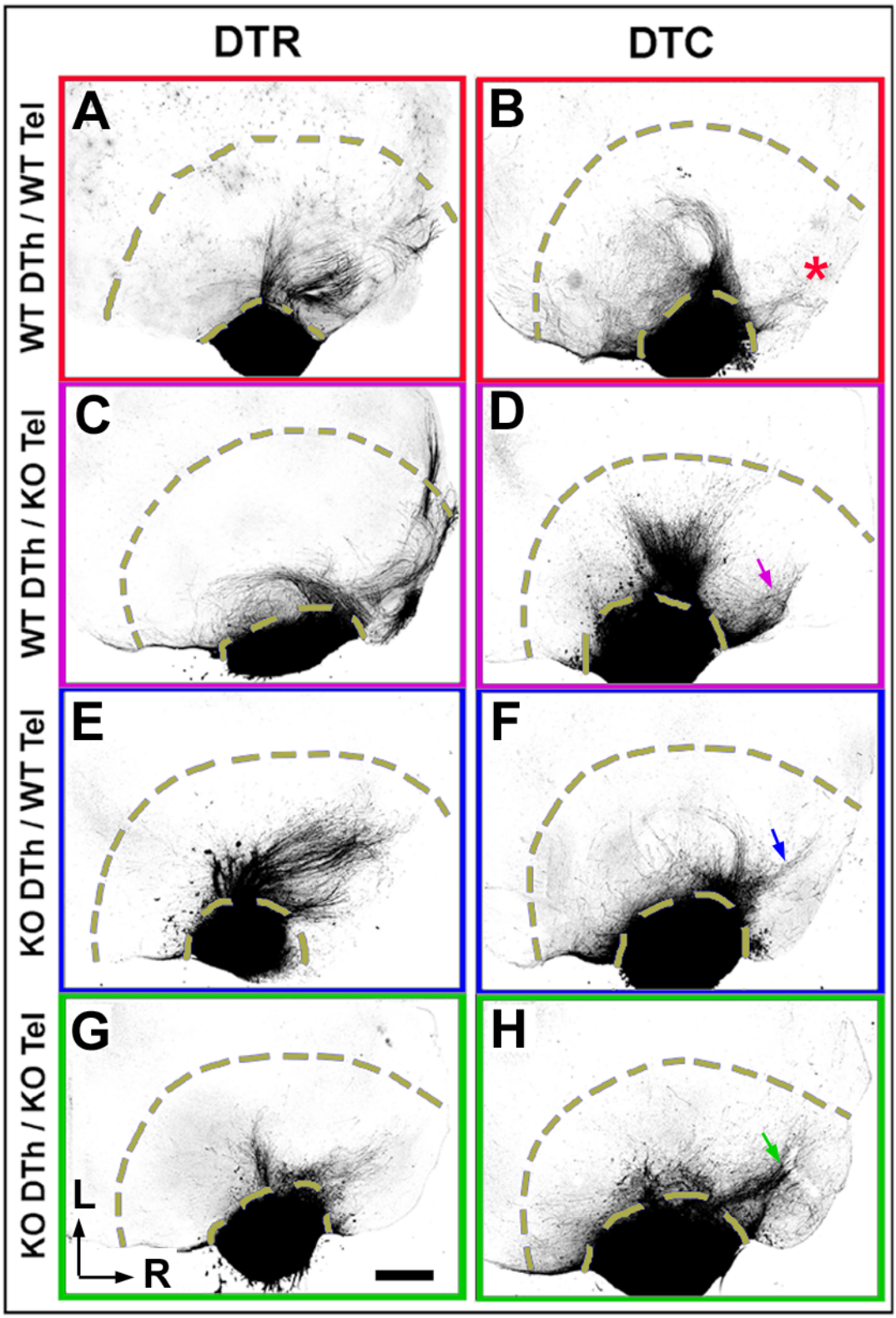

Figure 6. CHL1 in required on both thalamic and corticofugal axons for proper guidance of caudal but not rostral thalamic axons in the ventral telencephalon.

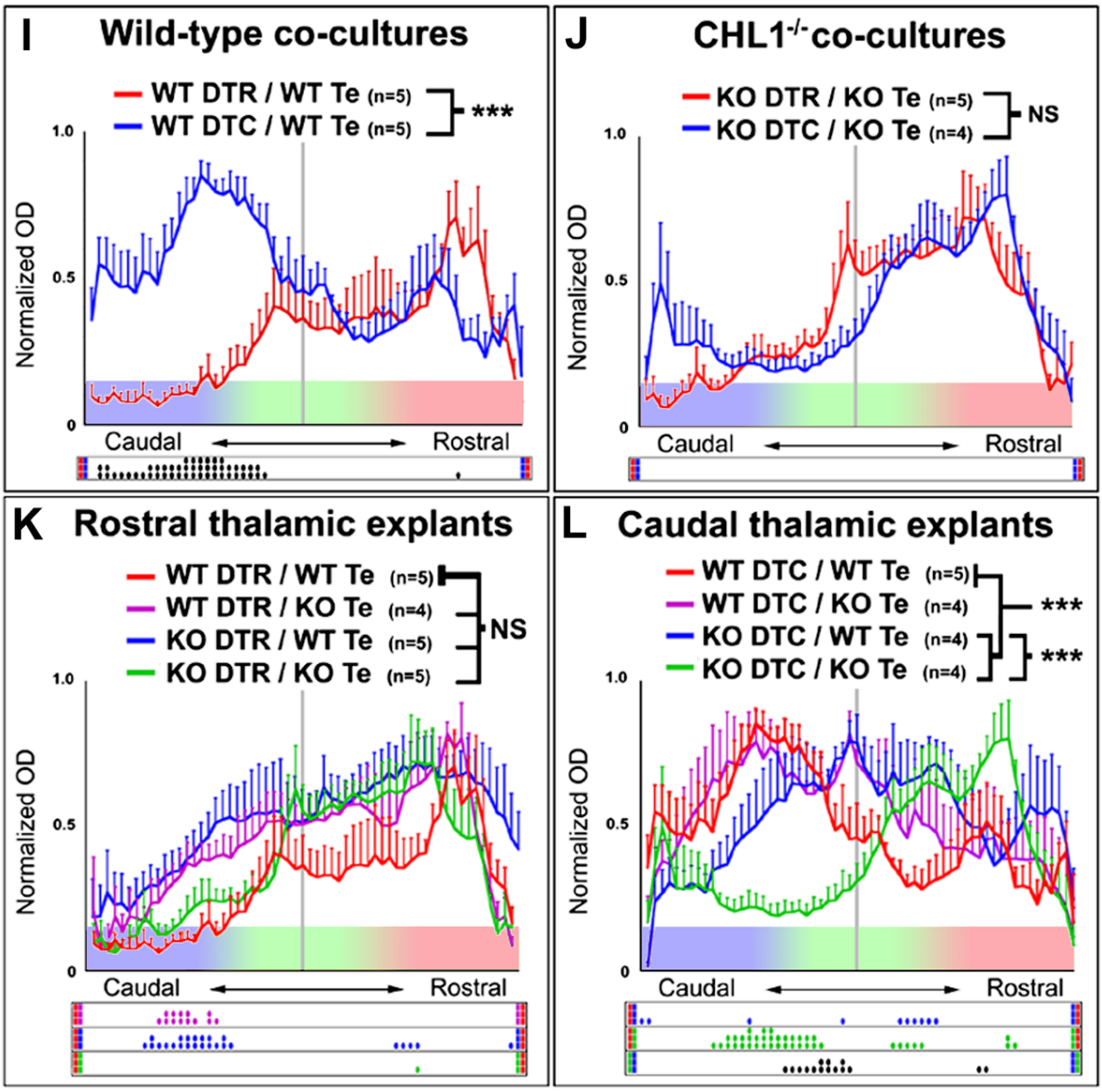

Figure 6. CHL1 in required on both thalamic and corticofugal axons for proper guidance of caudal but not rostral thalamic axons in the ventral telencephalon. Cont. (**A-H**) Combinations of E14.5 co-cultures using DTR explants (A-C-E-G) or DTC explants (B-D-F-H) with wholemount telencephalon isolated from control wild-type (A-B and E-F) or CHL1-/-. Note that DTR axons are not significantly affected by removal of CHL1 on corticofugal axons (C), thalamic axons (E) or both (G), whereas progressively more DTC axons are shifted rostrally when CHL1 is genetically removed from corticofugal (arrow in D), thalamic axons (arrow in F) or both (H). (**I-J**) Quantification of the normalized OD from EGFP+ axons originating from wild-type control DTR and DTC co-cultured with isochronic E14.5 wild-type wholemount telencephalon (I) or the same wholemount co-cultures done with CHL1-deificent E14.5 embryos (J). (**K-L**) Quantification of wholemount telencephalic co-cultures performed in A-H with combinations of CHL1+/- or CHL1-/- DTR explants (K) or DTC explants (L). Statistical analysis: *** $p<0.001$ ANOVA one-way test (overall effect: bins versus experimental conditions). The raster-like dot plot presented under each histogram (D and H) represents the significance of individual bins comparisons performed between the two experimental conditions according to a PLSD-post-hoc test (• $p<0.05$; •• $p<0.01$ and ••• $p<0.001$). Scale bar values: B-C, F-G, 150 microns.

Axon guidance cues are modulated by the environment through which an axon projects as well as the intracellular conditions

The proposed mechanism for the 'caudal handshake' describes an interesting interaction between a growing axon and the environment through which it is projecting. In discussions of axon guidance molecule receptor/ligand pairs, much time is spent regarding whether a given combination is attractive or repulsive. With several axon guidance receptors, whether an interaction with it's ligand is attractive or repulsive can be altered by intracellar conditions. An example of this is that the interaction of DCC with Netrin-1, generally described as attractive, can become a repulsive cue by decreasing cytosolic levels of cAMP (Ming et al. 1997).

Several extracellular interactions have also been shown to alter the directionality of DCC/Netrin-1 binding. Laminin-1, expressed at the optic disk of the retina, was shown to turn DCC/Netrin-1 based attraction into repulsion (Hopker et al. 1999). The proposed result of this modulation is that a single cue could attract RGC axons to the optic disk and then repulse them down the optic nerve. A recent study claimed that the DCC/Netrin-1 is normally repulsive but becomes attractive in the presence of serotonin (Bonnin et al. 2007). Unfortunately the functional consequences of these data are difficult to assess as serotonin protein in the embryonic brain is likely to come not just from the embryo, but via the bloodstream of mother.

DCC/Netrin-1 signaling is not the only axon guidance interaction known to be modulated by extracellular cues. Sema3A/Npn-1 repulsion can be turned into attraction or silenced by *cis* and *trans* interactions with L1 (Castellani et al. 2002). Our results show that *trans* interactions of TCA with CHL1 at least mollify the repulsion of Sema3A/Npn-1 interactions, possibly becoming a caudal attractive cue for caudal thalamic axons.

Considering CHL1 has an affect on DTC, and CHL1 is expressed in the caudal DTel, the identity and timing of cortical development could drastically affect TCA topography through indirect interactions of TCA with cues inside the VTel. Interestingly, in experiments where Fgf8 was

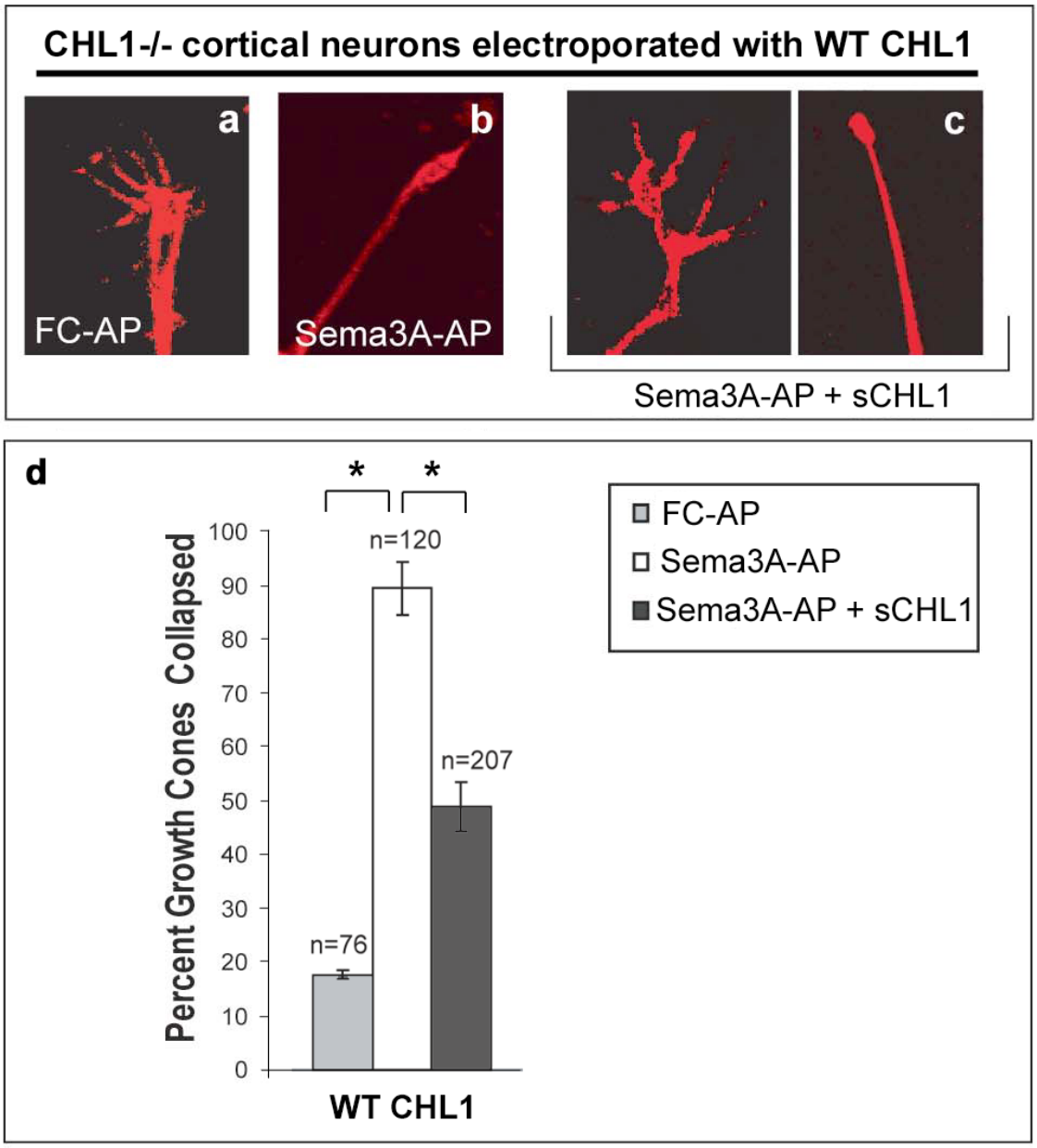

Figure 7. Application of soluble ectodomain of CHL1 reduces CHL1-mediated Sema3A growth cone collapse.

(**A-C**) Representative images of the growth cones of CHL1-/- cortical neurons transfected with full-length wild-type CHL1 incubated for 30 minutes with supernatant of 293T cells transfected with FC-AP fusion protein (A), Sema3A-AP fusion protein (B) or Sema3A-AP plus soluble (s)CHL1 (C). Growth cones were visualized with phalloidin staining of F-actin.

(**D**) Quantification of the percentage of growth cones collapsed in the three conditions shown in A-C. * $p<0.05$ Chi-square test. Each histogram represents growth cones counts (n number indicated) from three independent experiments. Experiment performed by Dr. Amanda Wright.

electroporated into the caudal cortex, forming an ectopic M1, the topography of TCA was not altered (Fukuchi-Shimogori and Grove 2001; Shimogori and Grove 2005). Despite an early change in cortical identity, at least in several markers for M1, no necessary cortical cues controlling TCA topography inside the VTel were altered. Experiments identifying the genes that control expression of CHL1 in caudal but not rostral CF axons may help identify other 'handshake' molecules.

Is Sema3A a caudal attractant for caudal thalamocortical axons?

Our data shows that *cis* and *trans* interactions of CHL1 with TCA, presumably via Npn-1 are required for caudal thalamic axons to enter the Sema3A rich caudal VTel. Whether this interaction is simply permissive, or is actually constitutes an attractive cue should be addressed. The only other cues identified to affect the topography of caudal TCA is Netrin-1, which was shown to repulse caudal axons from the Netrin-1 rich rostral VTel (Powell et al, 2007). Is the topography of caudal thalamic axons determined solely by varying degrees of repulsion, or is there a caudal attractive cue to caudal TCA?

This could be studied in several different ways. A series of experiments using the wholemount telencephalic co-culture assay could identify the role of Sema3A in establishing TCA topography inside the VTel. First, misexpress Sema3A in the rostral VTel, either by explanting a piece of the caudal VTel into the rostral VTel or using stably secreting cells. If Sema3A is a caudal attractive cue, a DTC explant should grow rostrally.

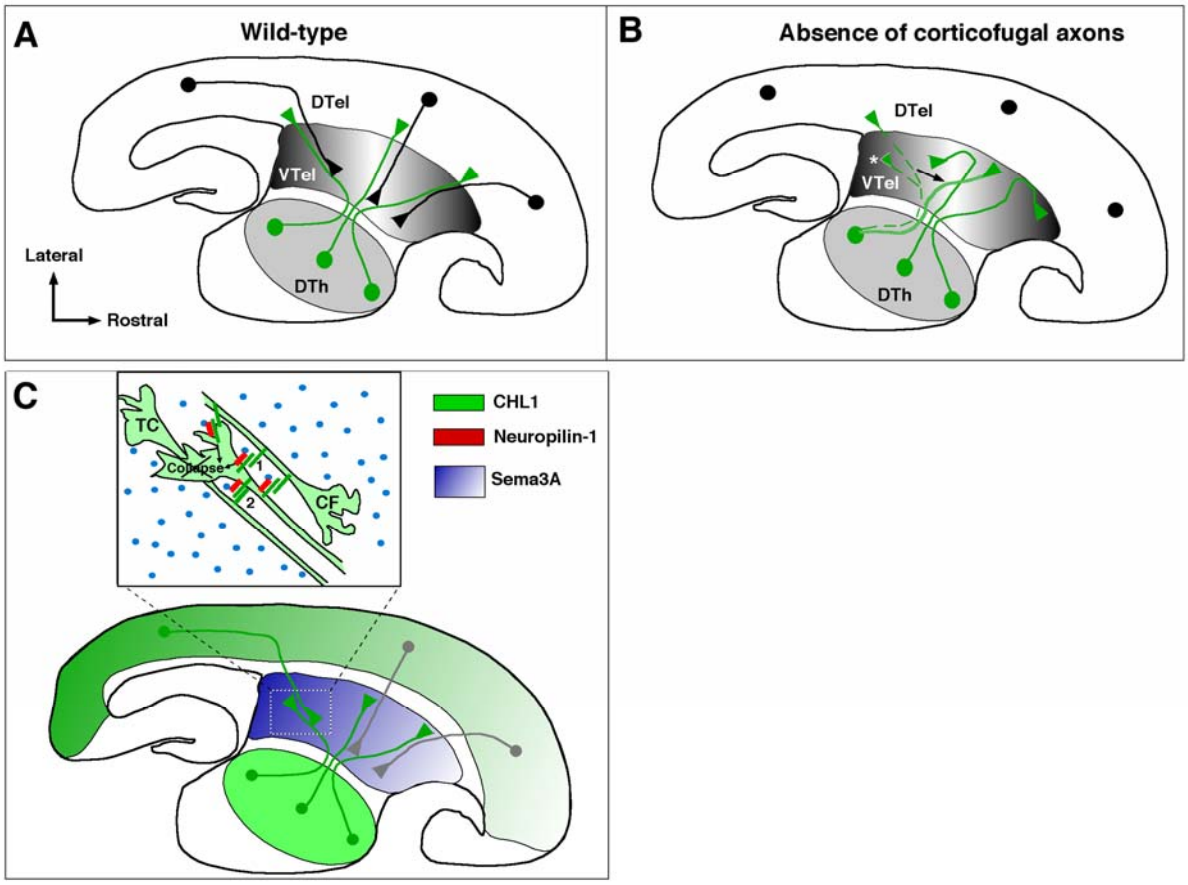

Figure 8. Model for the molecular mechanisms underlying the 'handshake' between thalamocortical and corticofugal axons.

(**A-B**) Summary of results where corticofugal axons are removed *ex vivo* (Figures 1 and 4) or *in vivo* (Figures 2 and 3) using co-culture or genetic approaches. When corticofugal axons are absent from the ventral telencephalon, the topographic guidance of axons originating from the caudal thalamus is affected (rostral shift indicated by arrow) but more rostral thalamic axons are not affected. However, in the absence of corticofugal axons, both rostral and caudal thalamic axons populations fail to properly cross the corticostriatal boundary. Furthermore, a significant proportion of axons originating from the caudal thalamus are stalled in the caudal part of the ventral telencephalon (star) and do not reach the CSB.

(**C**) Role of CHL1 expressed by corticofugal axons and thalamocortical axons growing in the caudal part of the ventral telencephalon in the silencing of Sema3A-mediated chemorepulsion of caudal thalamic axons. This model is based on combination of recently published data (Gates et al. 2007) and the present study suggesting that caudal thalamic axons are not repulsed from the Sema3A-rich caudal domain of the VTel because expression of CHL1 on both TC axons and CF axons (Figure 6) is required for silencing the chemorepulsion normally evoked by Sema3A (Figure 7).

EXPERIMENTAL PROCEDURES

Animals

Mice were used according to a protocol approved by the Institutional Animal Care and Use Committee at the University of North Carolina-Chapel Hill, and in accordance with NIH guidelines. Time-pregnant females were maintained in a 12-hr light/dark cycle and obtained by overnight breeding with males of the same strain. Noon following breeding is considered as E0.5. LKB1 conditional knockout mice were (abbreviated $LKB1^{F}$ allele; kindly provided by Dr Ron DePinho (Bardeesy et al. 2002)) were crossed with $Emx1^{Cre/+}$ mice ((Gorski et al. 2002); kindly provided by Dr Kevin Jones). CHL1 knockout mice were (kindly provided by Dr Melitta Schachner; (Montag-Sallaz et al. 2002)) were maintained as an homozygous line. Transgenic mice expressing EGFP under the control of CMV enhancer/chicken ßactin promoter were maintained by heterozygous crossing on a Balb/C background for more than 10 generations (Okabe et al. 1997).

Biotinylated Dextran Amine (BDA) anterograde axon tracing in live mouse embryos.

Briefly, isolated hemispheres from E14.5 to E18.5 mouse embryos were microinjected (PicoSpritzer III, General Valve Corp.) using a medial approach with a 10% solution of lysine-fixable BDA (3000 MW). Following incubation in oxygenated artificial cerebrospinal fluid (aCSF) for 5 hours at 37°C the hemispheres were immersion-fixed in 4% PFA. Injected hemispheres are sectioned coronally using a vibratome (LEICA VT1000S) at 100 microns-thick, permeabilized and incubated with Alexa546-conjugated Streptavidin (1:1000 in PBS + 0.1% Triton X-100 + 0.3% BSA) to reveal BDA. See (Powell et al. 2007) for details.

Wholemount telencephalic co-cultures and immunofluorescent staining

Wholemount telencephalon/dorsal thalamic co-cultures were maintained on organotypic slice culture inserts, fixed and stained for immunofluorescence as previously described (Polleux and Ghosh 2002; Seibt et al. 2003). The following primary antibodies were used: monoclonal anti-neurofilament 165kD (clone 2H3; Developmental Hybridoma Bank; 1:2000), polyclonal rat anti-L1 cell adhesion molecule (Chemicon; 1:1000) as well as polyclonal chicken and rabbit anti-GFP (Molecular Probes, 1:2000). The following secondary antibodies were used: Alexa-488, -546 and -647 conjugated goat anti-chicken, anti-rabbit or anti-mouse IgG (Molecular Probes; 1:2000).

Confocal microscopy

Fluorescent immunostaining was observed using a LEICA TCS-SL laser scanning confocal microscope equipped with an Argon laser (488 nm), green Helium-Neon laser (546nm) and red Helium-Neon laser line (633nm) mounted on an inverted DM-IRE2 microscope equipped with a Marzhauzer X-Y motorized stage allowing large scale tiling of wholemount telencephalic co-cultures obtained by scanning multiple fields using a long-working distance 10x objective followed by an automatic tiling function available from the LEICA confocal software.

Growth cone collapse assays

CHL1-minus thalamic embryonic (E14.5) neurons were obtained by isolating the thalamus and dissociating the cells in 3 ml of ice cold Hank's Balanced Salt Solution. Cells were further dissociated by trituration with a 10 ml pipette followed by a wide bore Pasteur pipette. Cells were then immediately co-transfected with pMax-GFP and pcDNA3-CHL1wt, or empty pcDNA using the Mouse Neuron Nucleofector Kit and the Amaxa Nucleofector Device (Amaxa, Gaithersburg, MD).

Briefly, 5 x 10^6 cells were centrifuged and resuspended in transfection buffer. DNA was added, and samples were transferred to electroporation cuvettes. Program O-05 was used to electroporate the DNA into the cells in the Amaxa Nucleofector Device. Cells were allowed to recover in RPMI medium (Gibco) for 5 minutes, and then plated on fibronectin-coated MatTek dishes in 10% fetal bovine serum and DMEM. The day after plating, the media was changed to Neurobasal media containing B27 supplement and glutamate (25uM) to select for neurons. After 48 hours of incubation to allow for neurite outgrowth, cells were treated with either FC-AP or Sema3A-AP fusion proteins (30 nM) for 30 minutes. Cells were then fixed with 4% PFA and permeabilized with 0.2% TritonX-100 for 5 min. After washing, cells were treated with rhodamine-conjugated phalloidin (Molecular Probes; 1:40) for 30 min at room temperature to visualize actin within the growth cone. Only cells expressing GFP were included in the analysis. Cells were mounted in Vectashield and growth cone morphology was observed using confocal microscopy.

ACKNOWLEDGMENTS

We would like to thank Dante Bortone for his initial help with Macro programming in Excel as well as all members of the Polleux laboratory for fruitful discussions. This project was funded by the NIH-National Institute of Neurological Disorders and Stroke (NS047701-01) (FP) and by the March of Dimes Foundation for Birth Defects (FP). This work benefited from the UNC-CH Confocal and Multiphoton Imaging Core facility and the In Situ Hybridization Core facility supported by the NINDS Institutional Center Core Grant to Support Neuroscience Research (P30 NS45892-01).

References

Bardeesy N, Sinha M, Hezel AF, Signoretti S, Hathaway NA et al. (2002) Loss of the Lkb1 tumour suppressor provokes intestinal polyposis but resistance to transformation. Nature 419(6903): 162-167.

Barnes AP, Lilley BN, Pan YA, Plummer LJ, Powell AW et al. (2007) LKB1 and SAD kinases define a pathway required for the polarization of cortical neurons. Cell 129(3): 549-563.

Braisted JE, Tuttle R, O'Leary D D (1999) Thalamocortical axons are influenced by chemorepellent and chemoattractant activities localized to decision points along their path. Dev Biol 208(2): 430-440.

Bulfone A, Smiga SM, Shimamura K, Peterson A, Puelles L et al. (1995) *T-Brain-1*: a homolog of *brachyury* whose expression defines molecularly distinct domains within the cerebral cortex. Neuron 15: 63-78.

Caviness VS, Jr., Frost DO (1980) Tangential organization of thalamic projections to the neocortex in the mouse. J Comp Neurol 194(2): 335-367.

Crandall JE, Caviness VS, Jr. (1984) Thalamocortical connections in newborn mice. J Comp Neurol 228(4): 542-556.

Demyanenko GP, Schachner M, Anton E, Schmid R, Feng G et al. (2004) Close homolog of L1 modulates area-specific neuronal positioning and dendrite orientation in the cerebral cortex. Neuron 44(3): 423-437.

Dupont JL, Gardette R, Crepel F (1983) Bioelectrical properties of cerebellar Purkinje cells in reeler mutant mice. Brain Res 274(2): 350-353.

Garel S, Rubenstein JL (2004) Intermediate targets in formation of topographic projections: inputs from the thalamocortical system. Trends Neurosci 27(9): 533-539.

Garel S, Huffman KJ, Rubenstein JL (2003) Molecular regionalization of the neocortex is disrupted in Fgf8 hypomorphic mutants. Development 130(9): 1903-1914.

Garel S, Yun K, Grosschedl R, Rubenstein JL (2002) The early topography of thalamocortical projections is shifted in Ebf1 and Dlx1/2 mutant mice. Development 129(24): 5621-5634.

Gates AG, Demyanenko GP, Powell A, Schachner M, Polleux F et al. (2007) Close Homolog of L1 (CHL1) is required for the area-specific targeting and guidance of thalamocortical axons. Journal of Neuroscience in press.

Gorski JA, Talley T, Qiu M, Puelles L, Rubenstein JL et al. (2002) Cortical excitatory neurons and glia, but not GABAergic neurons, are produced in the Emx1-expressing lineage. J Neurosci 22(15): 6309-6314.

Grigoriou M, Tucker AS, Sharpe PT, Pachnis V (1998) Expression and regulation of Lhx6 and Lhx7, a novel subfamily of LIM homeodomain encoding genes, suggests a role in mammalian head development. Development 125(11): 2063-2074.

Hevner RF, Miyashita-Lin E, Rubenstein JL (2002) Cortical and thalamic axon pathfinding defects in Tbr1, Gbx2, and Pax6 mutant mice: evidence that cortical and thalamic axons interact and guide each other. J Comp Neurol 447(1): 8-17.

Hohl-Abrahao JC, Creutzfeldt OD (1991) Topographical mapping of the thalamocortical projections in rodents and comparison with that in primates. Exp Brain Res 87(2): 283-294.

Liu Q, Dwyer ND, O'Leary DD (2000) Differential expression of COUP-TFI, CHL1, and two novel genes in developing neocortex identified by differential display PCR. J Neurosci 20(20): 7682-7690.

Metin C, Deleglise D, Serafini T, Kennedy TE, Tessier-Lavigne M (1997) A role for netrin-1 in the guidance of cortical efferents. Development 124(24): 5063-5074.

Molnar Z, Blakemore C (1995) How do thalamic axons find their way to the cortex? Trends Neurosci 18(9): 389-397.

Molnar Z, Cordery P (1999) Connections between cells of the internal capsule, thalamus, and cerebral cortex in embryonic rat. J Comp Neurol 413(1): 1-25.

Molnar Z, Adams R, Blakemore C (1998) Mechanisms underlying the early establishment of thalamocortical connections in the rat. Journal of Neuroscience 18(15): 5723-5745.

Montag-Sallaz M, Schachner M, Montag D (2002) Misguided axonal projections, neural cell adhesion molecule 180 mRNA upregulation, and altered behavior in mice deficient for the close homolog of L1. Mol Cell Biol 22(22): 7967-7981.

Okabe M, Ikawa M, Kominami K, Nakanishi T, Nishimune Y (1997) 'Green mice' as a source of ubiquitous green cells. FEBS Lett 407(3): 313-319.

Polleux F, Ghosh A (2002) The slice overlay assay: a versatile tool to study the influence of extracellular signals on neuronal development. Sci STKE 2002(136): PL9.

Powell A, Sassa T, Wu Y, Tessier-Lavigne M, Polleux F (2007) The attractive and repulsive functions of Netrin-1 are required for the topographic projection of thalamocortical axons in the ventral telencephalon. PLoS Biology: Accepted March 2008.

Seibt J, Schuurmans C, Gradwhol G, Dehay C, Vanderhaeghen P et al. (2003) Neurogenin2 specifies the connectivity of thalamic neurons by controlling axon responsiveness to intermediate target cues. Neuron 39(3): 439-452.

Vanderhaeghen P, Polleux F (2004) Developmental mechanisms patterning thalamocortical projections: intrinsic, extrinsic and in between. Trends Neurosci 27(7): 384-391.

Wright AG, Demyanenko GP, Powell AW, Polleux F, Maness PF et al. (2007) Journal of Neuroscience 27(50): 13667-13679.

CHAPTER FOUR

CONCLUSIONS

A new paradigm to study the topography of TCA projections.

The molecular mechanisms guiding thalamocortical axons to their proper target are only beginning to be uncovered. Including the data provided in this thesis, only two axon guidance molecules (ephrin-A5 and Netrin-1) have been definitively shown to control the segregation of subpopulations of TCA inside the ventral telencephalon (Dufour et al. 2003). While there are other families(Leighton et al. 2001) of axon guidance molecules shown to be involved in the formation of the internal capsule, they have yet to be studied using appropriate methodologies for assessing their role in establishing the topography of thalamocortical connections(Bagri et al. 2002; Lopez-Bendito et al. 2006).

To study topography in relation to axon guidance, there is the inherent need to segregate populations of axons in as precise a manner as possible. Pioneering studies of thalamocortical connectivity by Caviness and Frost employed techniques with the precision required to map topography in neonatal and adult mice with the resolution to map the innervation of cortical regions to individual neuron in the Dth (Caviness and Frost 1980; Frost and Caviness 1980). However, while these techniques are precise, they are not well suited for following the path of TCA through intermediate structures.

Later studies of TCA development used fluorescent carbocyanine dyes (DiI, DiA, DiO) in order to image axons inside the VTel (Molnar et al. 1998). However, the value gained from these experiments in terms of imaging came at the expense of precision, as the injections of these dyes often labeled massive regions of the Dth (Molnar et al. 1998). These dyes became the standard for identifying gross TCA guidance defects, although they lack the precision required to determine more subtle defects of topography. The novel BDA-based tracing technique designed during my thesis provides the first quantitative approach to study the topography of projection for small groups of thalamic neurons with high resolution. We suggest that this method should be employed for future studies of TCA topography (as well as other projections), as it is a low cost and low-tech solution for identifying the complex effects of interfering with a single axon guidance cue or receptor on precisely defined populations of thalamic axons.

A second methodological aspect of this thesis that should be expanded upon in future studies of TCA topography is the **telencephalic wholemount co-culture assay**. This method has evolved to probe the role of an axon guidance cue through a diverse array of manipulations (Dufour et al. 2003; Seibt et al. 2003). Schematized in **Figure 1**, the wholemount assay enables us to interfere with the role of an axon guidance molecule or receptor using multiple approaches like functional antibodies or genetic manipulations such as using shRNA against knocking out, or misexpressing genes in the dorsal thalamus or the ventral telencephalon. Using this assay, the topography of WT axons in control conditions segregate inside the VTel, with DTR axons growing rostrally and DTC growing caudally (**Figure 1A & B**). This allows us to establish normal growth patterns for the anatomically extreme regions of the DTh.

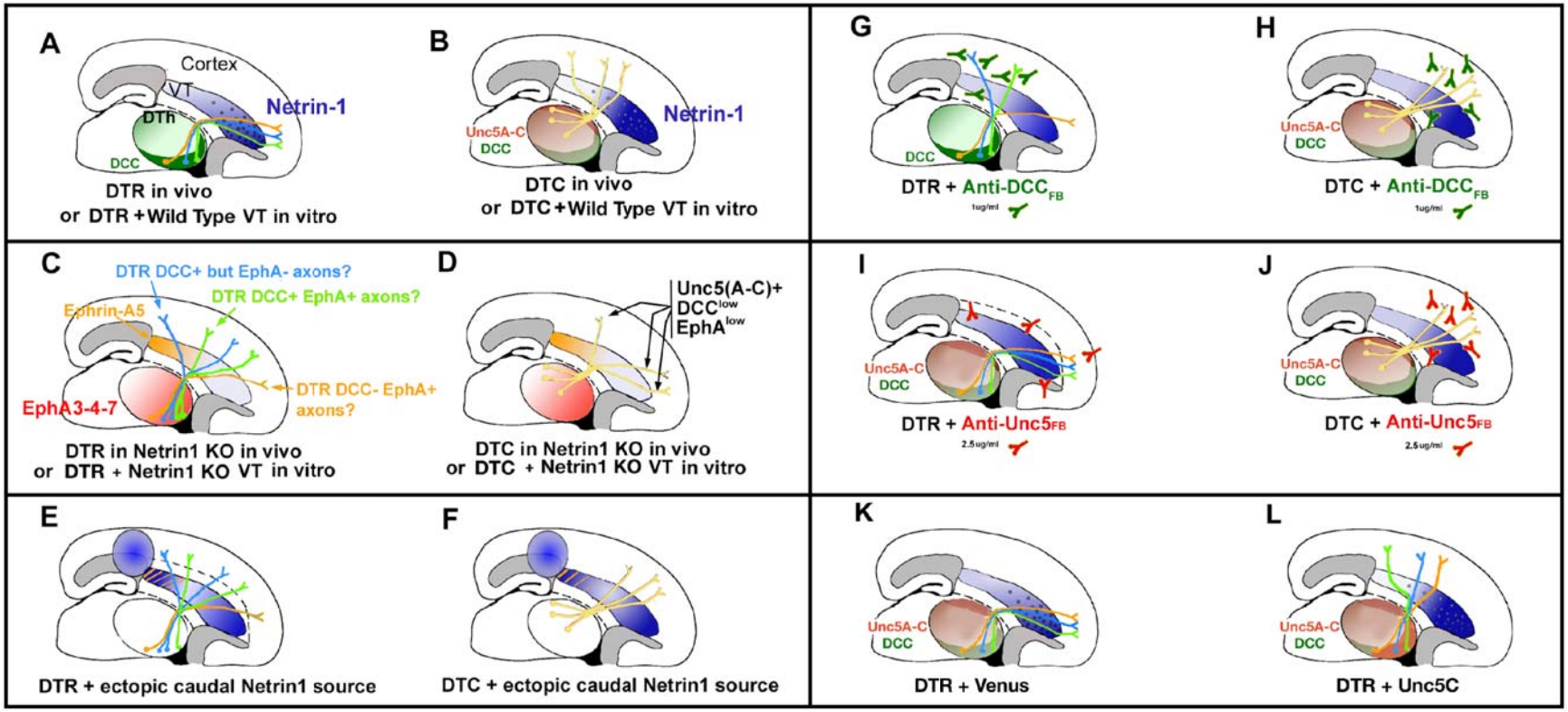

Figure 1 Netrin-1 controls the topography of thalamocortical axons via attraction and repulsion.
(**A-B**) Rostral TCA (DTR) are attracted to and caudal TCA (DTC) are repulsed by the rostral VTel by the high-rostral to low-caudal gradient of Netrin-1 (Blue). DCC receptors regulate rostral attraction while Unc5A-C regulate caudal repulsion. (**C-D**) In the Netrin-1-/-, DTR is caudalized, but maintain some rostral growth. This may be due in part to the repulsion of EphA3-4-7 expressing rostral TCA to the high-caudal to low-rostral gradient of ephrinA5 (Orange). DTC projects into the rostral VTel, consistent with the loss of a repulsive cue. (**E-F**) An ectopic source of caudal Netrin-1 attracts DTR to the caudal VTel while repulsing DTC rostrally. (**G-H**) Blocking DCC function caudalizes DTR, although ephrinA5 repulsion remains. DTC axons are rostralized (**I-J**) Blocking Unc5A&C function has no effect of DTR axons, DTC is rostralized, perhaps now attracted to Netrin-1. (**K-L**) Expressing Venus into DTR has no effect on growth. Expressing Unc5C in DTR axons turns Netrin-1 attraction into repulsion.

A common format for the whole mount assay is to use either a telencephalon or thalamic explant from a mutant mouse. The primary outcome measure of these experiments is the growth of DTh subpopulations inside the VTel. Additionally, this format allows for us to study whether a cue, receptor, or transcription factor has a cell-autonomous or cell-non-autonomous effect on TCA topography. For example, when Netrin-1 is genetically removed from the telencephalon using Netrin-1-/- mice, WT topography is completely disrupted. This shows that the effect of removing Netrin-1, which is expressed inside the DTh at E14.5, has a cell non-autonomous role in establishing TCA topography. Additionally, the remaining cues in the VTel guide the growth of DTR to random regions and DTC to the rostral regions (**Figure 1C & D**). Using this assay, cell-autonomous effects were described is a study by Seibt et al. (2002) where Ngn2 was shown to specify the rostral projection of DTR axons.

Secreted axon guidance molecules can be studied in a variety of ways using the whole mount assay, including the use of a small explant of cell lines (produced using the 'hanging drop' method) in order to disrupt the endogenous pattern of a protein's expression. As shown in **Figure 1E & F**, placing a small explant of Netrin-1 secreting 293 cells along the caudal domain of the VTel disrupts the normal Netrin-1 gradient. DTR axons are deflected caudally as they either follow the secreted Netrin-1 to high caudal concentrations or they can no longer differentiate between Netrin-1 concentrations, leaving the cue unable to provide topographic direction. DTC axons no longer project caudally, growing now to the rostral VTel. This implies that Netrin-1 is repulsive for caudal thalamic axons and the ectopic, secreted caudal Netrin-1 is of a higher concentration than the endogenous rostral Netrin-1.

A third manipulation that can be used to test the role of a hypothesized cue in the wholemount assay is to use function-blocking antibodies to axon guidance receptors. In the case of Netrin-1, there are function-blocking antibodies specific to DCC and a promiscuous antibody that blocks both Unc5A and Unc5C(Guijarro et al. 2006). By introducing these antibodies into the media of a wholemount assay, the effect of Netrin-1 receptors can be isolated further (**Figure 1G-J**). For

axons originating from DTR, blocking DCC receptors removes an attractive function of Netrin-1, which leads to a caudalized growth. Blocking DCC on DTC axons inhibits Netrin-1-mediated. Antibodies to Unc5A&C have no visible effect on DTR axons, showing they have little to no repulsive response to Netrin-1 endogenously. When Unc5A&C are blocked in DTC axons, the repulsive effect of Netrin-1 is abolished, leading to a re-direction of DTC axon growth towards the rostral domain of the VTel. We interpret these data as showing that the attractive response of Netrin-1 binding to low-DCC expressing DTC axons is sufficient to convert the chemorepulsion of control DTC axons into chemoattraction towards the Netrin-1-rich rostral domain of the VTelel.

A final manipulation of the wholemount assay described so far is to utilize electroporation-mediated gene transfer to overexpress a receptor in a subpopulation of DTh neurons (**Figure 1K & L**). Pioneered by Dr. Takayuki Sassa in our laboratory, plasmids expressing either myristoylated-(m)Venus alone or mVenus–IRES-Unc5C were electroporated into the DTh on 250microns-thick slices of WT mice. The resulting overexpression of Unc5C drastically caudalized DTR axons by modifying endogenous attractive Netrin-1 and DCC interactions into repulsive Unc5C based Netrin-1 interactions. This gain-of-function approach shows that expression of Unc5C in the rostral thalamic axons is sufficient to caudalize the outgrowth of DT axons in the VTel.

Are there other axon guidance cues patterning the topography of thalamocortical projections in the Ventral Telencephalon?

The organization of the mouse thalamocortical projections is defined by the specific connectivity of over 20 thalamic nuclei, each uniquely identified by the information relayed and the target tissue innervated. Including the data described in this thesis, there are only two axon guidance molecule/receptor pairs shown to affect topography beyond the level of a global axon guidance deficit.

There are two axon guidance molecules shown to regulate the topography of TCA inside the VTel, **ephrinA5** and **Netrin-1** (Dufour et al. 2003). EphrinA5, expressed at high levels in the caudal part of the Vtel, has been shown to repel TC axons from the rostro-medial DT expressing high levels of EphA3-A4-A7. These results explained why rostral DT axons avoid the caudal part of the VTel but do not explain why caudal DT axons specifically grow caudally in the Vtel. DTC axons do not express any detectable levels of EphAs and therefore should not be sensitive to ephrinA5 in the VTel, they could theoretically grow uniformly across the rostro-caudal axis of the VTel. These results suggested that EphA-ephrinA5 was not the only receptor-ligand couple involved in specifying the topography of TC projections in the VTel. This implies that other cue(s) control the repulsion of caudal DT axons from the rostral VTel or positively attract caudal TC axons toward the caudal domain of the VTel.

Our results demonstrate that Netrin-1 is a critical cue for TC axons in the VTel and plays a dual role in establishing TCA topography as it acts differentially on axons depending on whether the axon expresses DCC alone (attractive) or in combination with one of the Unc5 receptors (repulsive).

One of the most pressing remaining questions is whether additional cues exist inside the VTel that are required for establishing TCA topography. The balance of ephrinAs and Netrin-1 signaling

may provide enough specificity to pattern the internal capsule but there is an abundance of additional axon guidance molecules that have yet to be addressed.

Recently, studies in the Maness lab (Gates et al. 2007) done in collaboration with our lab have tested the role of Sema3A in establishing caudal TCA topography. The high-caudal to low-rostral expression of Sema3A in the VTel as well as the high-caudal to low-rostral expression of Npn1 in the DTh make this an intriguing molecule to study in more depth. Considering the interaction of Sema3A with Npn1 causes growth cone collapse (Nakamura et al. 1998), high levels of a caudal repulsive cue to the caudal thalamus appears to contradict the anatomy observed in WT mice an our own anatomical tracing. Our results from the CHL1-/- mice suggest that the repulsive action of Sema3A-Npn1 may be masked by the fasciculation of caudal TCA with CFA. Unlike other cues that mediate rostral projections via repulsion, this interaction appears to ensure that the only projections that reach the most caudal regions of the cortex are those that fasciculate with caudal CFA or express low levels of Npn1. Interestingly, Sema3A-dependent growth cone collapse may not be a result observed in rostral TCAs as they do not express Npn1, implying this may be a mechanism that primarily sorts axons from the caudal thalamus. This hypothesized interaction should be further examined, as it would constitute another cue that segregates TCA rostrally inside the VTel in a dose-dependent manner.

Another question that needs to be addressed is whether additional cues exist in the rostral VTel. To study this, we repeated a set of experiment from our Netrin-1 results. In particular, we used a whole mount telencephalic assay in which a heterogonous explant of a rostral VTel was grafted into the caudal Vtel. However, in order to ask whether additional cues are present in the rostral VTel, we explanted the rostral VTel of Netrin-1 -/- mice into WT telencephalons (**Figure 2A)**. Similar to our results in the Netrin-1 study, we would expect to see a caudal deflection by DTR axons if any attractive cues other than Netrin-1 exist in the rostral VTel.

Our results demonstrate that compared to control, homotypic explant conditions, growth of DTR axons is caudalized when using rostral Netrin-1 -/- VTel explants (**Figure 2D & E**).

Importantly, this deflection is significantly different than when a control, Netrin-1-expressing rostral VTel is grafted (**Figure 2C & E**). These data support the hypothesis that, from the perspective of a DTR axon, Netrin-1 is not the sole attractive molecule in the rostral VTel. What could the identity of this cue be?

There are several candidate axon guidance molecules whose roles have yet to be studied in the developing thalamocortical system. Considering the apparent long-range effect of the Netrin-1 -/- explant on DTR axons, it is likely that the unidentified guidance cue or cues are diffusible. One possibility is the morphogen Sonic Hedgehog (Shh), which has recently been identified as an axon guidance molecule (Charron et al. 2003). According to these studies, Shh has the additional role of as an axon guidance cue acting through the receptor, Smoothened (Charron et al. 2003). Interestingly, the directionality of Shh-dependent guidance occurs in a dose dependent manner, with low levels of Shh being attractive and high levels being repulsive to retinal ganglion cells, although the receptor responsible for this interaction was not identified (Kolpak et al. 2005).

The expression of Shh inside the VTel at E14.5 has not been thoroughly documented, but has been shown to be present in the rostral VTel ((Lee et al. 2001) and BGEM). As for the receptors to Shh, several well-characterized (Smoothend and Patched2) and one hypothesized receptor (Okada et al. 2006) all have intriguing expression patterns inside the DTh at E15. In particular, Boc is expressed in a high-rostral/medial to low caudal/lateral gradient in the DTh (Mulieri et al. 2002) while Smo and Ptch2 appear to primarily express in more caudal and lateral regions (BGEM). More precise expression patterns with the relevant scope of study should be performed.

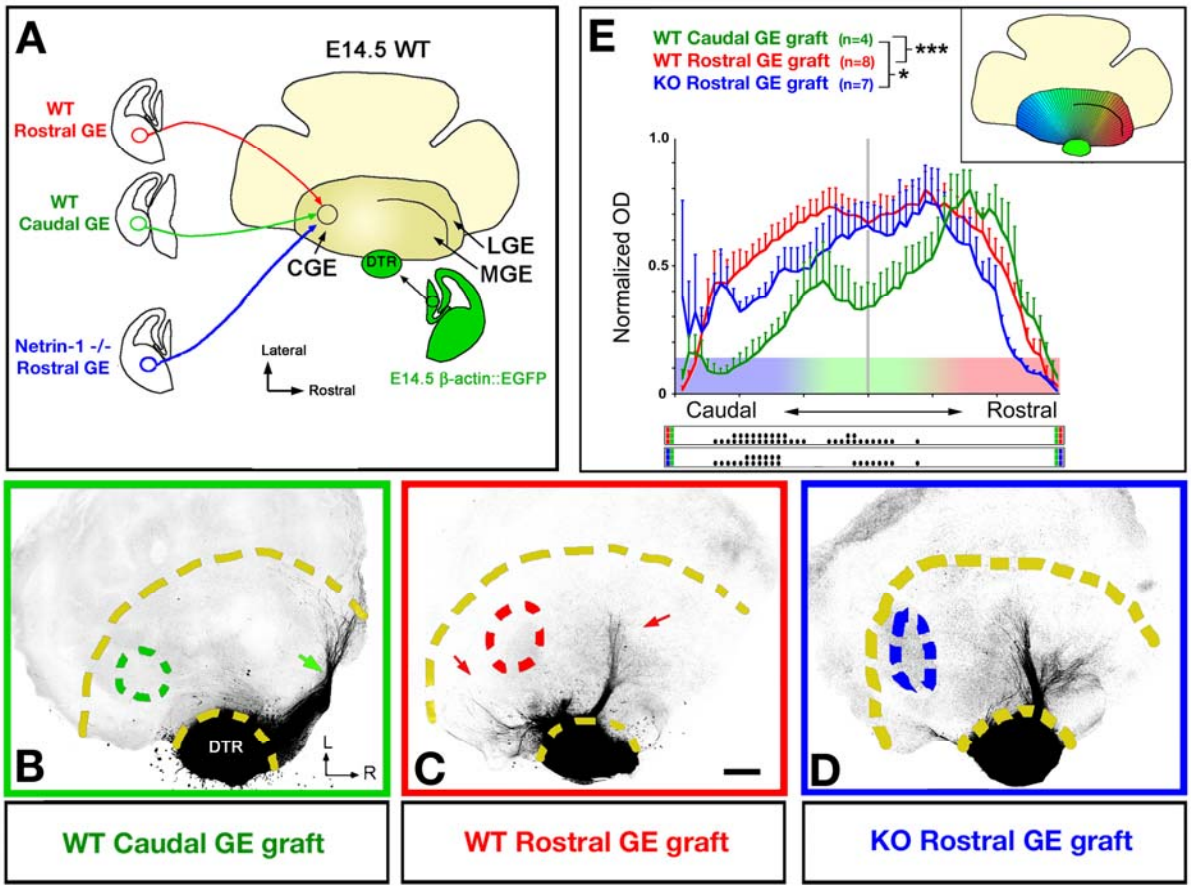

Figure 2. The rostral part of the VTel contains a second chemoattractant for rostral thalamic axons aside from Netrin-1.

(**A**) Rostral (red) or caudal (green) explants isolated from the mantle region of the VTel of WT mice were isolated from 250 microns-thick vibratome sections and grafted into the caudal part of the VTel of a recipient E14.5 wholemount telencephalic vesicle. The rostral VTel from a Netrin-1-/- mouse (blue) was also explanted into a WT VTel.
(**B**) Homotopic grafting (caudal VTel into caudal VTel) results in a normal outgrowth of rostral thalamic axons into the rostral domain of the VTel (arrow).
(**C**) In contrast, heterotopic grafting (rostral VTel into the caudal VTel) results in a pronounced change in the topography of DTR axon projections which invade more caudal territories (red arrows) than in control grafts (see B).
(**D**) Heterotopic grafting of a Netrin-1-/- VTel also results in a caudalization of DTR axons that is less severe.
(**E**) Quantification of the topography of rostral thalamic axon outgrowth in the VTel presenting WT homotopic (green), WT heterotopic (red), and KO heterotopic (blue) VTel graft into the caudal VTel.

*** $p<0.001$ & * $p<0.05$ ANOVA one-way test (overall effect: bins versus experimental conditions). The raster-like dot plot presented under the histograms represents the significance of individual bin comparisons between the two experimental conditions according to a PLSD-post-hoc test (• $p<0.05$; •• $p<0.01$ and ••• $p<0.001$). Scale bar value: B-D, 250 microns.

What role does the cortex have in TCA guidance inside the VTel other than the "Caudal Handshake?"

While our data shows that CFA affect the topography of caudal TCA inside the VTel, it is unclear to what extent additional cues originating from the dorsal telencephalon pattern the internal capsule. The requirement of CFA axons in patterning rostral TCA appears non-existent, or at least limited, however this does not rule out a contribution of secreted cues originating from the dorsal telencephalon. We initiated a series of experiments to ask whether the "Caudal Handshake" is the sole contribution from the cortex towards establishing TCA topography inside the VTel, and have preliminary data suggesting the existence of secreted cortical cues should be further addressed.

The dorsal telencephalon contains a regionally expressed attractant for rostrally projecting thalamocortical axons.

The results observed in rostral topography following genetic CFA ablation in the cortex-specific conditional LKB1knockout mice both *in vitro* and *in vivo* combined with physical removal of the cortex imply that cues originating from the cortex do not participate in this process. To conclusively test for the presence of cortical cues that influence rostral topography, we asked whether the organization of the cortex during the period of TC axon growth exerts a control over thalamocortical projections. Using our *in vitro* analysis, we manipulated the orientation of the cortex with regard to the ventral telencephalon and asked whether this would have an effect on rostral topography.

For our experimental condition, we severed the cortex from the VTel in a wholemount and inverted its orientation along the rostral-caudal axis (**Inverted Cortex: Fig 3A**). As a control experiment, we severed and reattached the cortex from the VTel of a wholemount it the original rostral-caudal orientation (**Severed Cortex: Fig 3A**). CF axons grow into the VTel following either

procedure, as seen when a cortex from an EGFP expressing cortex is co-cultured next to a wildtype VTel for both Severed and Inverted Cortex formats.

Following CF axotomy and reattachment of the cortex, DTR explants in Severed Cortex experiments are unaffected and project into the rostral VTel similarly to uncut, With Cortex wholemounts (**Fig 3B, C and E**). Additionally, when DTR axons reach the severed cortex, they cross into the DT with the same rostral specificity seen in uncut wholemount formats (**Fig 3F**). This experiment, even as a control, is quite impressive in that a procedure as drastic as a cortical transplant has no distinguishable *in vitro* affect on DTR topography in the either the VTel or the cortex.

In our Inverted Cortex condition, we finally observe an effect on rostral topography. When DTR axons are confronted with an inverted cortex, the growth becomes virtually randomized, although a rostral trend can still be detected (**Fig 3D and E**). Some populations of TC axons continue to project rostrally, while other populations grow to medial and caudal regions of the VTel.

Upon reaching the cortex, DTR axons display a complex set of behaviors depending on where they reach the CSB. Axons reaching their intended intermediate target of the rostral VTel, which now provides a barrier to the caudal cortex, appear to have difficulty crossing the CSB. These axons are sometimes deflected caudally, but eventually enter the cortex and grow with a trajectory similar to control conditions (**Blue Arrows Fig 3D and F**). For axons reaching more caudal regions of the VTel, this deflection is much more profound. DTR axons reaching the caudal CSB are deflected rostrally along the entire caudal region of the CSB (**Green arrows Fig 3D and F**). However, axons that do cross the CSB grow in a straight trajectory inside the cortex.

These results suggest that rostral-specific topographic cues originating from the cortex exist and are able to alter topography during early periods of growth through the VTel. Upon reaching the CSB, there are cues that are responsible for sorting TC axon entry into the cortex.

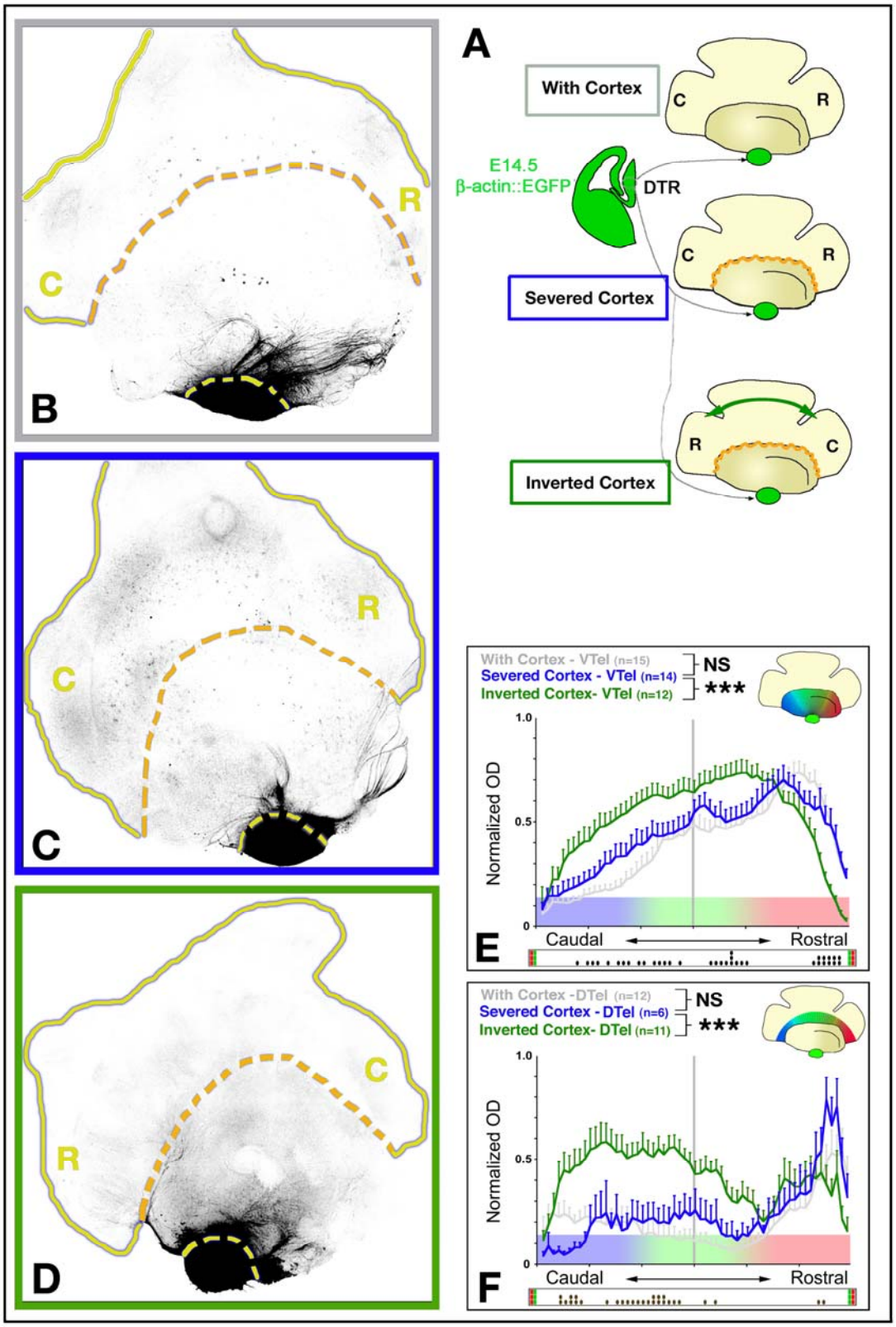

Figure 3. The cortex contains regionally expressed cues that affect the topography of thalamocortical projections.

Figure 3. The cortex contains regionally expressed cues that affect the topography of thalamocortical projections. Cont.

(**A**) Schema of the experimental paradigm: rostral (DTR) thalamic explants isolated from ß-actin::EGFP E14.5 embryos were co-cultured with E14.5 wholemount telencephalon from wild-type isochronic embryos under standard control conditions (grey: **With Cortex**) or on telencephalons which had undergone a complete cortectomy. The cortex was either replaced onto the telencephalon in the original orientation (blue: **Severed Cortex**) or with the rostro-caudal orientation reversed (green: **Inverted Cortex**) in order to test for the presence of regionally expressed cortical cues.

(**B**) DTR explants grown on With Cortex telencephalons grow to rostral regions of the VTel as shown before. Axons reaching the cortico-striatal boundary (CSB) cross into the cortex with no deflection (data not shown).

(**C**) DTR explants grown on Severed Cortex telencephalons also grow into the rostral VTel, with no measurable difference compared to With Cortex conditions. Similarly, axons reaching the CSB maintain their trajectory into the cortex (blue arrow).

(**D**) Explants grown on Inverted Cortex telencephalons are severely disrupted, growing into all regions of the VTel. While a rostral trend is still measureable, there is significantly more caudal growth. Axons passing through the rostral VTel encounter the caudal cortex and pass into with little deflection. Axons that grew into caudal regions of the VTel encounter the rostral cortex, but are severely deflected.

(**E**) Quantification of the topography of rostral thalamic axon outgrowth inside the VTel of With Cortex (grey), Severed Cortex (blue), and Inverted Cortex (green) conditions.

(**F**) Quantification of cortical entry by DTR axons in With Cortex (grey), Severed Cortex (blue), and Inverted Cortex (green) conditions.

*** $p<0.001$ ANOVA one-way test (overall effect: bins versus experimental conditions). The raster-like dot plot presented under the histograms represents the significance of individual bin comparisons between the two experimental conditions according to a PLSD-post-hoc test (• $p<0.05$; •• $p<0.01$ and ••• $p<0.001$).

Secreted cues from the cortex provide powerful long-range attractants to DTR axons.

Because DTR axon growth is disrupted immediately upon entering the VTel, it is unlikely that this is a result of direct interactions between CF and TC axons. Wholemounts with a GFP expressing Reattached or Inverted Cortex require 2-3 DIV before significant CF axon growth can be detected (Data not shown). This led us to ask whether DTR response to an inverted cortex is carried by secreted cortical cues. To achieve this, we inserted a 0.1 microns pored-membrane between the VTet and cortex of Inverted Cortex wholemounts to see if a caudalization of DTR axons is maintained (**Inverted w/Membrane Fig 4A**). The membrane pores do not allow axons to enter the VTel, but do allow for secreted molecules from the cortex to enter the VTel.

DTR axon growth through Inverted w/Membrane conditions is randomized, with peaks towards the rostral and caudal most regions of the VTel (**Fig 4B**). The pattern of growth is significantly different from both Severed and Inverted Cortex formats (**Fig 4C**), with a less uniform growth than Inverted conditions, and more caudal growth than in Severed conditions.

These results show that the cortex does contain secreted cues that are capable of caudalizing DTR axons inside the VTel. These secreted cues work independently of CF axons, as these axons are not present in the Inverted w/Membrane format. Additionally, the difference observed between Inverted and Inverted w/Membrane formats in the central regions of the VTel provide evidence that CF axons, while not required, can interact with rostral TC axons.

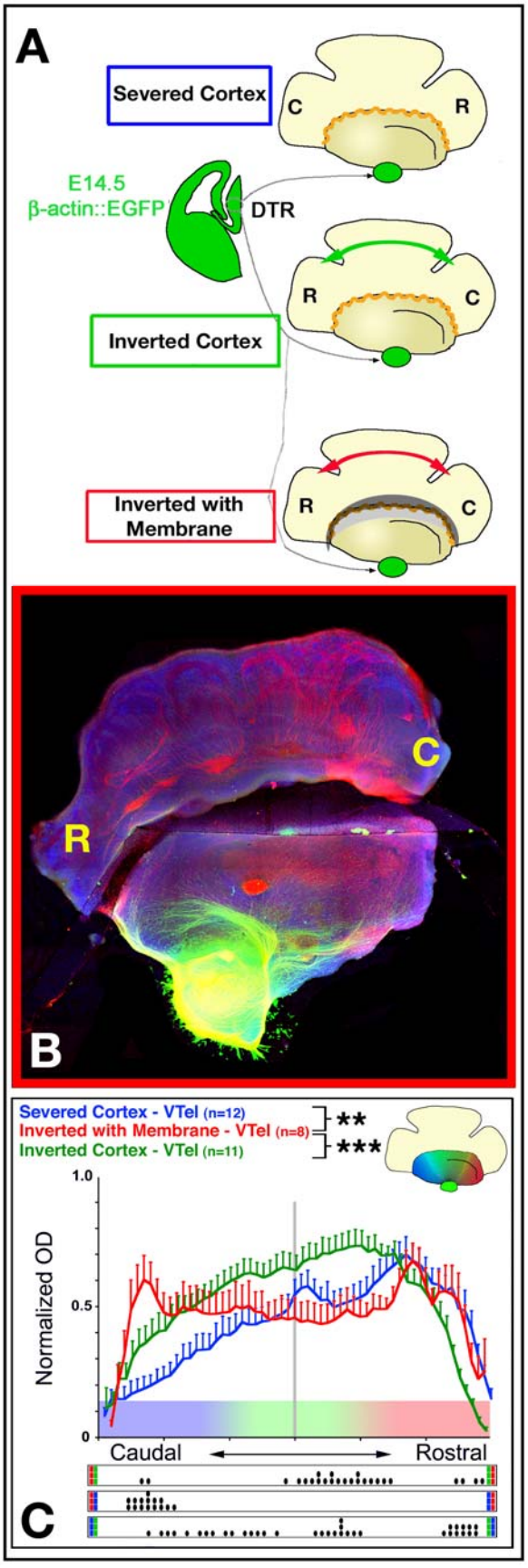

Figure 4. The rostral cortex contains a secreted cue that influences the topography of rostral thalamocortical axons inside the VTel.

(**A**) Schema of the experimental paradigm: rostral (DTR) thalamic explants isolated from ß-actin::EGFP E14.5 embryos were co-cultured with E14.5 wholemount telencephalon from wild-type isochronic embryos which had undergone a complete cortectomy. The cortex was either replaced onto the telencephalon in the original orientation (blue: **Severed Cortex**) or with the rostro-caudal orientation reversed (green: **Inverted Cortex**) in order to test for the presence of regionally expressed cortical cues. A final condition has a 0.1 microns-thick membrane positioned in between the cortex and the VTel (red: **Inverted with Membrane**).

(**B**) DTR explants grown on Inverted with Membrane telencephalons maintain some rostral growth, but a large contingent of axons is directed to caudal regions of the VTel. DTR axons and CFA are not able to cross the membrane. Red channel – NF165kd.

(**C**) Quantification of the topography of rostral thalamic axon outgrowth inside the VTel. DTR growth in Inverted with Membrane conditions is significantly different than both Severed and Inverted Cortex conditions. This implies that there are cortical cues affecting DTR growth. The membrane blocks CFA from entering the VTel, which shows that CFA are capable of influencing DTR growth. This also shows that there is a secreted cortical cue that can pass through the membrane.

*** $p<0.001$ & ** $p<0.05$ ANOVA one-way test (overall effect: bins versus experimental conditions). The raster-like dot plot presented under the histograms represents the significance of individual bin comparisons between the two experimental conditions according to a PLSD-post-hoc test (• $p<0.05$; •• $p<0.01$ and ••• $p<0.001$).

Further experiments should be performed to identify the secreted cues whose effects have been demonstrated in these experiments. As with our hypothesis of the possible involvement of Shh in patterning TCA inside the VTel, the identity of these cortical cues may not be traditionally thought of as axon guidance molecules. Long-range patterning molecules such as FGF8, which is expressed in the rostral dorsal telencephalon (BGEM), or Wnts, expressed in intriguing patterns along the CSB (Grove et al. 1998), are potential candidates.

The trajectory of thalamocortical axons reflects a continuous summation of interactions between environmental cues and axon responsiveness.

The mechanisms establishing the topography of the thalamocortical system can be difficult to study due to the amount of variables inherent in the system. There are heterogeneous populations of TCA expressing various combinations of axon guidance receptors, controlled in part by the combination of transcription factors they express. TCA response to axon guidance molecules is based not only upon these receptors, but the intracellular composition of the growth cone as well. There are multiple axon guidance molecules patterning the VTel during the period of TCA growth, including migrating populations of cells and the axons of neurons from distant regions. Finally, the three dimensional nature of the VTel increases the complexity of system.

The trajectory of a growing axon can be described as a continuous event during which an axon moves in a direction that is the summation of attractive and repulsive forces on the growth cone. Many of the experiments used in this thesis addressed the contribution of a single cue by assessing the result of a manipulation following 4 days *in vitro* or after significant *in vivo* development. It is important to remember that the resulting deficits are not the result of a single response by a TCA to the loss of an axon guidance molecule but a series of contiguous responses throughout the period of axon growth.

In the example of Netrin-1 as a topographic cue, DTR axon trajectories in mutant mice cannot be reduced to a single occurrence of a rostral axon reacting to a loss of Netrin-1. The resulting data are a summation of continuous events where a loss of Netrin-1 impacts the trajectory of a TCA in concert with the axon guidance molecules remaining in the VTel. While a DTR axon heavily expressing DCC may lose attraction to the rostral Vtel when Netrin-1 is removed, the presence of caudal ephrin-A5 still provides some rostral selectivity for axons expressing high levels of EphA4/5. For DTR axons expressing lower levels of EphA4/5 and high levels of DCC, the loss of Netrin-1 may result in a more severe caudalization. We predict that the level of redundancy of axon guidance mechanisms patterning the projection of TC axons in the ventral telencephalon is such that the effect of removing one cue (or one receptor in the DTh) at a time, might be masked by other axon guidance cues.

References

Bagri A, Marin O, Plump AS, Mak J, Pleasure SJ et al. (2002) Slit proteins prevent midline crossing and determine the dorsoventral position of major axonal pathways in the mammalian forebrain. Neuron 33(2): 233-248.

Caviness VS, Jr., Frost DO (1980) Tangential organization of thalamic projections to the neocortex in the mouse. J Comp Neurol 194(2): 335-367.

Charron F, Stein E, Jeong J, McMahon AP, Tessier-Lavigne M (2003) The morphogen sonic hedgehog is an axonal chemoattractant that collaborates with netrin-1 in midline axon guidance. Cell 113(1): 11-23.

Dufour A, Seibt J, Passante L, Depaepe V, Ciossek T et al. (2003) Area specificity and topography of thalamocortical projections are controlled by ephrin/Eph genes. Neuron 39(3): 453-465.

Frost DO, Caviness VS, Jr. (1980) Radial organization of thalamic projections to the neocortex in the mouse. J Comp Neurol 194(2): 369-393.

Grove EA, Tole S, Limon J, Yip L, Ragsdale CW (1998) The hem of the embryonic cerebral cortex is defined by the expression of multiple Wnt genes and is compromised in Gli3-deficient mice. Development 125(12): 2315-2325.

Guijarro P, Simo S, Pascual M, Abasolo I, Del Rio JA et al. (2006) Netrin1 exerts a chemorepulsive effect on migrating cerebellar interneurons in a Dcc-independent way. Mol Cell Neurosci 33(4): 389-400.

Kolpak A, Zhang J, Bao ZZ (2005) Sonic hedgehog has a dual effect on the growth of retinal ganglion axons depending on its concentration. J Neurosci 25(13): 3432-3441.

Lee JD, Kraus P, Gaiano N, Nery S, Kohtz J et al. (2001) An acylatable residue of Hedgehog is differentially required in Drosophila and mouse limb development. Dev Biol 233(1): 122-136.

Leighton PA, Mitchell KJ, Goodrich LV, Lu X, Pinson K et al. (2001) Defining brain wiring patterns and mechanisms through gene trapping in mice. Nature 410(6825): 174-179.

Lopez-Bendito G, Cautinat A, Sanchez JA, Bielle F, Flames N et al. (2006) Tangential neuronal migration controls axon guidance: a role for neuregulin-1 in thalamocortical axon navigation. Cell 125(1): 127-142.

Molnar Z, Adams R, Blakemore C (1998) Mechanisms underlying the early establishment of thalamocortical connections in the rat. Journal of Neuroscience 18(15): 5723-5745.

Mulieri PJ, Kang JS, Sassoon DA, Krauss RS (2002) Expression of the boc gene during murine embryogenesis. Dev Dyn 223(3): 379-388.

Nakamura F, Tanaka M, Takahashi T, Kalb RG, Strittmatter SM (1998) Neuropilin-1 extracellular domains mediate semaphorin D/III-induced growth cone collapse. Neuron 21(5): 1093-1100.

Okada A, Charron F, Morin S, Shin DS, Wong K et al. (2006) Boc is a receptor for sonic hedgehog in the guidance of commissural axons. Nature 444(7117): 369-373.

Powell AW, Sassa T, Wu Y, Tessier-Lavigne M, Polleux F (2008) The attractive and repulsive functions of Netrin-1 are required for the topographic projection of thalamocortical axons in the ventral telencephalon. PLoS Biology: Accepted March 2008.

Seibt J, Schuurmans C, Gradwhol G, Dehay C, Vanderhaeghen P et al. (2003) Neurogenin2 specifies the connectivity of thalamic neurons by controlling axon responsiveness to intermediate target cues. Neuron 39(3): 439-452.

Wright AG, Demyanenko GP, Powell AW, Polleux F, Maness PF et al. (2007) Journal of Neuroscience 27(50): 13667-13679.